

# The effects of different cure cycles on the mechanical performance of thick-walled composites

Guyonne Alleman



Copyright © Guyonne Alleman  
All rights reserved.

# The effects of different cure cycles on the mechanical performance of thick-walled composites

MASTER OF SCIENCE THESIS

For obtaining the degree of Master of Science in Aerospace Engineering  
at Delft University of Technology

Guyonne Alleman

May 16, 2018

## GRADUATION COMMITTEE

Chair holder:

Prof.dr.ir. R. Benedictus

Committee members:

Dr. J.J.E. Teuwen

Dr.ir. J.M.J.F. van Campen

Dr. G. Struzziero



---

# Abstract

A composite wind turbine blade is partially thick-walled to comply with high strength criteria. When the manufacturer's recommended cure cycle (MRCC), which is designed for thin-walled components, is used for thick-walled components, the exothermic reaction of the resin will cause through-thickness temperature distributions. This thermal anisotropy through the thickness can introduce residual stresses which will lead to warpage, matrix cracks and delaminations. Therefore the cure cycle needs to be optimised for thick-walled composites to reduce the residual stresses.

Because residual stresses are mainly compressive, they can have a positive effect on the tensile strength of the composite, while they can have a detrimental effect on the compression and shear strength of the composite. Residual stresses can be reduced by using very long cure cycle times, but this is economically infeasible. Therefore, the objective of this research is to make recommendations on the cure cycle of thick-walled composites made by vacuum infusion to simultaneously minimise residual stresses and cycle time by experimental investigation of different cure cycles.

Adjusting the cure cycle parameters will change the thermophysical properties of the resin. Therefore a cure kinetics model is developed that describes the influence of temperature and time on the degree of cure of the epoxy resin. The DiBenedetto model expresses the relation between degree of cure and the  $T_g$  of the resin. This information is used to describe the curing behaviour of the composite.

Nine two-dwell cure cycles were designed and compared with the single dwell MRCC. The cure cycles are made distinct by choosing different values for the first dwell temperature, first dwell time, ramp rate and second dwell temperature. Every laminate was separated with peel plies into nine sub-laminates of which three were selected for mechanical testing to determine the influence of the cure cycle parameters on the through-thickness temperature distribution and the mechanical performance of the composite. The mechanical performance is tested with an in-plane shear test with acoustic emission (AE) to detect the defects due to the manufacturing process.

The aim is to obtain laminates with a low exothermic peak, a high maximum in-plane shear stress ( $\tau_{12}^m$ ) and low AE activity while minimising the cure cycle time. The main conclusions of this research are that  $\tau_{12}^m$  of the laminate made with MRCC is significantly lower than all two-dwell cure cycles. Increasing the first dwell temperature will decrease the exothermic peak temperature, decrease  $\tau_{12}^m$ , not affect the AE activity and not affect time. Increasing the first dwell time will decrease the exothermic peak temperature, increase  $\tau_{12}^m$ , decrease AE activity and increase time. Increasing the ramp rate will increase the exothermic peak temperature, result in a peak in  $\tau_{12}^m$  at 50°C/h, increase AE activity and decrease time. Increasing the second dwell temperature will decrease  $\Delta T$  between the exothermic peak temperature and the second dwell temperature, decrease  $\tau_{12}^m$ , increase AE activity and not affect time.

It is recommended to use a two-dwell cure cycle compared to MRCC for thick-walled components with this material combination in order to reduce residual stresses and cycle time. Using a second dwell temperature of 70°C is beneficial for the mechanical performance while time is not affected. Increasing the first dwell time will be beneficial for the mechanical performance but the time is increased considerable and a trade-off should be made by the manufacturer.



---

# Acknowledgements

The master thesis project is, as it is for many, my final act as a student. This stage of life is and almost was a very rewarding and fulfilling experience, creating knowledge, skills and friendships. All three of which I hope to keep and expand upon in the future. I would like to thank my parents, my boyfriend and my future parents in law for their love and support during all these years. I would also like to thank dr. Julie Teuwen and dr. Giacomo Struzziero for their guidance and advice during my master thesis. The lab technicians for their help and finally my friends for making my time at the TU Delft unforgettable.

Guyonne Alleman



“Keep your dreams alive. Understand to achieve anything requires faith and belief in yourself, vision, hard work, determination, and dedication. Remember all things are possible for those who believe.”

— *Gail Devers*



---

# Table of Contents

<b>1</b>	<b>Introduction</b>	<b>1</b>
1.1	Background . . . . .	1
1.2	Literature study . . . . .	2
1.2.1	Thermophysical properties . . . . .	2
1.2.2	Mechanisms of residual stress formation . . . . .	2
1.2.3	Effects of residual stresses . . . . .	3
1.2.4	Cure cycle optimisation . . . . .	3
1.3	Research questions . . . . .	8
1.4	Thesis outline . . . . .	9
<b>2</b>	<b>Material characterisation</b>	<b>11</b>
2.1	Chemical characterisation . . . . .	11
2.1.1	Dynamic DSC . . . . .	11
2.1.2	Isothermal DSC . . . . .	13
2.2	Thermal characterisation . . . . .	14
2.2.1	Degradation temperature . . . . .	14
2.2.2	Glass transition temperature . . . . .	16
2.2.3	Specific heat . . . . .	16
2.3	Thermo-mechanical characterisation . . . . .	18
2.3.1	Elastic modulus . . . . .	19
2.3.2	Coefficient of thermal expansion . . . . .	22
2.3.3	Density resin . . . . .	24
2.3.4	Cure shrinkage . . . . .	26

---

<b>3</b>	<b>Methodology</b>	<b>27</b>
3.1	Vacuum infusion . . . . .	27
3.1.1	Layup . . . . .	27
3.1.2	Infusion . . . . .	29
3.1.3	Cure cycles . . . . .	29
3.2	Mechanical testing . . . . .	30
3.2.1	Density and volume fraction . . . . .	32
3.2.2	In-plane shear test . . . . .	32
3.2.3	Short-beam test . . . . .	33
<b>4</b>	<b>Results</b>	<b>35</b>
4.1	Temperature analysis . . . . .	35
4.1.1	Temperature profiles . . . . .	36
4.1.2	Exothermic peak temperature . . . . .	36
4.1.3	Thermal anisotropy in time . . . . .	38
4.1.4	Inside-out vs. outside-in curing . . . . .	40
4.2	Density composite . . . . .	41
4.3	Volume fractions . . . . .	41
4.4	In-plane shear test . . . . .	43
4.4.1	Shear stress . . . . .	43
4.4.2	Shear modulus . . . . .	45
4.4.3	Maximum shear strain . . . . .	46
4.4.4	Offset shear strength . . . . .	46
4.4.5	Acoustic emission . . . . .	46
4.5	Short-beam test . . . . .	50
4.6	Time optimisation . . . . .	51
<b>5</b>	<b>Discussion</b>	<b>53</b>
<b>6</b>	<b>Conclusions</b>	<b>57</b>
<b>7</b>	<b>Recommendations</b>	<b>59</b>
	References	61
<b>A</b>	<b>Dynamic DSC integration</b>	<b>65</b>
<b>B</b>	<b>Determination of the glass transition temperature</b>	<b>67</b>
<b>C</b>	<b>Malfunction of TMA</b>	<b>69</b>
<b>D</b>	<b>Resin crystallisation</b>	<b>71</b>

---

# List of Figures

1.1	Vitrification point . . . . .	2
1.2	Residual stress due to resin shrinkage. . . . .	3
1.3	$\alpha_{cross}$ close to $\alpha_{AGP}$ . . . . .	4
1.4	Temperature profile cure cycle Sorrentino et al. . . . .	5
1.5	Cure cycle Bogetti and Gillespie. . . . .	6
1.6	Cure cycle Antonucci et al. . . . .	6
1.7	Cure cycle Kim and Lee. . . . .	7
1.8	Cure cycle Kim et al. . . . .	7
1.9	Flowchart. . . . .	10
2.1	Differential Scanning Calorimeter. . . . .	12
2.2	$\alpha$ vs. temperature Airstone 780E/785H measured with a ramp rate of 1°C/min. . . . .	13
2.3	$\alpha$ vs. time with cure kinetics model for Airstone 780E/785H. . . . .	15
2.4	% weight loss vs. temperature for Airstone 780E/785H. . . . .	15
2.5	DiBenedetto model for Airstone 780E/785H. . . . .	17
2.6	Modulated ramp rate DSC. . . . .	18
2.7	$C_p$ determined with mDSC for Airstone 780E/785H. . . . .	19
2.8	Mould for epoxy samples. . . . .	20
2.9	Storage modulus with $\alpha = 0.94$ for Airstone 780E/785H. . . . .	21
2.10	Storage modulus with 1 Hz for Airstone 780E/785H. . . . .	21
2.11	Storage modulus at room temperature for Airstone 780E/785H. . . . .	22
2.12	Typical probe position vs. temperature graph for Airstone 780E/785H. . . . .	23
2.13	Density vs. $T_g$ . . . . .	25
2.14	Density vs. temperature for Airstone 780E/785H. . . . .	26

3.1	Vacuum infusion layup. . . . .	28
3.2	Infusion. . . . .	29
3.3	Typical two dwell cure cycle. . . . .	30
3.4	Two-dwell cure cycles. . . . .	31
3.5	Sub-laminates used for mechanical testing. . . . .	32
3.6	Geometry mechanical testing. . . . .	33
3.7	Selected region for DIC measurements. . . . .	33
4.1	Temperature profile of laminate made with MRCC. . . . .	37
4.2	Temperature profiles of sub-laminate E. . . . .	37
4.3	Exothermic peak temperature distribution through the thickness. . . . .	38
4.4	Through-thickness temperature distribution of the laminate made with MRCC at different points in time. . . . .	39
4.5	Through-thickness temperature distribution of the laminate made with CC9 at different points in time. . . . .	39
4.6	Maximum in-plane shear stress. . . . .	44
4.7	Chord shear modulus of elasticity. . . . .	45
4.8	Offset shear strength. . . . .	47
4.9	$\tau_{12}$ vs. average cumulative hits of the laminate made with MRCC. . . . .	47
4.10	AE cumulative hits at $\tau_{12} = 40$ MPa. . . . .	48
4.11	AE cumulative hits at $\tau_{12} = 50$ MPa. . . . .	49
4.12	Short-beam strength. . . . .	50
A.1	Integration of first dynamic DSC test. . . . .	65
A.2	Integration of second dynamic DSC test. . . . .	66
B.1	Determination of $T_g$ using the Pyris DSC software. . . . .	68
B.2	Cure cycle to determine $T_g$ . . . . .	68
C.1	Malfunction of probe with TMA. . . . .	69
D.1	Exothermic peak temperature of laminates made with a good and bad resin system. . . . .	72
D.2	$\frac{d\alpha}{dt}$ of laminates made with a good and bad resin system. . . . .	73

---

## List of Tables

2.1	Total heat of reaction of Airstone 780E/785H epoxy measured with a ramp rate of 1°C/min. . . . .	12
2.2	Degree of cure reached with isothermal tests for Airstone 780E/785H. . . . .	14
2.3	Constants used in cure kinetics model for Airstone 780E/785H. . . . .	14
2.4	Constants used in $C_p$ model for Airstone 780E/785H. . . . .	18
2.5	Samples mechanical characterisation. . . . .	19
2.6	$CTE_{glass}$ per degree of cure for Airstone 780E/785H. . . . .	24
2.7	Density per degree of cure for Airstone 780E/785H. . . . .	24
3.1	Cure cycles. . . . .	31
4.1	$\alpha_{AGP}$ vs. $\alpha_{cross}$ . . . . .	40
4.2	Density per sub-laminate for two glass fibre - epoxy laminates. . . . .	41
4.3	Volume fractions per sub-laminate for the laminate made with CC7. . . . .	42
4.4	Volume fractions per sub-laminate for the laminate made with CC1. . . . .	43
4.5	Time to $\alpha_{max}$ . . . . .	51



---

# Chapter 1

---

## Introduction

In this master thesis project the effects of different cure cycles on the mechanical performance of thick-walled composites made by vacuum infusion are investigated. First some background information about vacuum infusion and cure cycles will be given (1.1). A literature study about the change in thermophysical properties during curing, the mechanisms and effects of residual stress and cure cycle optimisation (1.2) will result in research questions to be answered during this project (1.3). Finally, a thesis outline will describe the remaining structure of this report (1.4).

### 1.1 Background

Vacuum infusion is a composite manufacturing technique that uses a solid mould on one side and a disposable vacuum bag on the other side of the fibres. A pressure difference between inlet and outlet is used to infuse the resin into the preform. After infusion the resin is either cured at room temperature or at elevated temperatures using a heated mould or an oven. Vacuum infusion is extensively used in aerospace and wind energy industries where large composite parts are required [1]. It results in high performance composite materials with low cost manufacturing [2, 3].

A wind turbine blade, made by vacuum infusion, is partially thick-walled to comply with high strength criteria. The manufacturer's recommended cure cycle (MRCC) is designed for thin-walled components and is often time conservative [4] and inadequate for thick components due to the exothermic reaction which causes through-thickness temperature distributions [5, 6]. This thermal anisotropy through the thickness can introduce residual stresses which will lead to warpage, matrix cracks and delaminations [6–9]. The thermal anisotropy can be reduced by decreasing the cure temperature, increasing the time to reach that temperature and increasing the time at that temperature. But this results in a longer cycle time which makes it economically infeasible [4]. Therefore the MRCC needs to be optimised for thick-walled composites in order to reduce the residual stresses and cycle time.

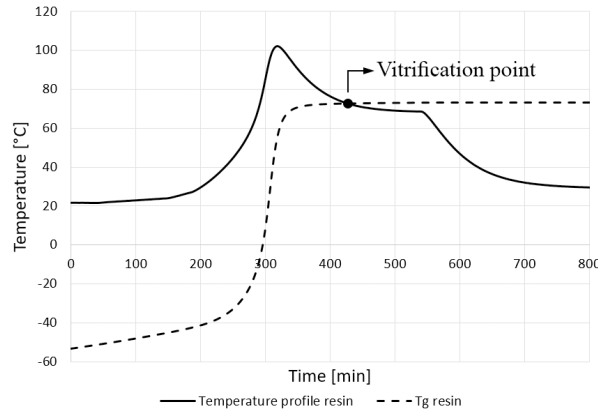


Figure 1.1: Vitrification point

## 1.2 Literature study

Curing is a chemical process that refers to the hardening of a thermoset material. The material is irreversibly converted from a liquid into a solid by cross-linking polymer chains which create a 3D network. The degree of cure can be described by a number between 0 and 1 in which 0 means that the material has not experienced any curing and 1 relates to a fully cross-linked material. This literature review focuses on the curing of an epoxy resin. During the curing process the thermophysical properties of the material will change (1.2.1). Curing an epoxy resin can result in the formation of residual stresses (1.2.2) which can have both a beneficial and a detrimental effect on the composite material (1.2.3). To reduce the negative effects of residual stresses, the cure cycle can be optimised in order to improve the quality of the composite laminate (1.2.4).

### 1.2.1 Thermophysical properties

During the curing process of an epoxy resin, molecules are crosslinked to form a 3D network, which results in a change in thermophysical properties. The glass transition temperature ( $T_g$ ) of the resin will increase with the degree of cure, the specific heat ( $C_p$ ) will increase with temperature and the coefficient of thermal expansion (CTE) will be constant below and above  $T_g$ , but will jump at the  $T_g$  [6, 10]. The volume of the resin and thus its density will also change during cure due to cure shrinkage [11, 12]. The elastic modulus will decrease drastically when the resin is in its rubbery phase (above  $T_g$ ) and then remains low until vitrification. Vitrification is the process at which the  $T_g$  exceeds the temperature of the resin (Fig. 1.1). After vitrification the elastic modulus will increase. [10]

### 1.2.2 Mechanisms of residual stress formation

Residual stresses are stresses that remain in the material after cure in an unloaded state. Although residual stresses occur in both thin and thick laminates, they become more significant with increasing thickness. Residual stresses in thick-walled composites are mainly caused by three mechanisms. Firstly, the exothermic reaction of the epoxy resin and the low

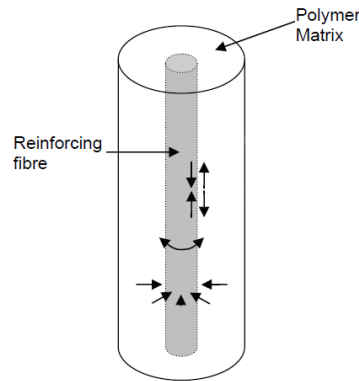


**Figure 1.2:** Residual stress due to resin shrinkage where  $\rightarrow\leftarrow$  indicate residual compressive stresses and  $\leftarrow\rightarrow$  indicate residual tensile stresses. Figure from Parlevliet [12].

thermal conductivity of the resin and fibres cause thermal anisotropy through the thickness of the laminate which will lead to an unequal degree of cure [5,6]. Secondly, cure shrinkage of the resin results in residual stresses at micromechanical level due to the large difference in shrinkage between fibres and matrix [7,12]. Lastly, differences in CTE between fibres and matrix causes residual stresses at micro- and macromechanical level [12–14].

### 1.2.3 Effects of residual stresses

The residual stresses in thick-walled composites will have multiple effects on the composite laminate. It can cause matrix cracking, fibre-matrix debonding, fibre waviness, delaminations and warpage [14–16]. Residual stress in a laminate can have both a beneficial and a detrimental effect on its mechanical properties, depending on the applied load and its direction (Fig. 1.2). Cure shrinkage and differences in CTE between matrix and fibre cause residual compressive stresses in the fibre along its longitudinal axis. These stresses will be beneficial for the tensile strength of the composite in the fibre direction, but are detrimental for the compressive strength of the composite in fibre direction. [14,17,18]

Transverse to the fibre direction, the ultimate strength depends on the fibre-matrix bonding and the strength of the matrix. Radial compressive residual stresses in the matrix will increase the fibre-matrix bonding and therefore increase the ultimate transverse tensile strength. Residual stress will have a detrimental effect on the compressive strength of the material in transverse direction as the compressive residual stress will increase the compressive load on the matrix. [17–19]. The residual stress in a laminate will have a detrimental effect on the shear and fatigue properties [14,17–19].

### 1.2.4 Cure cycle optimisation

In order to cure the epoxy resin, a certain cure cycle is required. The manufacturer recommends a cure cycle, called the MRCC. However, the MRCC is designed for thin-walled components and is often time conservative [4] and inadequate for thick composites due to the high levels of residual stress [5,6]. To improve the quality of the composite laminate, the MRCC must be optimised. Certain objectives can be defined that will minimise the formation

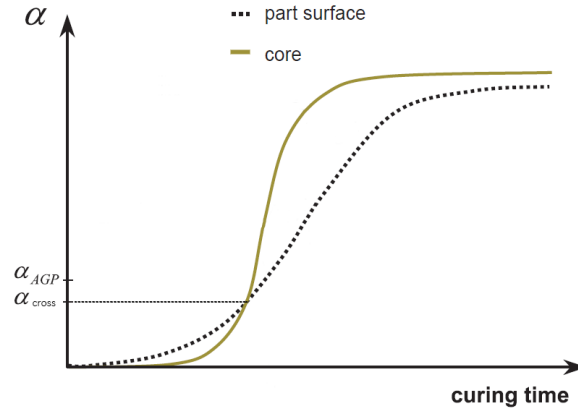


**Figure 1.3:**  $\alpha_{cross}$  close to  $\alpha_{AGP}$ , figure modified from [9].

of residual stress and maximise the efficiency of the process [4, 9, 20]. As the composite is heated from the outside, the curing process always starts as outside-in curing. At some point the exothermic reaction starts and the temperature inside the laminate will gain upon the temperature on the outside of the laminate as the heat cannot escape. Temperature is related to degree of cure and therefore the curing process changes from outside-in to inside-out curing. This is called the crossover point, denoted by  $\alpha_{cross}$  (Fig. 1.3). The degree of cure at the vitrification point, or After Gel Point (AGP), is denoted by  $\alpha_{AGP}$ . At this point, the resin modulus starts to increase and therefore  $\alpha_{cross}$  should ideally be below  $\alpha_{AGP}$ . Below  $\alpha_{AGP}$ , stresses caused by outside-in curing can relax because the resin is still in its liquid phase. After  $\alpha_{AGP}$ , the curing process should be changed to inside-out curing to prevent matrix cracking and delaminations. [3, 9, 20]

Besides this objective there are more objectives to optimise the cure cycle. The laminate must have a maximum degree of cure throughout the thickness to increase the mechanical performance, but the time must be minimised to reduce costs. The peak temperature inside the laminate must be minimised to prevent thermal degradation. Thermal anisotropy must be prevented to obtain a uniform degree of cure through the thickness. Finally, the curing and cooling stresses must be as low as possible to reduce the formation of residual stress. [9]

## Optimisation

Satisfying all objectives to a maximum extent is not feasible in practice as certain objectives will contradict others. For example the highest degree of cure and minimum time is reached with the highest curing temperature. However, a high curing temperature will result in a high exothermic peak and high curing and cooling stresses. Therefore optimisation of the cure cycle is necessary in order to compromise between the different objectives. Multiple authors have tried to perform this optimisation, an overview is given below.

Kim and Daniel [21] experimentally determined the influence of different cure cycles on the curvature of asymmetric laminates made by Resin Transfer Moulding (RTM). The curvature is used as a means to visualise residual stresses. The material used is an epoxy resin with carbon fibre to make a  $[0_4/90_4]$  layup with a thickness of 1 mm. The  $T_g$  of the resin is  $135^\circ\text{C}$ . They investigated three different cure temperatures:  $160^\circ\text{C}$ ,  $135^\circ\text{C}$  and  $110^\circ\text{C}$  and

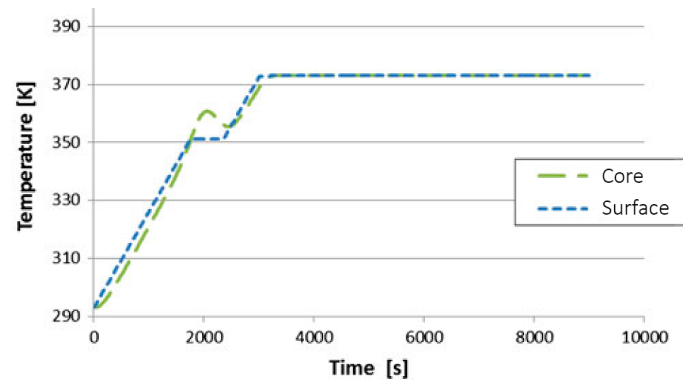


**Figure 1.4:** Temperature profile cure cycle Sorrentino et al.. Figure modified from Sorrentino et al. [20].

found a large decrease in curvature from  $135^{\circ}\text{C}$  to  $110^{\circ}\text{C}$ . This matches with the theory that a lower cure temperature reduces the peak temperature, thermal gradients, curing stresses and cooling stresses and thus reduces residual stresses and curvature. However, by reducing the cure temperature from  $160^{\circ}\text{C}$  to  $135^{\circ}\text{C}$  a small increase in curvature is observed. This was explained by the fact that curing above  $T_g$  causes a relaxation of the residual stresses. They also determined the influence of different ramp rates on the curvature of the laminate and tested three different ramp rates:  $4^{\circ}\text{C}/\text{min}$ ,  $2.75^{\circ}\text{C}/\text{min}$  and  $0.5^{\circ}\text{C}/\text{min}$ . No difference in curvature was found between  $4^{\circ}\text{C}/\text{min}$  and  $2.75^{\circ}\text{C}/\text{min}$ , but an increase in curvature was observed with  $0.5^{\circ}\text{C}/\text{min}$ . For the samples of  $4^{\circ}\text{C}/\text{min}$  and  $2.75^{\circ}\text{C}/\text{min}$ , most of the cure occurred at the cure temperature while the  $0.5^{\circ}\text{C}/\text{min}$  sample was already cured for 82% when the cure temperature was reached. This means that stresses caused by differences in CTE between fibre and matrix cannot relax because the resin is already partially gelled and thus the amount of residual stress will increase.

Sorrentino et al. [20] optimised the cure cycle of a 10 mm thick carbon fibre - epoxy laminate. They found that adding a second temperature dwell in the cure cycle creates a temperature profile that reduces residual stresses (Fig. 1.4). This is because the exothermic peak in the core of the laminate will occur at the first dwell, resulting in a lower  $\alpha_{cross}$  and a lower peak temperature after the second dwell.

Struzziero and Skordos [4] optimised the cure cycle of a 24 mm thick laminate made of carbon fibre with RTM6 epoxy resin and found that higher ramp rates increase the overshoot temperature while a higher second dwell temperature has a limited influence on the overshoot temperature.

Bogetti and Gillespie [7] determined with a one-dimensional cure simulation analysis of a 25.4 mm thick glass fibre - polyester laminate the influence of ramp rates on residual stress formation. They simulated ramp rates of 0.25, 0.5 and  $1.0^{\circ}\text{C}/\text{min}$  (Fig. 1.5) and found the preferred inside-out curing with the 0.25 and  $0.5^{\circ}\text{C}/\text{min}$  ramp rates and outside-in curing with  $1.0^{\circ}\text{C}/\text{min}$ .

Balvers [22] measured the process-induced strains using Fibre Bragg Gratings (FBG) in a 25 mm thick glass fibre - epoxy composite. He found that a higher cure temperature leads to higher process induced strains, but the maximum strain is reached at the gelation temperature of the matrix. Increasing the cure temperature above  $T_g$  will decrease the amount of process

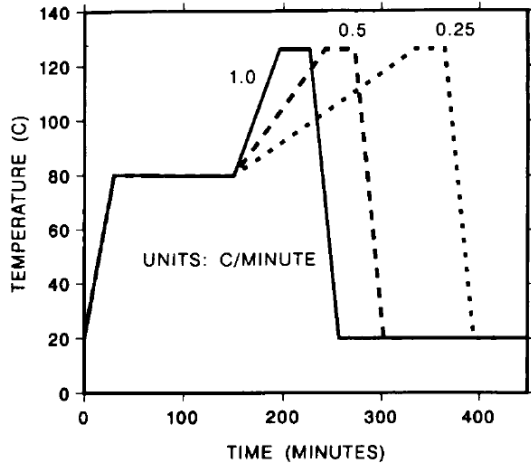


**Figure 1.5:** Cure cycle Bogetti and Gillespie. Figure from Bogetti and Gillespie [7].

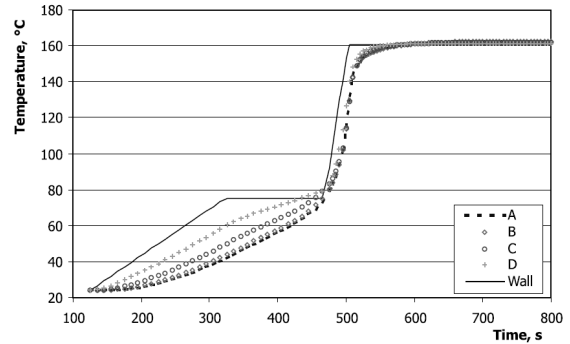


**Figure 1.6:** Cure cycle Antonucci et al.. A-D are thermocouples measuring the temperature across the thickness. The wall temperature is the applied temperature on the part. Figure from Antonucci et al. [2].

induced strain.

Antonucci et al. [2] used a scaling analysis of the energy balance equation to minimise the thermal gradients in a 10 mm thick composite of polyester resin with random glass fibres made by RTM. They used a two-dwell cure cycle whereby the temperature during the first dwell was held until the through-thickness temperature distribution was uniform. Then the temperature was raised to the second dwell to complete the cure. This resulted in no temperature gradients through the thickness after the first dwell (Fig. 1.6). Also  $\alpha_{cross}$  was found to be lower than  $\alpha_{AGP}$  which resulted in minimum residual stresses in the part.

Kim and Lee [23] used a finite difference method to reduce the temperature overshoot due to the exothermic reaction in a 15 and 30 mm thick carbon fibre - epoxy laminate by introducing cooling and reheating steps in the cure cycle without an increase in processing time. The cooling step is initiated just before the start of the exothermic reaction which minimised the exothermic peak (Fig. 1.7). Due to the exothermic reaction, the temperature inside the laminate will remain constant. After a certain time reheating is initiated to keep the temperature in the laminate constant. This optimised cure cycle reduced the temperature overshoot and resulted in a uniform degree of cure throughout the thickness.

Li and Tucker [24] determined the effect of increasing the number of dwells and concluded that using three dwells instead of two will reduce the processing time by 2 minutes. This does not outweigh the increased complexity of the cure cycle.

Sicot et al. [25] experimentally determined the influence of cooling rate and number of dwells on the level of residual stress of a 2 mm carbon fibre - epoxy laminate. They found a reduction in residual stress of 20% by reducing the cooling rate from 10 °C/min to 0.55 °C/min. However, the cycle time increased with 280 minutes by applying this cooling rate. Introducing a third dwell in the process without increasing the cycle time resulted in a reduction of the residual stress (10-27%) compared to a two-dwell cure cycle.

Kim et al. [26] studied the influence of a cooling cycle after the first dwell on the process-induced strains using dielectrometry and FBG sensors on a carbon fibre - epoxy laminate.

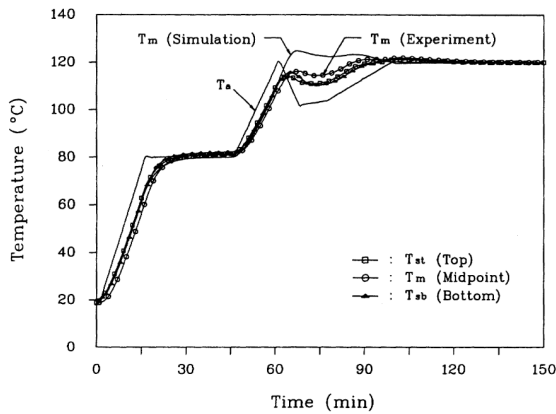


**Figure 1.7:** Cure cycle Kim and Lee.  $T_a$  is the autoclave temperature. Figure from Kim and Lee [23].

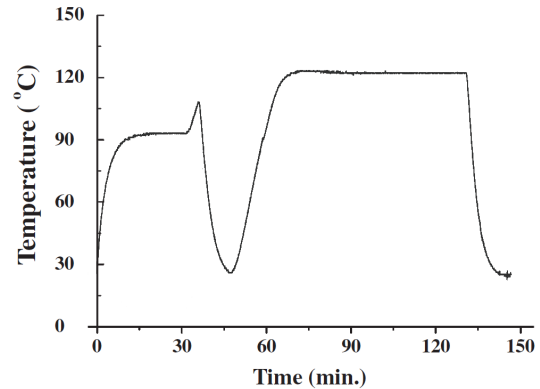


**Figure 1.8:** Cure cycle Kim et al.. Figure modified from Kim et al. [26].

Their MRCC consists of a conventional two-dwell cycle. The improved cycle adds a cooling cycle between the first and second dwell, without increase in processing time and reduced the process-induced strains up to 48.6% (Fig. 1.8).

## Conclusions

The optimisation methods discussed above lead to some similarities and contradictions:

- Increasing the dwell temperature will reduce the processing time and increase the maximum degree of cure, but it will enhance the amount of residual stress, with a maximum at the  $T_g$ . However, curing at too high temperatures can cause thermal degradation. [21, 22]
- Low ramp rates will result in inside-out curing while high ramp rates result in outside-in curing. Too low ramp rates will also increase the residual stress as the laminate is already partially cured before reaching the dwell temperature. Higher ramp rates will increase the exothermic peak temperature. [4, 7, 21]
- Multiple authors used a two-dwell cure cycle whereby the exothermic reaction occurs during the first dwell and the second dwell is used to fully cure the part [2, 4, 7, 20]. No distinct results are obtained by using a three dwell cure cycle to improve the residual stresses and cycle time [24, 25].
- Kim and Lee [23] and Kim et al. [26] optimised their cure cycle by adding a cooling stage before the final dwell to minimise the exothermic peak.

## 1.3 Research questions

The literature review on cure cycle optimisation shows that multiple authors have tried to optimise the cure cycle for thick-walled components. However, only some guidelines can be made on the optimum cure cycle because this will differ for every material combination. No literature is found on cure cycle optimisation for the material combination used in this project: non-crimp biaxial glass fibre with Airstone 780E/785H epoxy resin. Therefore this master thesis project focuses on the influence of different cure cycle parameters on the mechanical performance of this material combination. In order to do so, first the thermophysical properties of the resin and fibres must be determined. After this, laminates with different cure cycles are manufactured and mechanically tested to determine the influence of the cure cycle parameters on the residual stress formation. And finally a recommendation is made for improvement of the cure cycle for thick-walled composites.

### Research objective

The research objective is to make recommendations on the cure cycle of thick-walled composites made by vacuum infusion to minimise residual stresses and cycle time by experimental investigation of different cure cycles.

### Sub-goals

- To determine the thermophysical properties of epoxy resin and its composite by material characterisation techniques.
- To determine the influence of different cure cycles on the mechanical properties of thick-walled composites.

### Research questions

The research objective and sub-goals lead to the following research questions:

- What is the influence of temperature and degree of cure on the thermophysical properties of epoxy resin and composite laminates?
  - What is the influence of temperature on the curing behaviour of the resin?
  - What is the total heat of reaction to fully cure the resin?
  - What is the influence of degree of cure on the glass transition temperature of the resin?
  - What is the influence of temperature and degree of cure on the specific heat of the resin?
  - What is the influence of temperature and degree of cure on the coefficient of thermal expansion of the resin?
  - What is the amount of cure shrinkage of the resin?
  - What is the influence of temperature and degree of cure on the density of the resin?
  - What is the influence of temperature and degree of cure on the elastic modulus of the resin?
  - What is the density of the composite?

- What is the fibre volume fraction of the composite?
- What is the influence of different ramp rates, dwell temperatures and dwell times on the through-thickness temperature distribution and the mechanical properties of thick-walled composites?
  - What is the influence of different ramp rates, dwell temperatures and dwell times on the through-thickness temperature distribution of the laminate?
  - What is the influence of different ramp rates, dwell temperatures and dwell times on the in-plane shear strength of the sub-laminates?
  - What is the influence of different ramp rates, dwell temperatures and dwell times on the interlaminar shear strength of the sub-laminates?
- Which recommendations can be made for improvement of the cure cycle of thick-walled composites made by vacuum infusion in order to minimise the residual stresses and cycle time?

## 1.4 Thesis outline

This master thesis project is performed in cooperation with a postdoctoral researcher, dr. Giacomo Struzziero. An overview of the total project is visualised in a flowchart (Fig. 1.9). Curing the composite laminate requires the use of a cure cycle which can be adjusted by changing cure cycle parameters. Different dwell temperatures, dwell times and ramp rates will change the thermophysical properties of the epoxy resin and composite laminate. The chemical and thermal properties are used to generate a heat transfer model, which will determine the degree of cure and temperature distribution at any given time. The thermo-mechanical properties together with the heat transfer model will result in a thermo-mechanical model. This model will, besides the degree of cure and temperature distribution, determine the residual stresses in the composite laminate. According to the objectives described in paragraph 1.2.4, the aim is to maximise the degree of cure, minimise the thermal anisotropy through the thickness and minimise the residual stresses in the laminate. Therefore, the cure cycle needs to be optimised by adjusting the cure cycle parameters. This master thesis project focuses on the determination of the thermophysical properties and the experimental validation of the heat transfer and thermo-mechanical model. The models will be made by dr. Giacomo Struzziero.

First, material characterisation will be performed in order to determine the thermophysical properties of the epoxy resin and its composite (chapter 2). After that, the methodology describes the steps to manufacture the thick composite laminates with different cure cycles and to mechanically test these laminates (chapter 3). The results of the through-thickness temperature distribution, in-plane shear strength and interlaminar shear strength are presented in chapter 4 and discussed in chapter 5. This leads to conclusions to answer the research questions (chapter 6). Finally, recommendations will be given for further research (chapter 7).

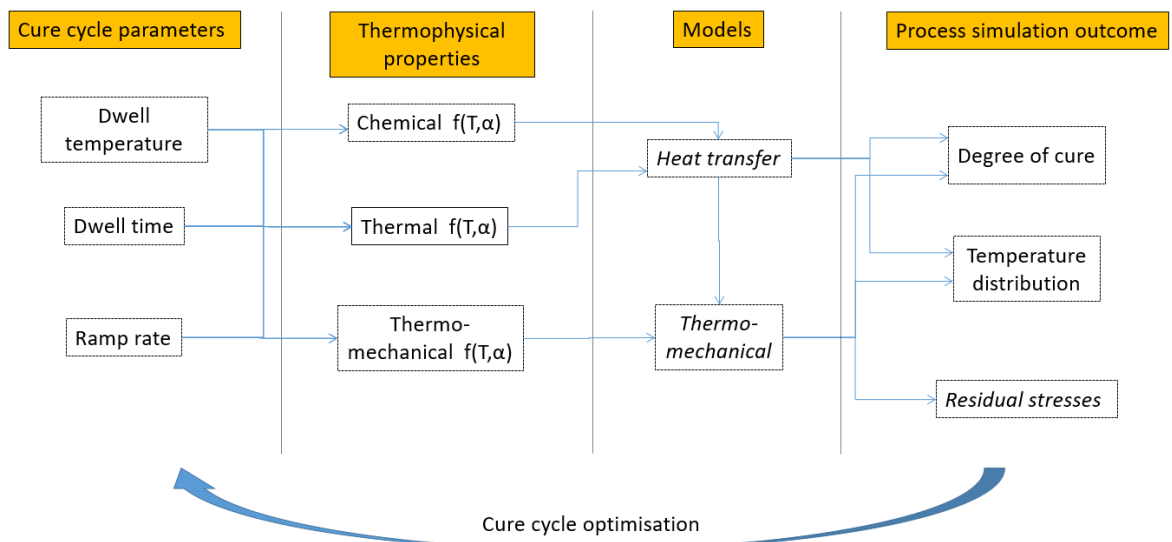


**Figure 1.9:** Flowchart. The parts indicated in italic will be performed by dr. Giacomo Struzziero.

# Material characterisation

Adjusting the cure cycle parameters of a cure cycle will change the thermophysical properties of the resin. Therefore material characterisation is performed in order to understand the influence of temperature and degree of cure on the thermophysical properties of the resin. In chapter 4 this information will be used to describe the curing behaviour of a composite laminate. The resin used in this thesis is Airstone 780E/785H epoxy. Material characterisation can be divided into three sections: chemical, thermal and thermo-mechanical characterisation. During chemical characterisation, the influence of temperature and time on the degree of cure is characterised (2.1). The material's response to temperature changes is determined with thermal characterisation (2.2). With thermo-mechanical characterisation the influence of degree of cure on the mechanical properties of the material is determined (2.3).

## 2.1 Chemical characterisation

Curing epoxy resin is an exothermic reaction. The heat generated during the reaction can be characterised with cure kinetics. This will reveal information about the relation between temperature, time and degree of cure. A Differential Scanning Calorimeter (DSC) measures the heat flow needed to increase the temperature of the sample. It will measure the difference in amount of heat required to raise the temperature in a reference and a reactive sample (Fig. 2.1) [27]. The reference pan is empty while the other pan contains the sample. Both pans will have equal temperature throughout the experiment. The outputs of the measurement are time, temperature and heat flow ( $dH/dt$ ). With a DSC, dynamic and isothermal scans can be performed. Dynamic scans have a constant ramp rate to be able to determine the total heat of reaction (2.1.1) while isothermal scans are performed at a constant temperature to determine the degree of cure at any given time (2.1.2) [10, 28, 29].

### 2.1.1 Dynamic DSC

With a dynamic DSC scan, the temperature will change as a function of time with a constant ramp rate to determine the total heat of reaction. The DSC will measure the heat flow ( $\frac{dH}{dt}$ )

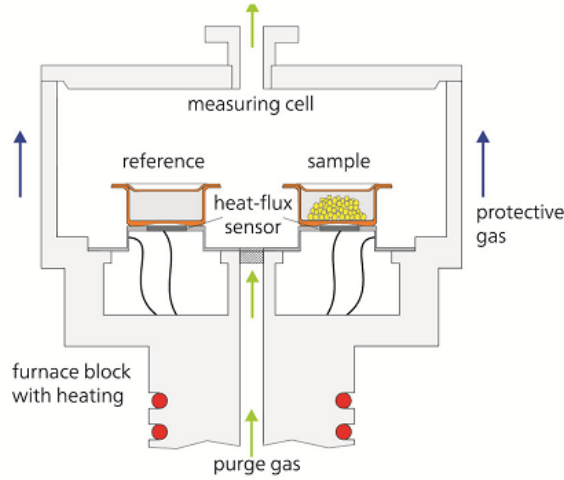


**Figure 2.1:** Differential Scanning Calorimeter. Figure from Reading and Hourston [30].

**Table 2.1:** Total heat of reaction of Airstone 780E/785H epoxy measured with a ramp rate of 1°C/min.

Sample	$H_t$
1	435.7 J/g
2	434.7 J/g
Average	435.2 J/g

required to raise the temperature of the sample. The integral of the heatflow vs. time graph will give the total heat of reaction ( $H_t$ ) according to [28]:

$$H_t = \int_0^t \frac{dH}{dt} dt \quad (2.1)$$

A proportional baseline is used to calculate  $H_t$  [31]. The Perkin Elmer Pyris Sapphire DSC with aluminium pans is used for all DSC tests. Two samples of uncured epoxy resin with a mass between 1 and 5 mg are heated from  $-25^\circ\text{C}$  to  $180^\circ\text{C}$  with a ramp rate of  $1^\circ\text{C}/\text{min}$ . The integration is visualized in Appendix A. The total heat of reaction is shown in Table 2.1. The average total heat of reaction is 435.2 J/g with a standard deviation of 0.5 J/g.

Now the total heat of reaction from this dynamic DSC test is known, the degree of cure ( $0 \leq \alpha \leq 1$ ) at any given time can be obtained according to [6, 10, 27, 28]:

$$\alpha = \frac{1}{H_t} \int_0^t \frac{dH}{dt} dt \quad (2.2)$$

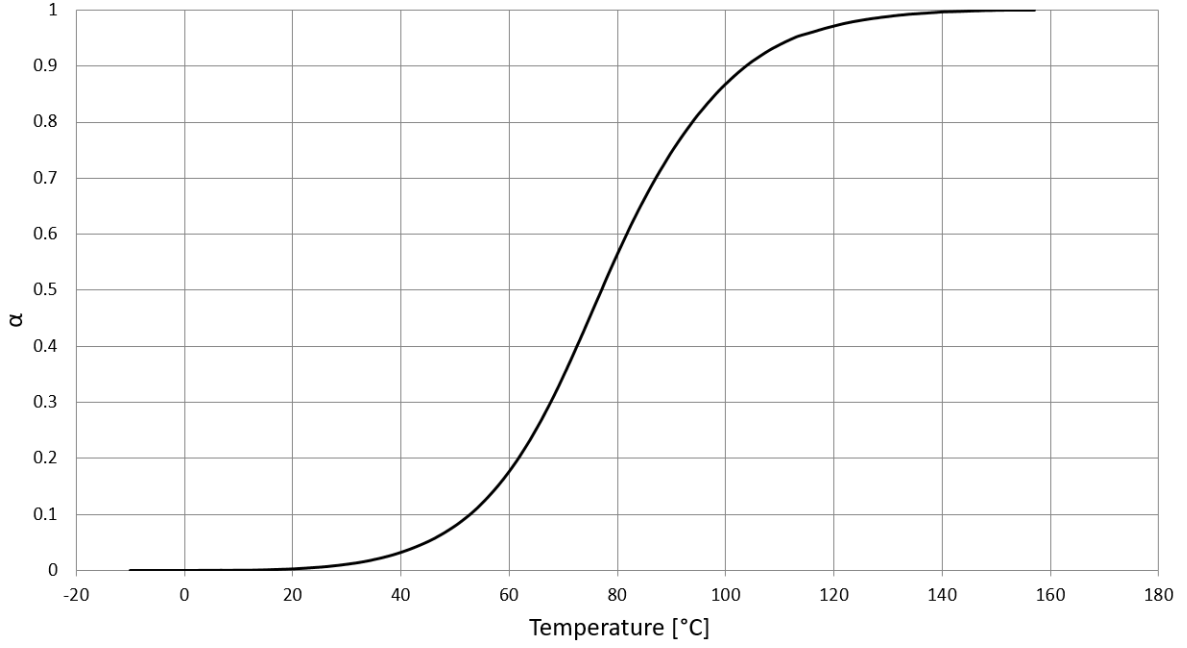


**Figure 2.2:**  $\alpha$  vs. temperature Airstone 780E/785H measured with a ramp rate of  $1^\circ\text{C}/\text{min}$ .

As the ramp rate is  $1^\circ\text{C}/\text{min}$ , the degree of cure at a given time can be converted to the degree of cure at a given temperature, shown in Fig. 2.2.

### 2.1.2 Isothermal DSC

Isothermal DSC scans are performed at a constant temperature for a given amount of time to determine the degree of cure at any given time. The DSC will measure the heat flow required to keep the temperature of the sample constant. The degree of cure at any given time can be obtained using Eq. 2.2. Isothermal tests are performed at four different temperatures: 50, 70, 90 and  $110^\circ\text{C}$ . The ramp rate towards the isothermal temperature is as fast as possible and approximately  $23^\circ\text{C}/\text{min}$ . The degree of cure as a function of time is plotted in Fig. 2.3. The maximum degree of cure that can be reached with a certain temperature and time is stated in Table 2.2. The semi-empirical model of Khoun et al. [10] is used to model the degree of cure as a function of time according to:

$$\frac{d\alpha}{dt} = K \frac{\alpha^m (1 - \alpha)^n}{1 + \exp[C(\alpha - (\alpha_{C0} + \alpha_{CT}T))]} \quad (2.3)$$

in which

$$K = A \exp\left(\frac{-E_a}{RT}\right) \quad (2.4)$$

This model contains a diffusion factor, represented as the denominator in Eq. 2.3 which will slow down  $\frac{d\alpha}{dt}$  when  $\alpha$  is close to 1.  $E_a$  is the activation energy calculated as the slope of the  $\ln(d\alpha/dt)$  vs  $1/T$  graph at low degrees of cure.  $\alpha_{C0}$  and  $\alpha_{CT}$  are fitting parameters

**Table 2.2:** Degree of cure reached with isothermal tests for Airstone 780E/785H.

Temperature [°C]	Time [min]	$\alpha$
50	505	0.79
70	265	0.90
90	132	0.92
110	67.5	0.96

**Table 2.3:** Constants used in cure kinetics model for Airstone 780E/785H.

Parameter	Value
E [J/mol]	61762.95
A [1/s]	1474423.40
n	1.66
m	0.069
C	30.72
$\alpha_{C0}$	0.65
$\alpha_{CT}$	0.0029

from a linear fit of the ultimate degree of cure ( $\alpha_{max}$ ) vs.  $T_g$  graph.  $R$  is the universal gas constant and the other parameters ( $m$ ,  $n$ ,  $C$  and  $A$ ) are obtained using a least squares non-linear regression between the experimental results and the model.  $\alpha$  and  $T$  are variables. All constants for Eq. 2.3 and Eq. 2.4 are presented in Table 2.3. The model is visualized as the black line in Fig. 2.3.

## 2.2 Thermal characterisation

The material's response to temperature changes is determined with thermal characterisation. Before thermal characterisation can be performed, it is necessary to determine the degradation temperature as this is the upper use temperature of the resin (2.2.1). The  $T_g$  at any given degree of cure can be calculated using the DiBenedetto equation (2.2.2). The specific heat of the resin is determined with a modulated DSC (mDSC) (2.2.3).

### 2.2.1 Degradation temperature

The degradation temperature of a polymer is the temperature at which polymer chains will break and the mechanical properties of the material will change permanently. Therefore the degradation temperature is the upper use temperature of the resin. Thermal degradation can be identified with Thermogravimetric Analysis (TGA) which measures the weight loss during temperature increase. This test is performed according to ASTM E2550. For this experiment the Perkin Elmer TG/DTA is used which is a combination of a TGA and a

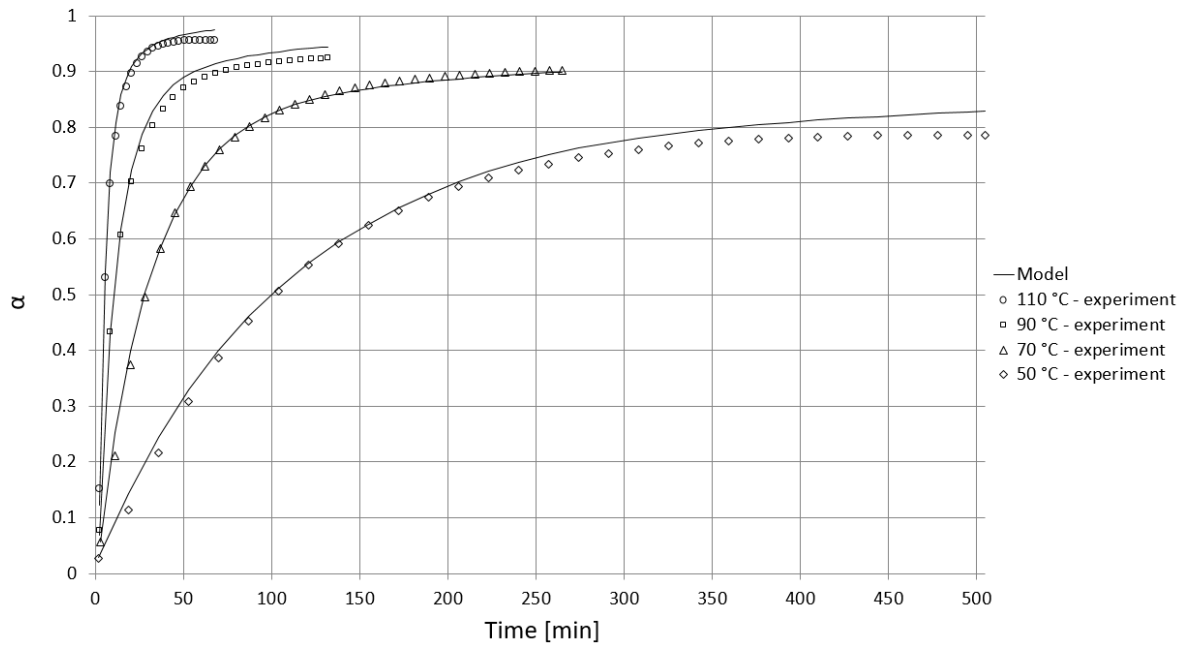


Figure 2.3:  $\alpha$  vs. time with cure kinetics model for Airstone 780E/785H.

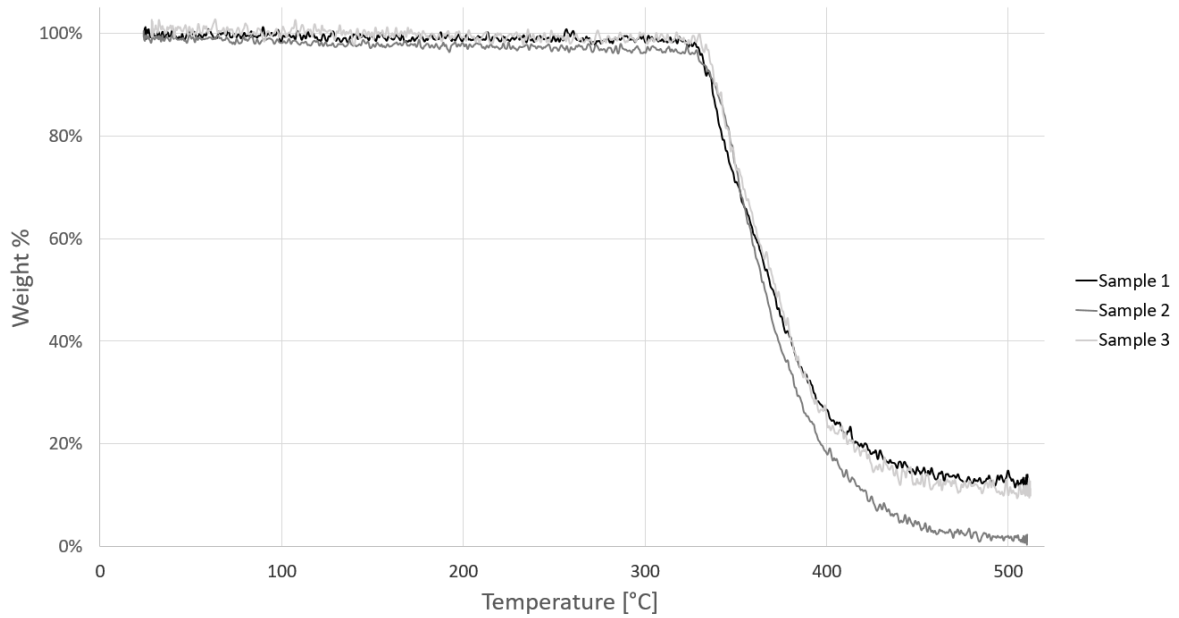


Figure 2.4: % weight loss vs. temperature for Airstone 780E/785H.

Differential Thermal Analysis (DTA) machine. Only TGA data is used in this experiment. Three samples with a mass between 7.5 and 11.6 mg are tested in aluminium pans from room temperature to 500°C with a ramp rate of 10°C/min. Results are shown in Fig. 2.4. It can be seen that at a certain temperature the weight drastically starts to decrease. The degradation temperature is calculated as the onset of this weight reduction. The average degradation temperature of the three samples is 329°C with a standard deviation of 1.3°C. According to ASTM E2550 the results are considered reliable if the standard deviation of the degradation temperature is below 6°C, which means that these results are reliable.

## 2.2.2 Glass transition temperature

During the curing process of epoxy, the  $T_g$  will increase with degree of cure. This can be modelled using the DiBenedetto equation [6, 10, 22, 32, 33]:

$$\frac{T_g - T_{g0}}{T_{g\infty} - T_{g0}} = \frac{\lambda\alpha}{1 - (1 - \lambda)\alpha} \quad (2.5)$$

in which  $T_{g0}$  and  $T_{g\infty}$  are respectively the glass transition temperatures of the uncured and fully cured resins,  $\alpha$  is the degree of cure and  $\lambda$  is a fitting parameter based on experimental results. Experimental data is obtained by partially curing epoxy resin using the Perkin Elmer Pyris Sapphire DSC by heating the sample from 0°C to a set temperature with 1°C/min. The set temperatures are chosen from 50 to 130°C with a step size of 10°C. Then the sample is quickly cooled to 30°C below the expected  $T_g$  value with 50°C/min to ensure no further cure of the resin. The degree of cure of the sample can be calculated using Fig. 2.2. The  $T_g$  of the sample is calculated with a second DSC run by heating from 30°C below the expected  $T_g$  to 30°C above the expected  $T_g$  with a ramp rate of 10°C/min. At  $T_g$ , there will be a stepwise decrease in heatflow. The midpoint of this stepwise decrease is considered as  $T_g$  (Appendix B). This test is performed with three to five samples per set temperature with a mass between 7.5 and 13.8 mg. The average  $T_g$  and standard deviation per degree of cure is shown in Fig. 2.5.  $T_{g0}$  is -55°C and is obtained with the same procedure as described above but without partially curing the sample.  $T_{g\infty}$  is 89°C and is obtained by heating until the end temperature of the resin. The end temperature is the temperature at which no further increase of  $T_g$  will take place. The end temperature is determined at 153°C. When the experimental data is obtained,  $\lambda$  is calculated by minimising the error between the experimental data and the model. With  $\lambda = 0.438$  the error is minimised and the resulting model is visualised as the black line in Fig. 2.5.

## 2.2.3 Specific heat

The specific heat ( $C_p$ ) is the amount of energy required in order to raise the temperature of 1 gram of material with 1 Kelvin.  $C_p$  is determined with a modulated DSC (mDSC) because an mDSC can separate the curing process of epoxy resin from the  $T_g$  transition while with a DSC both events are combined. This can be further described by the heat flow equation of Gray [34]:

$$\frac{dH}{dt} = Cp_s \frac{dT_s}{dt} + \frac{T_p - T_s}{R} \quad (2.6)$$

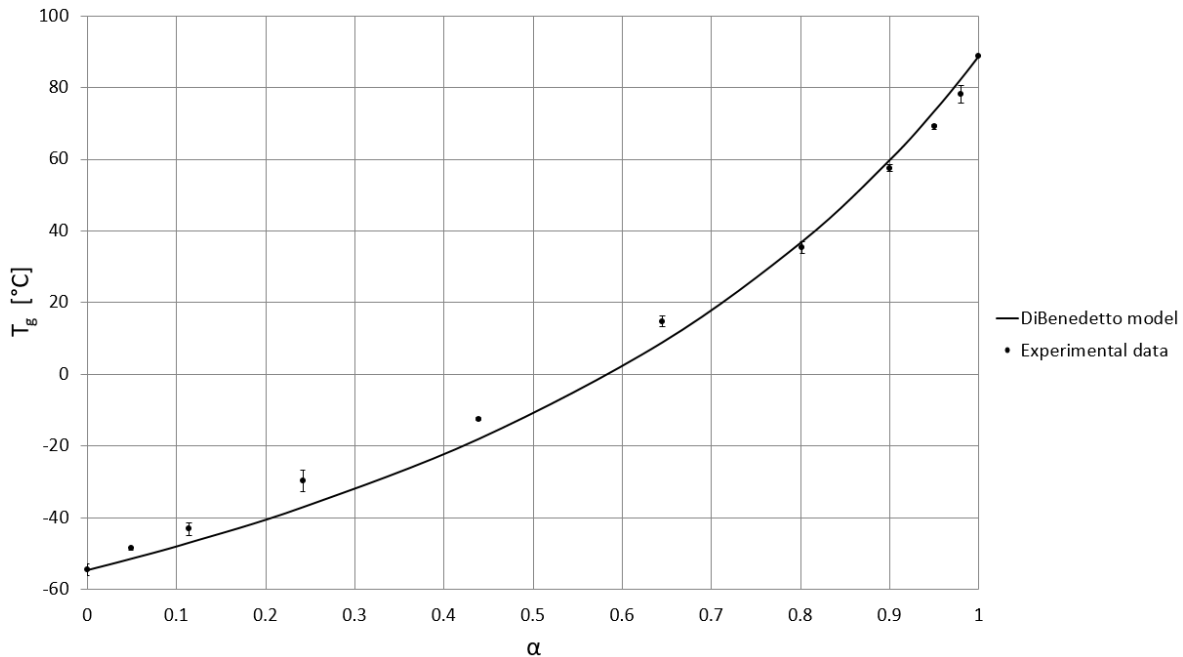
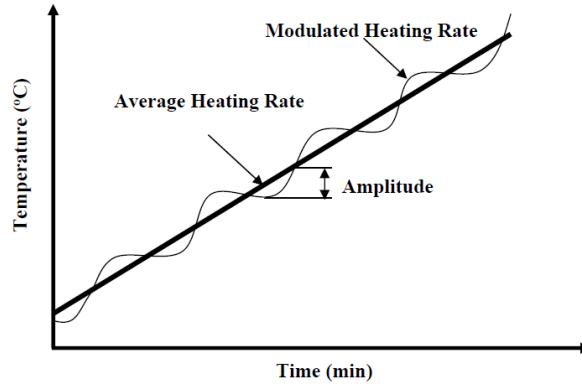


Figure 2.5: DiBenedetto model for Airstone 780E/785H.

in which  $Cp_s$  is the specific heat of the sample and container,  $T_s$  is the temperature of the sample and container,  $T_p$  is the temperature of the energy source and  $R$  is the thermal resistance between the sample and container and the energy source. The first term on the right hand side of Eq. 2.6 describes the energy necessary to raise the temperature of the sample and sensor and the second term describes the heat developed or absorbed by the sample over time and temperature [27]. Because the heat flow ( $dH/dt$ ) measured with a DSC has two contributing terms, the  $C_p$  cannot be directly related to the heat flow. An mDSC is able to isolate these two terms into separate signals which means that kinetic events (second term in Eq. 2.6) can be separated from non-kinetic events (first term in Eq. 2.6) to be able to determine  $C_p$  [27, 29]. This separation is done with a different ramp rate. With a normal DSC a linear ramp rate is used while an mDSC performs both a linear and a modulated ramp rate (Fig. 2.6). With the modulated ramp rate  $dT/dt$  will vary and at some points  $dT/dt = 0$ . This means that the first term on the right hand side of Eq. 2.6 will cancel and  $dH/dt$  will only depend on the second term. By subtraction of the dynamic ramp rate at  $dT/dt = 0$  from the total ramp rate, also the first term on the right hand side of Eq. 2.6 is known. This term is necessary to calculate  $C_p$ .

Two mDSC tests are performed with the TA Instruments DSC Q2000, one at 70°C and one at 90°C with a mass of respectively 7.7 and 7.3 mg. The samples were cooled down to -30°C as quickly as possible and held for 10 minutes at -30°C to create a baseline  $C_p$  at a temperature where almost no reaction takes place. Then the samples are heated to 70°C or 90°C at 20°C/min and a modulation of 1°C/min. The samples were held at the isothermal temperatures respectively 435 and 147 minutes. The  $C_p$  vs. time graph for both tests is visualised in Fig. 2.7.

A model is made for both temperatures according to the model described by Struzziero and Skordos [4]:



**Figure 2.6:** Modulated ramp rate DSC, figure from [27].

**Table 2.4:** Constants used in  $C_p$  model for Airstone 780E/785H.

Parameter	Value	Unit
$A_{C_p}$	0.008833	$Jg^{-1}C^{-2}$
$B_{C_p}$	0.308906	$Jg^{-1}C^{-2}$
$\Delta_{C_p}$	-0.34372	$Jg^{-1}C^{-2}$
$C_{C_p}$	0.585234	$^{\circ}C^{-1}$
$\sigma$	13.79599	$^{\circ}C$

$$C_p = A_{C_p}T + B_{C_p} + \frac{\Delta_{C_p}}{1 + e^{C_{C_p}(T-T_g-\sigma)}} \quad (2.7)$$

in which the constants  $A_{C_p}$  and  $B_{C_p}$  describe the linear relation of  $C_p$  of uncured resin on temperature.  $\Delta_{C_p}$ ,  $C_{C_p}$  and  $\sigma$  are constants describing respectively the strength, width and temperature shift of the step reduction in  $C_p$  during  $T_g$  transition. The constants are reported in Table 2.4 and the model is visualised in Fig. 2.7.

During the mDSC tests the epoxy resin will cure. For the test at  $70^{\circ}C$  the  $C_p$  will have a step reduction during vitrification as  $T_{g\infty}$  is  $89^{\circ}C$ . For the test at  $90^{\circ}C$  there is no step reduction in  $C_p$  because the curing temperature is always above  $T_g$  and thus no vitrification takes place.

## 2.3 Thermo-mechanical characterisation

Testing mechanical properties requires the use of solid materials. Therefore, the epoxy resin must be cured until the gel point of the resin to perform thermo-mechanical characterisation. To determine if a relation exists between degree of cure and the mechanical properties, four samples are manufactured with different degrees of cure. Uncured epoxy resin is poured in an aluminium mould with inner dimensions  $170 \times 110 \times 2.5$  mm (Fig. 2.8) and cured in an oven. A thermocouple is located in the epoxy resin. The aim is to obtain samples with  $\alpha = 0.65$ ,  $\alpha = 0.75$ ,  $\alpha = 0.85$  and  $\alpha = 0.95$ . The different degrees of cure are obtained with

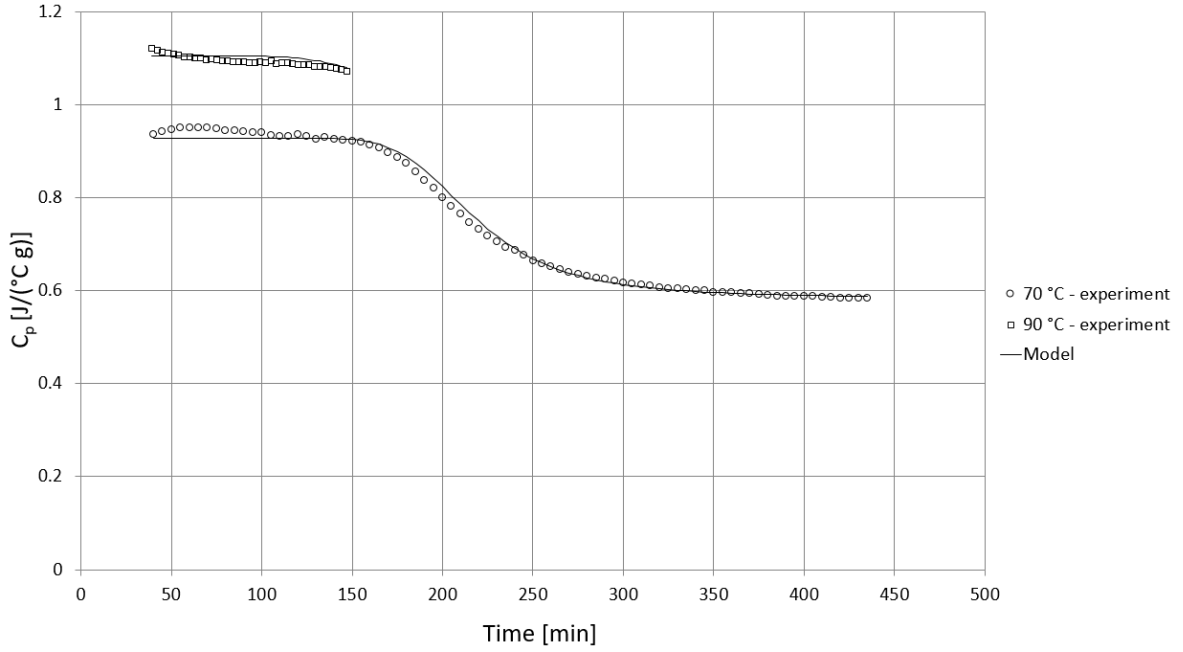


**Figure 2.7:**  $C_p$  determined with mDSC for Airstone 780E/785H.

**Table 2.5:** Samples mechanical characterisation.

$\alpha$	Cure temperature [°C]	Cure time [min]
0.71	70	45
0.78	70	95
0.82	70	255
0.94	110	135

cure cycles determined with the cure kinetics model (2.1.2). The cure cycles used and the final degree of cure obtained per sample are stated in Table 2.5. The final degree of cure is calculated with the thermal history of the resin using data of the thermocouples. It can be seen that the aimed degrees of cure differs 1 – 6% from the final degrees of cure but the final degrees of cure are spread enough to continue. After the samples are cured they are cut into the correct dimensions for mechanical characterisation with the Struers Secotom-10 cut-off machine. With these samples, mechanical tests are performed to determine the elastic modulus (2.3.1), CTE (2.3.2) and density (2.3.3) of the four samples with different degrees of cure. With the difference in volume between cured and uncured samples the amount of cure shrinkage can be calculated (2.3.4).

### 2.3.1 Elastic modulus

The elastic modulus for four degrees of cure is determined with the Perkin Elmer Dynamic Mechanical Analyser (DMA) which measures the material's response during an oscillating

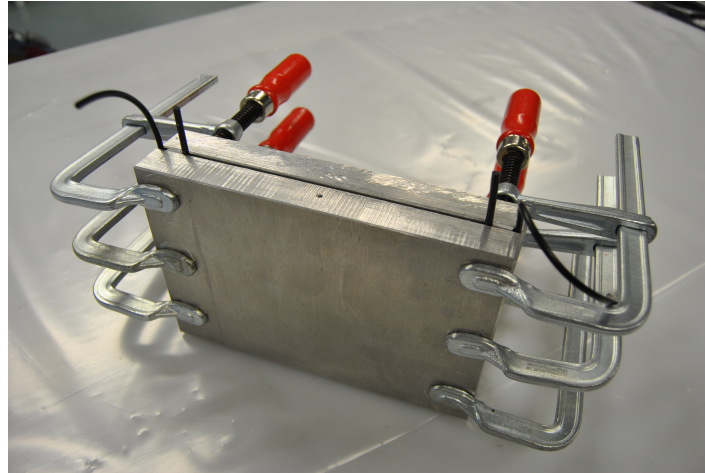


**Figure 2.8:** Mould for epoxy samples.

stress. For this test the material is tested in a 3-point bending mode according to ASTM D4065-01. The 3-point bending mode is used as this mode does not take into account any clamping effects and thus measures pure bending instead of bending + extension as with the single- or double cantilever mode [35]. The sample size is 50 x 10 x 2.5 mm and two samples are tested per degree of cure for repeatability. The sample is heated from  $-50$  to  $210^{\circ}\text{C}$  with a ramp rate of  $2^{\circ}\text{C}/\text{min}$ . This ramp rate will give accurate results as the temperature difference between sample and oven is minimised while keeping the testing time acceptable. Five different frequencies are tested per sample: 0.2 Hz, 1 Hz, 5 Hz, 10 Hz and 20 Hz. The DMA measures storage and loss modulus and calculates  $\tan(\delta)$ . Only storage modulus ( $E'$ ) is used in this report as this relates to the Young's modulus when the material is in its elastic region. The storage modulus for each frequency with  $\alpha = 0.94$  is shown in Fig. 2.9.  $T_g$  is defined as the onset of the drop in storage modulus. What can be seen is that a higher frequency results in a higher  $T_g$  [35, 36]. This conclusion is similar for the other degrees of cure. The storage modulus for all degrees of cure with a frequency of 1 Hz is plotted in Fig. 2.10. 1 Hz is typically used for  $T_g$  calculation [36]. The  $T_g$  will increase with increasing degree of cure. Above  $T_g$  the partially cured samples will cure and will eventually end at the same storage modulus in the rubbery state. The average storage modulus from the two samples at room temperature ( $20^{\circ}\text{C}$ ) for all frequencies and degrees of cure is plotted in Fig. 2.11. Significance is tested with the Kruskal-Wallis test in SPSS as the data is not normal distributed. Although there is no significant difference between the storage modulus at different frequencies and degrees of cure, it can be seen that the storage modulus at room temperature will increase with increasing frequency. However, since there is no significant difference between the samples, an average is taken from all degrees of cure and frequencies. The average storage modulus at  $20^{\circ}\text{C}$  is 4.50 GPa with a standard deviation of 0.28 GPa. All samples will eventually reach the maximum degree of cure in this test as the samples are heated to  $210^{\circ}\text{C}$ . Therefore the storage modulus above  $T_g$  is only calculated for  $\alpha = 0.94$ . Again the storage modulus will increase with increasing frequency but no significant difference is found. The average storage modulus above  $T_g$  at  $213^{\circ}\text{C}$  is 48.24 MPa with a standard deviation of 1.79 MPa.

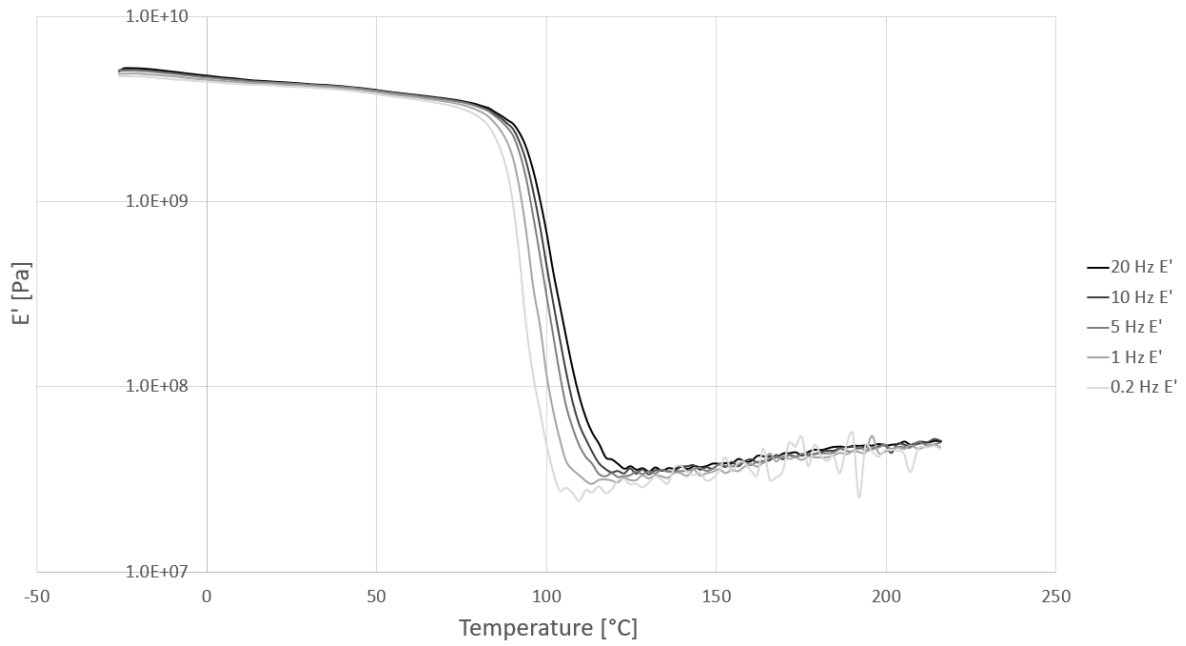


Figure 2.9: Storage modulus with  $\alpha = 0.94$  for Airstone 780E/785H.

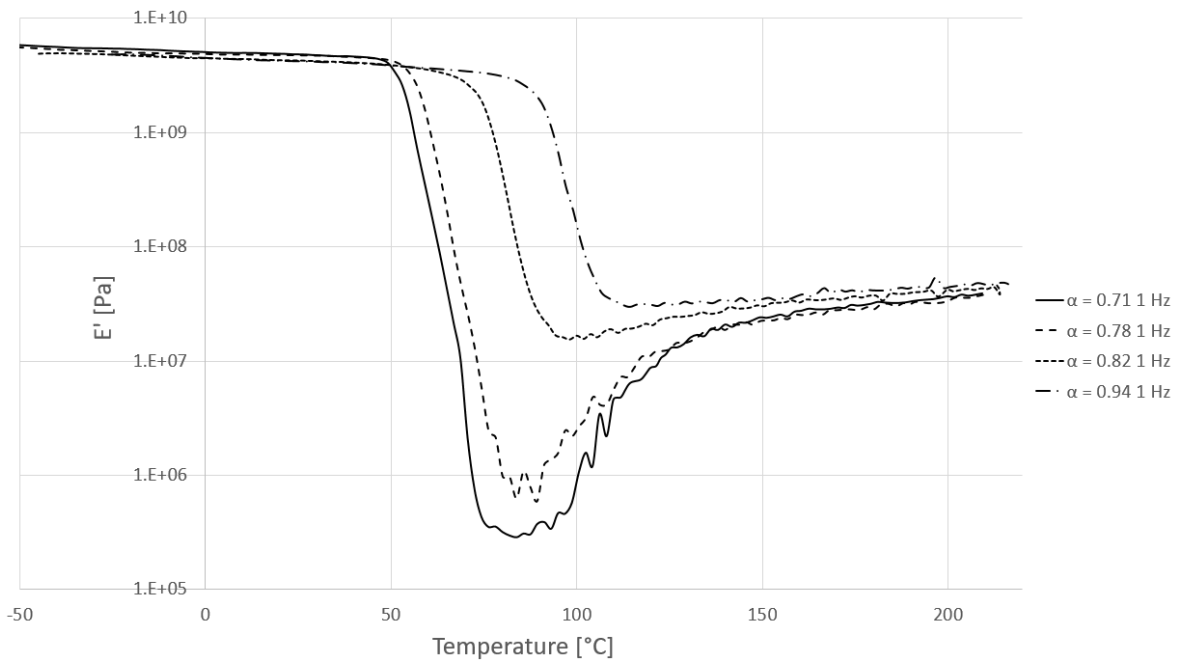


Figure 2.10: Storage modulus with 1 Hz for Airstone 780E/785H.

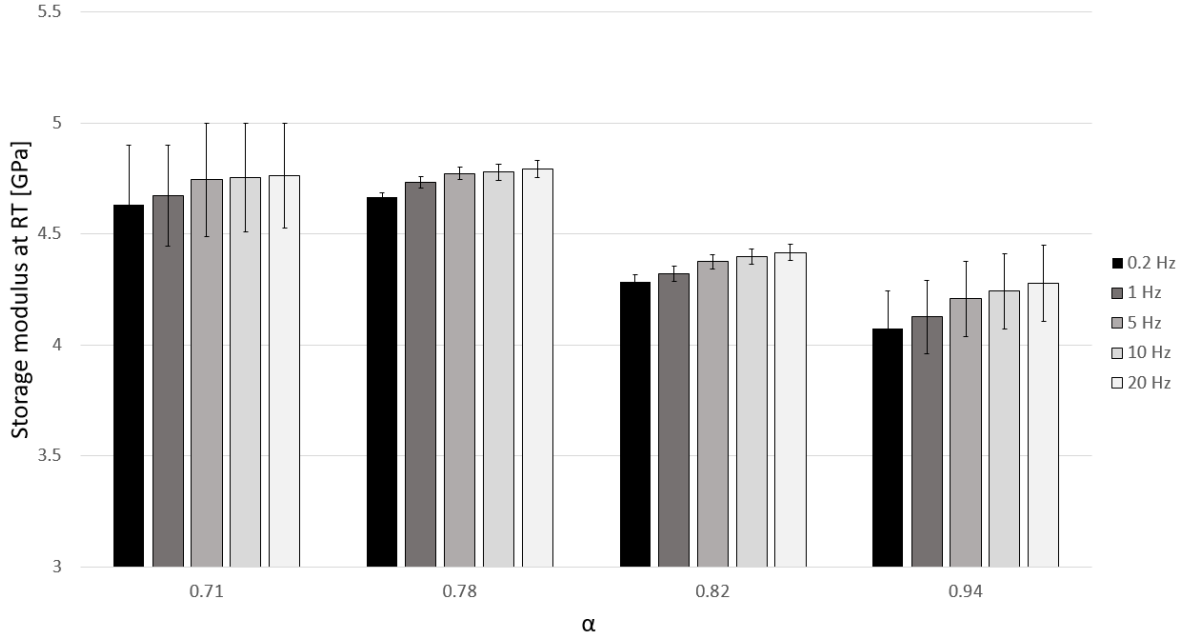


Figure 2.11: Storage modulus at room temperature for Airstone 780E/785H.

### 2.3.2 Coefficient of thermal expansion

The CTE is determined with the Perkin Elmer Thermomechanical Analyser (TMA) which measures the expansion of the sample by changing temperature. It is executed according to ASTM E831-14. The samples with different degrees of cure are tested in a temperature range of  $-50$  to  $170^{\circ}\text{C}$  with a heating/cooling rate of  $5^{\circ}\text{C}/\text{min}$ . The sample size is  $5 \times 5 \times 2.5$  mm. A typical probe position vs. temperature graph is shown in Fig. 2.12. CTE is calculated in a linear range of the probe position vs. temperature graph according to:

$$CTE = \frac{\Delta L}{L \cdot \Delta T} \quad (2.8)$$

in which  $\Delta L$  and  $\Delta T$  are respectively the probe position and temperature range in which CTE is calculated and  $L$  is the initial length at room temperature. Fig. 2.12 can be divided into 7 zones. First the sample is cooled from room temperature to  $-60^{\circ}\text{C}$  (1). Then the sample is heated to  $170^{\circ}\text{C}$  (2–4). Zone 2 indicates the CTE below  $T_g$ , zone 3 shows the glass transition and zone 4 illustrates the CTE above  $T_g$ . Then the sample is cooled again whereby zone 5 shows the CTE above  $T_g$ , zone 6 indicates the glass transition and zone 7 illustrates the CTE below  $T_g$ . As this test is performed with samples that are partially cured, the samples will post-cure during the test. Cure shrinkage of the resin is linearly related with degree of cure and cure shrinkage happens until the resin is fully cured [36, 37]. Therefore the resin will shrink during post-cure and the probe position vs. temperature graph will not be linear. CTE will be equal during heating and cooling in the same temperature range and therefore zone 1 is used to calculate  $CTE_{glass}$  for every degree of cure to minimise the effect of cure shrinkage on the CTE calculation. To determine  $CTE_{rubber}$  zone 5 is used as it is assumed that the resin is fully cured after reaching  $170^{\circ}\text{C}$  and the material will not experience cure

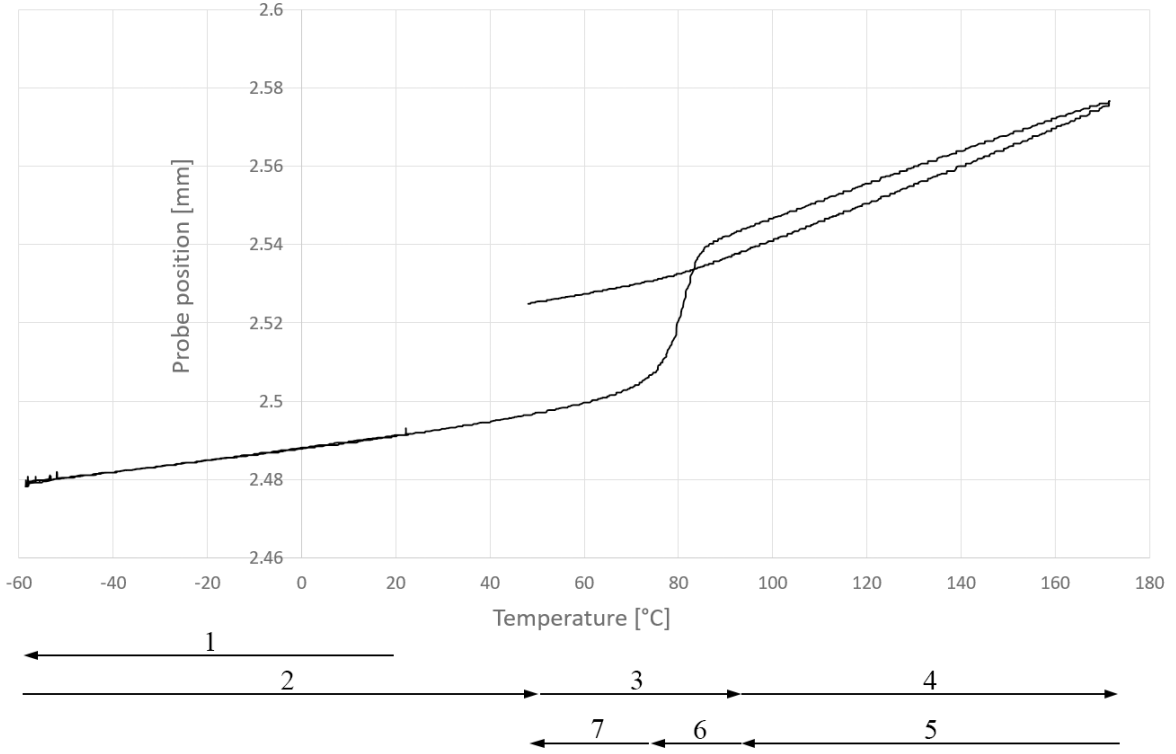


**Figure 2.12:** Typical probe position vs. temperature graph for Airstone 780E/785H.

shrinkage during cooling. As the samples are fully cured in zone 5 it is impossible to measure  $CTE_{rubber}$  for partially cured samples in this test.

CTE is expected to be constant below and above  $T_g$ , whereby  $CTE_{glass} < CTE_{rubber}$  [36]. However, some tests show a constant probe position with increasing temperature ( $CTE = 0$ ) at low temperatures (Appendix C). As this happens randomly and  $CTE = 0$  is physically not possible with this resin system, these results are removed from the data. 3 to 8 samples are tested per degree of cure and  $CTE_{glass}$  and  $CTE_{rubber}$  are calculated as described above. The results of  $CTE_{glass}$  per degree of cure are shown in Table 2.6. It can be seen that there is no relation between degree of cure and  $CTE_{glass}$ . This is confirmed by using a one-way ANOVA test in SPSS. Also Jansen et al. [38] and Khoun et al. [10] found the same conclusion. The average CTE in the glassy state is  $CTE_{glass} = 24.01 \mu m/(m^\circ C)$  with a standard deviation of  $2.22 \mu m/(m^\circ C)$ . In the rubbery state it is only possible to calculate  $CTE_{rubber}$  of fully cured samples. The average CTE in rubbery state is  $CTE_{rubber} = 71.42 \mu m/(m^\circ C)$  with a standard deviation of  $4.80 \mu m/(m^\circ C)$ .

**Table 2.6:** CTE<sub>glass</sub> per degree of cure for Airstone 780E/785H.

$\alpha$	CTE <sub>glass</sub> [ $\mu m/(m^\circ C)$ ]	Standard deviation [ $\mu m/(m^\circ C)$ ]
0.71	23.84	0.75
0.78	24.24	0.32
0.82	23.54	0.89
0.94	24.41	1.02
Average	24.01	2.22

**Table 2.7:** Density per degree of cure for Airstone 780E/785H.

$\alpha$	Density [ $g/cm^3$ ]	Standard deviation [ $g/cm^3$ ]
0.71	1.1579	0.0002
0.78	1.1574	0.0002
0.82	1.1565	0.0001
0.94	1.1566	0.0003

### 2.3.3 Density resin

The resin density of the four samples with different degrees of cure is calculated with the Archimedes' principle according to ASTM D792-13. By measuring the sample weight in air and in liquid, the density can be obtained according to:

$$\rho = \frac{A}{A - B}(\rho_0 - \rho_L) + \rho_L \quad (2.9)$$

in which  $A$  and  $B$  are respectively the weight of the sample in air and in liquid,  $\rho_0$  is the density of the liquid which is adjusted to the temperature of the liquid and  $\rho_L$  is the density of air ( $0.0012 g/cm^3$ ). The liquid used in this experiment is ethanol as the sample density is too close to water to test the sample in water. Four samples per degree of cure with a sample size of 25 x 25 x 2.5 mm are tested and the results are shown in Table 2.7.

A one-way ANOVA in SPSS indicates that there is no significant difference in density between  $\alpha = 0.71$  and  $\alpha = 0.78$  and between  $\alpha = 0.82$  and  $\alpha = 0.94$ . There is a significant difference in density between  $\alpha = 0.78$  and  $\alpha = 0.82$ . However, a trend in the results is identified that concludes that density will decrease with increasing degree of cure. This conclusion is confirmed by experiments of Fisch et al. [39] and Pang and Gillham [40]. Pang and Gillham [40] determined the density of partially cured epoxy at room temperature. They used  $T_g$  as a measure of degree of cure and found that the density experiences a peak by increasing  $T_g$  (Fig. 2.13). This peak occurs around  $T_{gel}$  of the resin. The initial increase in density is the result of cure shrinkage of the resin. The decrease in density above  $T_g$  is caused by two mechanisms [40]:

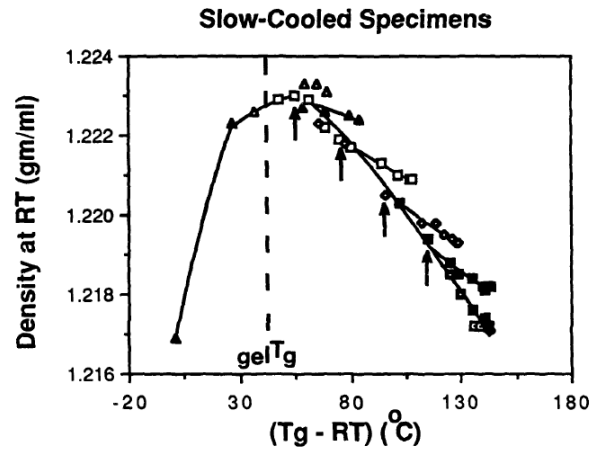
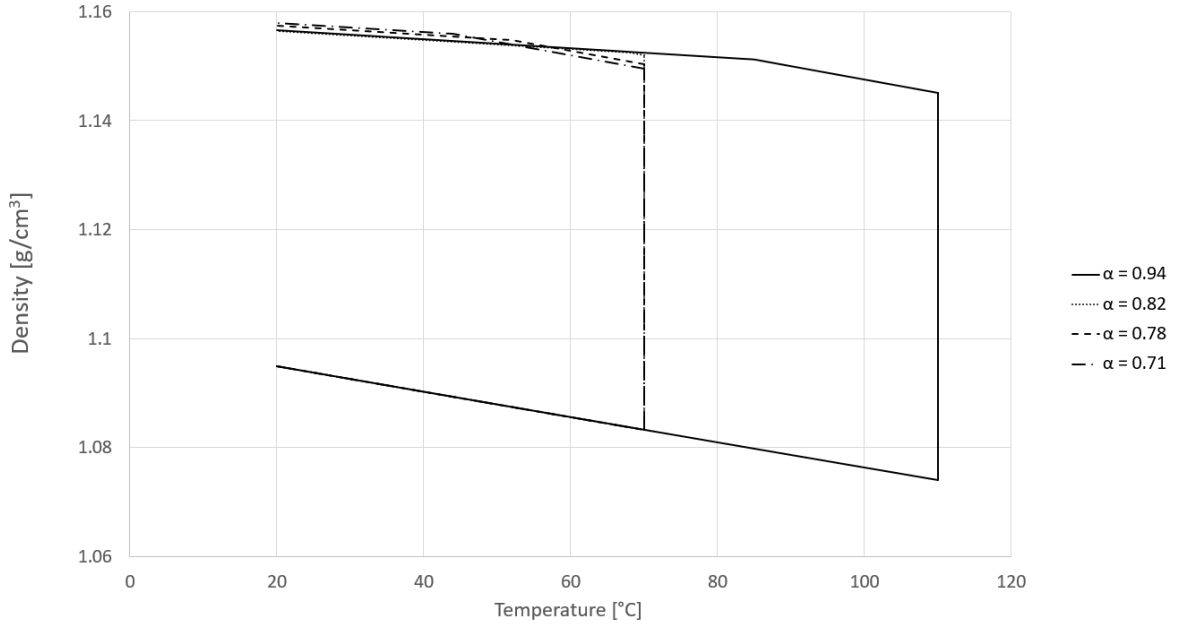


Figure 2.13: Density vs.  $T_g$ . Figure from Pang and Gillham [40].

- Materials with a higher degree of cure have a higher crosslink density and higher  $T_g$ . Materials with a higher crosslink density will relax less during cooling than materials with a lower crosslink density because the polymer chains are more constrained.
- As discussed in paragraph 2.3.2,  $CTE_{glass} < CTE_{rubber}$ . Materials with a lower  $T_g$  will experience more cooling during  $CTE_{rubber}$  than materials with a higher  $T_g$ . Therefore materials with a lower  $T_g$  will contract more during cooling and will end up with a higher density than materials with a higher  $T_g$ .

The latter can be further explained by looking at the change in density during the cure cycle of the four epoxy samples (Fig. 2.14) [39]. The initial density of the uncured epoxy resin is calculated with the volumetric mixing ratio of resin and hardener according to the data sheet. 100 parts of resin with a density of  $1.15 \text{ g/cm}^3$  mixed with 38 parts of hardener with a density of  $0.95 \text{ g/cm}^3$  results in a density of  $1.0949 \text{ g/cm}^3$ . The samples are cured according to the cure cycles described in Table 2.5. First the samples are heated towards the cure temperature. The density will decrease as the material will expand during heating.  $CTE_{rubber}$  is used as the uncured resin has a  $T_g$  of  $-55^\circ\text{C}$ . During cure the resin will shrink and the density will increase. The higher the degree of cure the higher the amount of cure shrinkage [37]. Then the material contracts during cooling according to  $CTE_{rubber}$  above  $T_g$  and  $CTE_{glass}$  below  $T_g$ . It can be seen that, for the samples cured at  $70^\circ\text{C}$ , the lower the degree of cure, the more the material contracts during  $CTE_{rubber}$ . Therefore, a higher degree of cure results in a lower density. This graph is an idealized representation of the change in density during cure. However, in practice cure shrinkage will already happen during heat up.



**Figure 2.14:** Density vs. temperature for Airstone 780E/785H.

### 2.3.4 Cure shrinkage

Cure shrinkage is measured as the difference in volume between fully uncured and cured samples at room temperature according to [11]:

$$Shrinkage = \frac{V_{cured} - V_{uncured}}{V_{uncured}} \quad (2.10)$$

in which  $V$  represents the volume of the resin. Eq. 2.10 is rewritten in terms of density according to:

$$V = \frac{m}{\rho} \quad (2.11)$$

to get:

$$Shrinkage = \frac{\rho_{uncured}}{\rho_{cured}} - 1 \quad (2.12)$$

in which  $m$  and  $\rho$  are respectively the mass and density of the resin.  $\rho_{cured}$  is calculated using  $\rho_{\alpha=0.94} = 1.1566 \text{ g/cm}^3$  and  $\rho_{uncured} = 1.0949 \text{ g/cm}^3$ . The amount of shrinkage is 5.3%.

---

## Chapter 3

---

# Methodology

Chapter 2 described the influences of temperature and degree of cure on the thermophysical properties of the resin. Now the thermophysical properties of the resin are known, this information can be used to describe the curing behaviour of a composite laminate. Ten laminates are manufactured with vacuum infusion and cured according to different cure cycles (3.1). Each laminate can be divided into nine sub-laminates of which three are selected for mechanical testing (3.2).

### 3.1 Vacuum infusion

Vacuum infusion is a manufacturing technique that uses a solid mould on one side and a disposable vacuum bag on the other side of the composite. Between the mould and the bag layers of dry glass fibre are stacked in different directions (3.1.1). After the vacuum bag is applied the dry fibres are infused with resin (3.1.2). When the laminate is infused it is cured in the oven according to different cure cycles (3.1.3).

#### 3.1.1 Layup

A schematic overview of the layup for the vacuum infusion is shown in Fig. 3.1.

##### **Mould**

The mould used in this project is a 2 mm thick flat aluminium plate. The plate is treated with Marbocote 227 release agent before every use to prevent that the laminate will adhere to the mould. The edges of the plate are covered during the Marbocoat treatment to ensure good adhesion of the tacky tape. Cytac LTS 90B tacky tape is applied on the edge of the plate to attach the vacuum bag to the plate. A second mould is used on top of the vacuum bag to ensure symmetric heat transport. This second mould is applied after infusion to keep track of the infusion speed.

##### **Infusion mesh**

The infusion mesh will transport the resin from the inlet to the fibres. Airtech greenflow 75

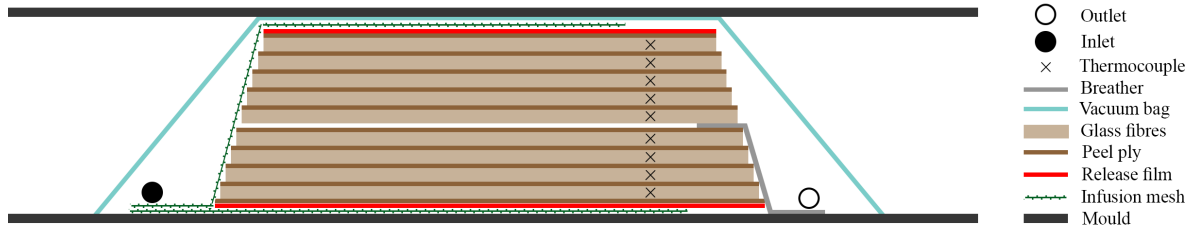


Figure 3.1: Vacuum infusion layup.

is used on top and on the bottom of the fibres for symmetry and to ensure full wetting of the fibres. On all sides except the inlet side, the infusion mesh is 100 mm shorter than the fibres to allow the resin to penetrate through the thickness.

### Release film

The Airtech WL3900RP perforated release film is used to separate the infusion mesh and the peel ply layer to allow easy separation after infusion.

### Peel ply

A peel ply layer with PTFE coating (Airtech release ease 234 TFP) allows easy separation of the sub-laminates after infusion. It is applied between every sub-laminate and between the release film and the first and last sub-laminate to ensure the same surface finish for all sub-laminates.

### Fibres

The reinforcement used in this project is the non-crimp biaxial glass fibre fabric from Saertex with  $812g/m^2$  and the NEG 2001/2002 sizing. The layers of  $45/-45^\circ$  are stitched together in  $0^\circ$  and  $90^\circ$  direction. Six layers are used per sub-laminate to comply with the test standards for mechanical testing. To create a laminate of about 30 mm thick, 9 sub-laminates are made. This means that each sub-laminate is 3.5 mm thick and the total laminate thickness is 31.5 mm with 54 glass fibre layers. The layup of every sub-laminate is  $[45, -45]_{3s}$ , which makes the layup of both the sub-laminates and the total laminate symmetric. This is done by flipping the top three glass fibre layers of every sub-laminate and rotate these layers by  $90^\circ$ . Every sub-laminate is equipped with a k-type thermocouple located halfway the thickness of the sub-laminate, about 100 mm from the outlet side and halfway the width and measures the temperature every 30 seconds. One thermocouple is located in the oven. The first sub-laminate from the lower mould has a length and width of 500 mm. The size of the sub-laminates decreases towards the top with 10 mm per sub-laminate such that the top sub-laminate has a length and width of 420 mm. This is done to prevent resin runners on the edge of the laminate because the vacuum bag cannot follow the steep thickness increase of the laminate. Two pieces of Airweave N10 breather of 50 mm wide are located on the outlet side between sub-laminate 4 and 5 about 10 mm inside the fibres to allow resin flow from the laminate towards the outlet. As the resin flows from the top infusion mesh downwards and from the bottom infusion mesh upwards, the resin will arrive at the breather when the laminate is completely infused.

### Vacuum bag

The Airtech Wrightlon 8400 nylon film is used to create a vacuum bag. The bag is attached to the tacky tape that was applied on the edge of the lower mould.

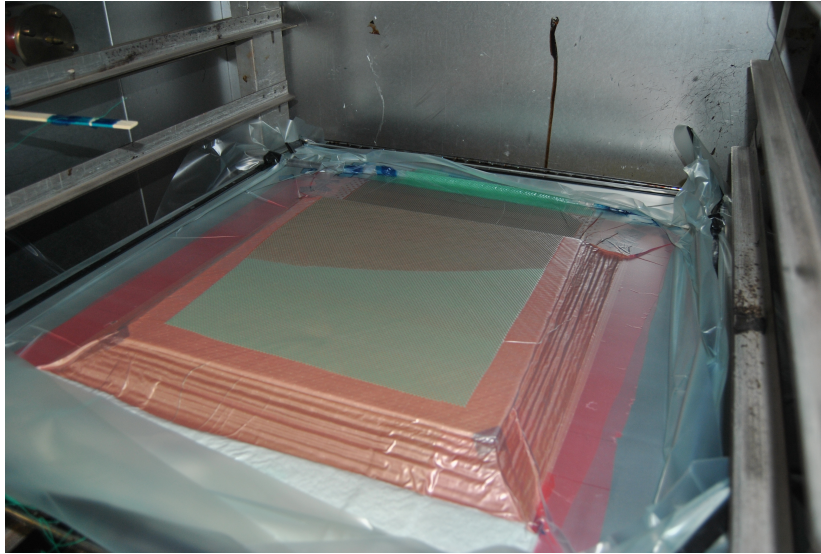


Figure 3.2: Infusion.

### 3.1.2 Infusion

The infusion of the glass fibre laminate will take place in the oven at room temperature to maintain vacuum during infusion and curing (Fig. 3.2). The bucket of resin is connected to the inlet tube which is connected to the infusion mesh. The outlet, which lays on top of the breather, is connected to the vacuum pump. During infusion the pressure difference between inlet and outlet will be 950 mbar. After infusion the inlet is closed and the pressure will be increased to 500 mbar according to industry standards. For the infusion a total of 6 litres of resin system is made. The resin is degassed for 20 minutes before infusion to reduce the amount of air bubbles. The laminates were infused in 98 – 130 minutes.

### 3.1.3 Cure cycles

After infusion the oven (Vötsch VTL 100/150) is closed and the cure cycle starts. Every laminate has experienced a different cure cycle (CC), specified in Table 3.1 and Fig. 3.4. The MRCC is a one-dwell cure cycle with a ramp rate of 20°C/hour up to 70°C. All other cure cycles are two-dwell cure cycles, as this results in lower residual stresses and a reduced cycle time compared to a one-dwell cure cycle, but a three-dwell cure cycle will not give a considerable improvement compared to a two-dwell cure cycle according to the literature described in paragraph 1.2.4. Literature also revealed that adding a cooling stage in between the two dwells will decrease the residual stresses. However, this will result in too many variables and will not be feasible in the given amount of time. Therefore, a two-dwell cure cycle is chosen. In a two-dwell cure cycle eight variables can be distinguished (Fig. 3.3): 1) the starting temperature, 2) the ramp rate to the first dwell, 3) the temperature of the first dwell, 4) the time of the first dwell, 5) the ramp rate to the second dwell, 6) the temperature of the second dwell, 7) the time of the second dwell and 8) the cooling rate. To minimise the amount of variables the starting temperature will be the same as the outside air temperature and the two ramps will have equal ramp rate. The time of the second dwell is set to 400

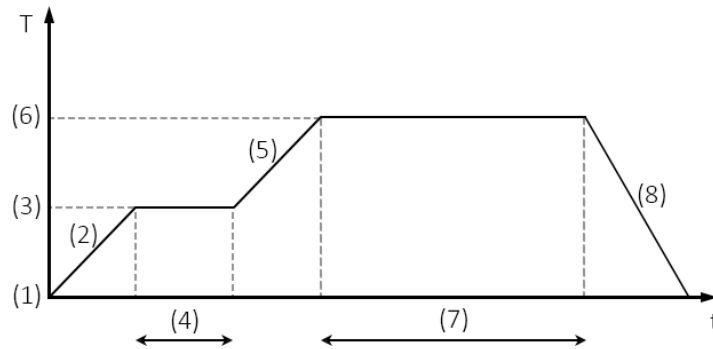


**Figure 3.3:** Typical two dwell cure cycle.

minutes to make sure that all laminates are fully cured. Later, the time to reach a fully cured laminate can be determined with the cure kinetics model in order to compare the curing time for different cure cycles. After the second dwell, heating is stopped and the oven will slowly cool down to outside air temperature. No cooling is applied. The remaining variables are first dwell temperature, first dwell time, ramp rate and second dwell temperature.

Cure cycle 2 functions as a baseline cure cycle and every other cure cycle differs with only 1 parameter from the baseline cure cycle. The values of the parameters are based on the literature study on cure cycle optimisation (paragraph 1.2.4) and industry standards. For example, for the second dwell temperature three temperatures are chosen: 70, 80 and 100°C. 70°C is chosen as it is the same as the MRCC to determine if adding a second dwell to the MRCC will influence the mechanical properties. 80°C and 100°C are chosen as they represent temperatures below and above  $T_g$  to determine the influence of curing above  $T_g$  on the mechanical properties. The first dwell temperatures are chosen in between outside air temperature and the second dwell temperature of 70°C and the first dwell times and ramp rates are based on literature. The laminates will not be subjected to a post-cure cycle as this will relax the residual stresses in the laminates which makes comparison more difficult.

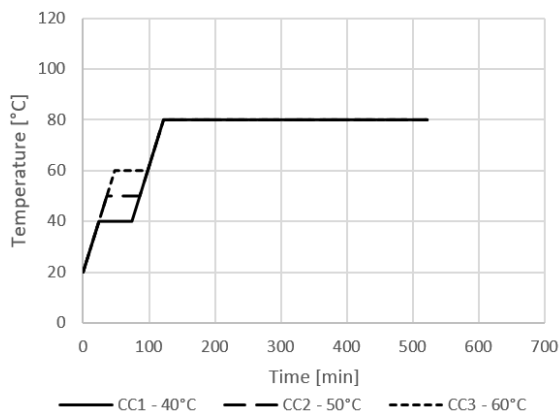
## 3.2 Mechanical testing

After curing the laminate is separated into the nine sub-laminates using a chisel and a hammer on the sides of the laminate. The sub-laminates are labelled from A to I from bottom to top (Fig. 3.5). As the layup of the laminate is symmetric and heating is applied all around, it is assumed that the through-thickness temperature distribution is symmetric. Therefore, only the sub-laminates A, C and E are selected for mechanical testing. The three sub-laminates are bonded together with double-sided tape and then the edges are cut such that the three sub-laminates have equal dimensions (440 x 440 mm). Then samples are cut with the Proth 3060AH with a diamond cutting blade according to Fig. 3.6. In Fig. 3.6 the infusion direction is always from top to bottom. The edges of the laminate (95 mm) are cut to avoid edge effects and it is assumed that the temperature is uniform in longitudinal and lateral direction in the area that is selected for testing.

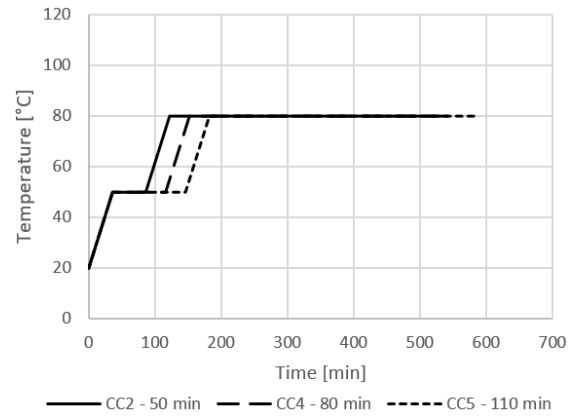
The density and volume fractions of two laminates are tested to determine if the resin is uniformly infused through the thickness (3.2.1). Literature described that residual stress mainly influences the compression and shear strength of the laminates (1.2.3). However,

**Table 3.1:** Cure cycles.

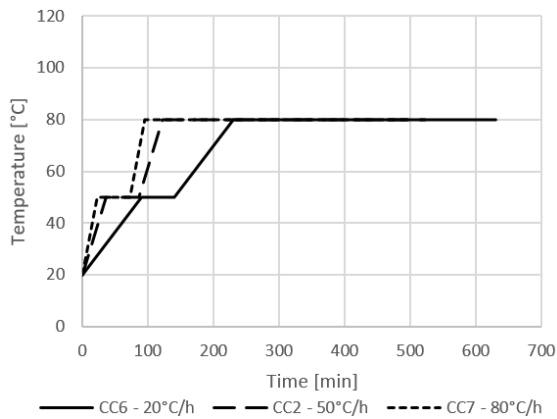
Cure cycle	First dwell temperature (°C)	First dwell time (min)	Ramp rate (°C/hour)	Second dwell temperature (°C)	Second dwell time (min)
MRCC	70	240	20		
1	40	50	50	80	400
2	50	50	50	80	400
3	60	50	50	80	400
4	50	80	50	80	400
5	50	110	50	80	400
6	50	50	20	80	400
7	50	50	80	80	400
8	50	50	50	70	400
9	50	50	50	100	400



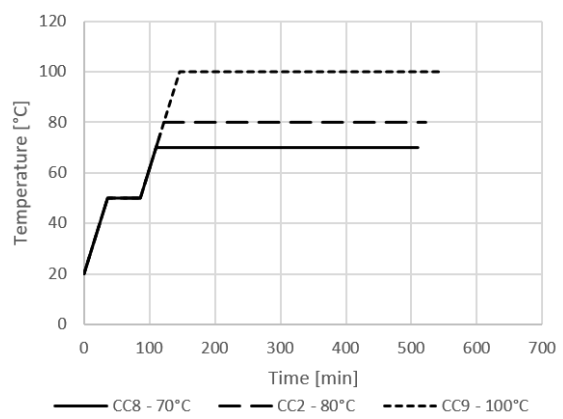
**(a)** Varying the first dwell temperature.



**(b)** Varying the first dwell time.



**(c)** Varying the ramp rate.



**(d)** Varying the second dwell temperature.

**Figure 3.4:** Two-dwell cure cycles.

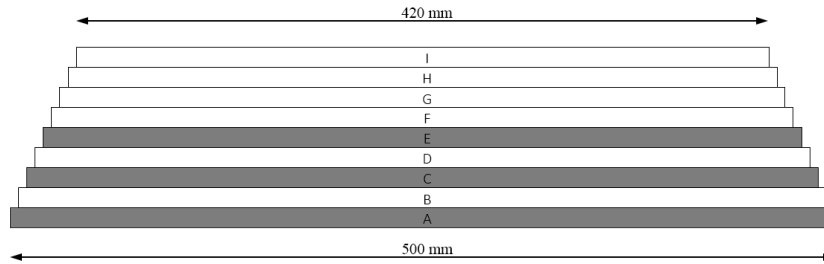


**Figure 3.5:** Labels used for sub-laminates. The grey sub-laminates are used for mechanical testing.

performing compression tests is very difficult and time consuming as the fibres must be perfectly aligned with the test direction. Therefore it is chosen to perform two types of shear strength tests: in-plane shear test (ASTM D3518/D3518M)(3.2.2) and interlaminar shear test, also known as short-beam test (ASTM D2344) (3.2.3). Where possible, the results are statistically compared with IBM SPSS to test significance. A significance level of 95% is used. A one-way ANOVA will indicate the significance when the data is normal distributed and the Kruskal Wallis test is used when the data is not normal distributed. Normality is tested with the Shapiro wilk test. A post-hoc test will individually the compare data. The post-hoc test Tukey is used when there is homogeneity of variances and Games-Howell is used when there is no homogeneity of variances.

### 3.2.1 Density and volume fraction

For two laminates density/volume fraction samples are cut for all nine sub-laminates to determine if there is a difference in density and volume fractions through the thickness. The volume fractions that are tested are fibre volume fraction (FVF), matrix volume fraction (MVF) and void volume fraction (VVF). It is made sure that all samples are cut at the same longitudinal and lateral position in the laminate. The same samples can be used for the density test and the volume fraction test. The density test is performed according to ASTM D792 and the volume fraction test according to D3171 procedure G. Four samples are cut with dimensions 20 x 10 mm.

### 3.2.2 In-plane shear test

For the in-plane shear test, ASTM D3518/D3518M prescribes samples of dimension 25 x 250 mm in  $\pm 45$  direction. Six samples are cut to meet the requirement of a minimum of five samples. The Zwick 20kN is used to apply and measure the force on the sample. No tabs are applied on the samples. Digital Image Correlation (DIC) with a sampling rate of 0.2Hz is used to measure the strain during testing. As there is no expected difference in strain along the sample, an average will be taken from a rectangle according to Fig. 3.7.

Two acoustic emission (AE) sensors are applied during testing to measure the AE activity. As described in paragraph 1.2.3, residual stress in fibre reinforced composites causes, among others, more matrix cracking, fibre-matrix debonding and delaminations than composites without residual stress. The amount of residual stress is altered by changing the cure cycle

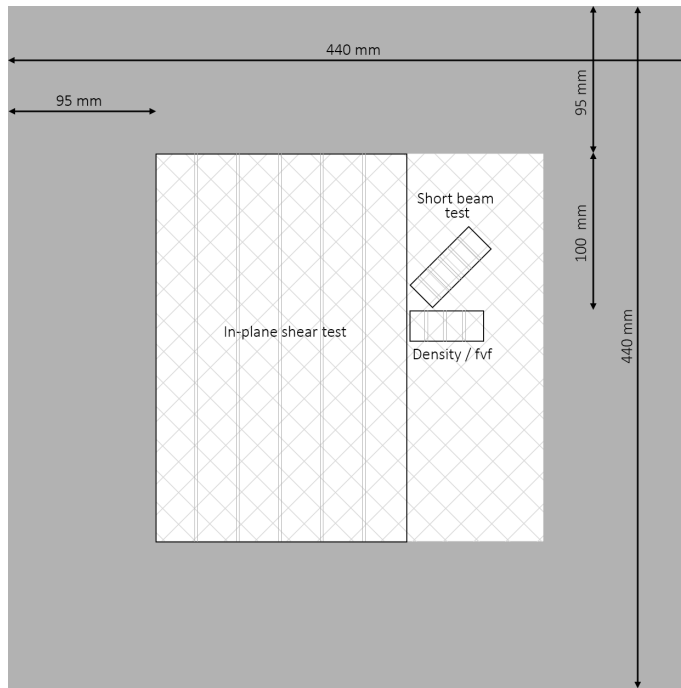


**Figure 3.6:** Geometry mechanical testing.

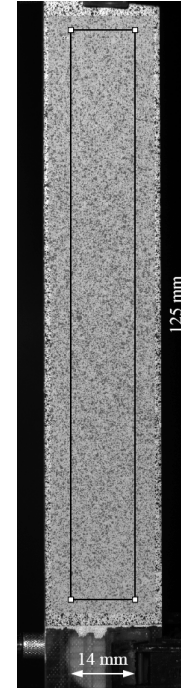


**Figure 3.7:** Selected region for DIC measurements.

parameters of the cure cycle. Although the amount of residual stress is unknown, the amount of defects due to the manufacturing process can be quantified by using the AE system [41,42]. The AE sensors detect acoustic events caused by the defects described before. An acoustic event is called a hit. In this research, the AE system is used to compare the number of hits at a certain load between samples that have seen different cure cycles to determine the influence of different cure cycles on the amount of defects in the composite laminates. The AMSY-6 (Vallen Systeme GmbH, Icking, Germany), 8 channel AE system is used during the in-plane shear test. Two wide-band piezoelectric sensors (VS900M) with an external 34 dB pre-amplifier are attached approximately 75 mm above and below the horizontal centreline of the specimen with ultrasonic coupling gel and a clamping device. The AE system continuously measures the AE activity with a sampling rate of 2 MHz until failure of the specimen.

### 3.2.3 Short-beam test

For the short-beam test, ASTM D2344 prescribes a length of 6 x thickness and a width of 2 x thickness. It also prescribes that there are at least 10% 0° fibres in the span direction of the beam. Therefore the samples are cut with a 45° angle to ensure a 0/90° layup. With an average thickness of 3.5 mm six samples are cut with dimensions 21 x 7 mm. The Zwick 10kN is used to apply the force on the sample. During the test the force and displacement is recorded.



---

# Chapter 4

---

## Results

Ten laminates are manufactured and cut according to the methodology described in chapter 3. The current chapter focuses on the results only, a discussion of the results will follow in chapter 5. Temperature is measured at nine different through-thickness positions to measure the thermal anisotropy due to the exothermic reaction (4.1). It must be proven that there is no difference in density (4.2) and volume fractions (4.3) through the thickness of the laminates to be able to compare the mechanical properties of the sub-laminates. Then three out of nine sub-laminates are tested with the in-plane shear test (4.4) and the short-beam test (4.5) to test the mechanical properties through the thickness. Finally, the time needed to obtain the maximum degree of cure of the laminate is calculated (4.6).

### 4.1 Temperature analysis

The temperature of the composite during cure is measured halfway the thickness of every sub-laminate at about 100 mm from the outlet side and halfway the width (Fig. 3.1). The results are analysed in four different ways. To determine the influence of different cure cycles on the temperature profile during cure, the profiles of middle sub-laminate are compared (4.1.1). Due to the exothermic reaction of the epoxy, the through-thickness temperature distribution is not uniform. Different cure cycles result in different through-thickness temperature distributions (4.1.2). This through-thickness temperature distribution evolves in time as the material is heated from the outsides but slowly the inside temperature will gain upon the temperature on the outsides (4.1.3). Therefore the process changes from outside-in curing to inside-out curing. With the cure kinetics model this crossover point ( $\alpha_{cross}$ ) and the after gel point ( $\alpha_{AGP}$ ) can be calculated (4.1.4). It must be said that every cure cycle is applied only once, which makes the variability of the temperature profiles unknown. However, three more laminates are infused and cured with a resin system that encountered some problems. A description of the problems and a comparison between the temperature profiles of these laminates is explained in Appendix D.

### 4.1.1 Temperature profiles

The temperature profile of the laminate made with MRCC is shown in Fig. 4.1. It can be seen that the temperature of the laminate is exceeding the maximum temperature of the cure cycle due to the exotherm by 32 – 46°C, depending on its through-thickness position. The temperature profile of sub-laminate E for every other cure cycle is visualised in Fig. 4.2. Based on Fig. 4.2 the following observations are noticed:

- Increasing the first dwell temperature will decrease the exothermic peak temperature (Fig. 4.2a).
- Increasing the first dwell time will decrease the exothermic peak temperature (Fig. 4.2b).
- Increasing the ramp rate from 50°C/hour to 80°C/hour won't affect the exothermic peak temperature. However, decreasing the ramp rate to 20°C/hour decreases the exothermic peak temperature (Fig. 4.2c).
- Decreasing the second dwell temperature to 70°C will decrease the exothermic peak temperature while there is no difference in exothermic peak temperature between the second dwell temperatures of 80°C and 100°C (Fig. 4.2d).
- The difference between the exothermic peak temperature and the second dwell temperature of the cure cycle ( $\Delta T$ ) is 34.1°C, 37.3°C and 13.5°C for the second dwell temperatures of respectively 70°C, 80°C and 100°C. This means that increasing the second dwell temperature to 100°C will decrease  $\Delta T$  while there is no difference in  $\Delta T$  between the second dwell temperatures of 70°C and 80°C (Fig. 4.2d).

### 4.1.2 Exothermic peak temperature

The exothermic peak temperature through the thickness for every cure cycle is plotted in Fig. 4.3. No thermocouple data is available for CC7 sub-laminate G. The effects of different cure cycle parameters on the exothermic peak temperature are similar as for the temperature profiles described in paragraph 4.1.1.

It can be seen that the temperature profiles for the laminates made with MRCC, CC2 and CC3 are asymmetric with respect to the middle layer while all other cure cycles behave in a more symmetric way. Guo et al. [5] and Lahuerta Calahorra [43] also found asymmetric temperature distributions through the thickness with thick-walled composite laminates. Lahuerta Calahorra [43] found that an increase in first dwell temperature results in a more asymmetric temperature distribution. However, this is not true for the temperature distributions of Fig. 4.3a as CC3 (first dwell temperature of 60°C) is more symmetric than CC1 (first dwell temperature of 40°C) and CC2 (first dwell temperature of 50°C).

The layup of the laminates made by Guo et al. [5] and Lahuerta Calahorra [43] were not symmetric as both used a bleeder layer on top of the laminate. According to Oh and Lee [44] increasing the thickness of the bleeder will increase the temperature on the side of the bleeder. This can explain the asymmetric temperature distributions of Guo et al. [5] and Lahuerta Calahorra [43]. However, the layup of the laminates made in this project are symmetric and no bleeder is used (Fig. 3.1). Shi [8] also used a symmetric layup for a 32 mm thick glass-fibre

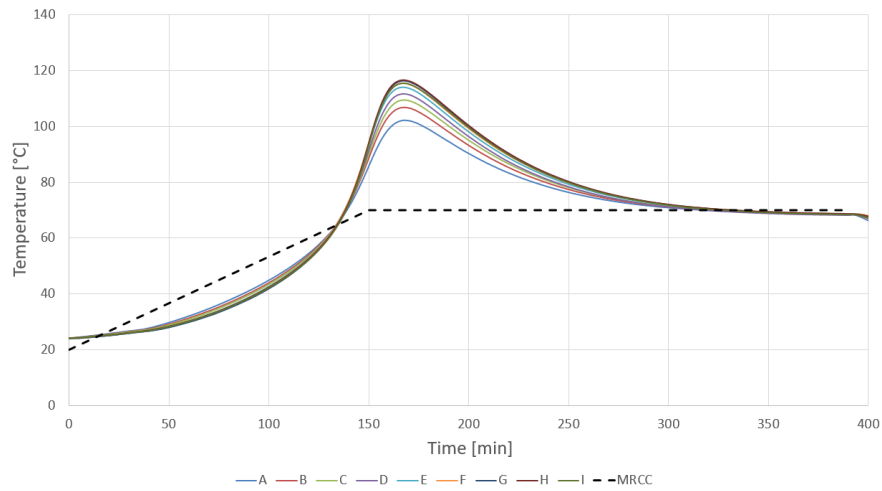
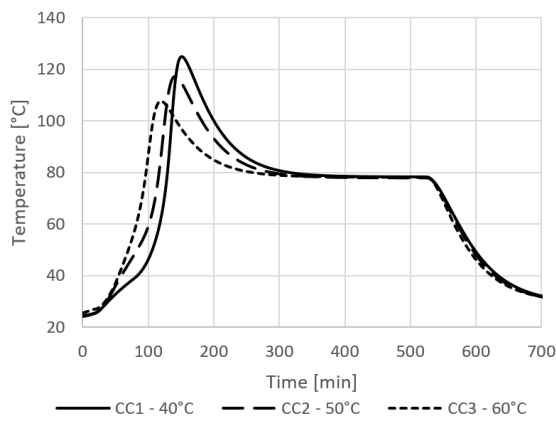
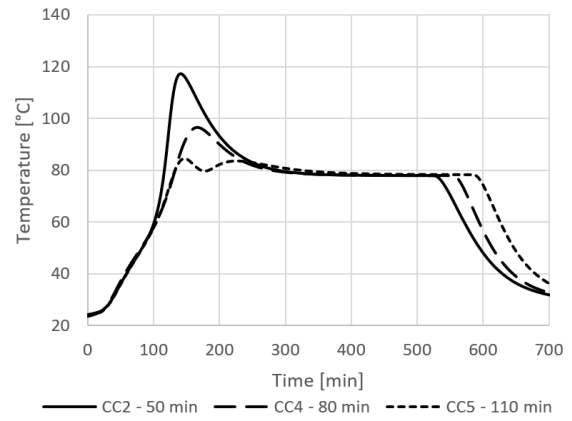


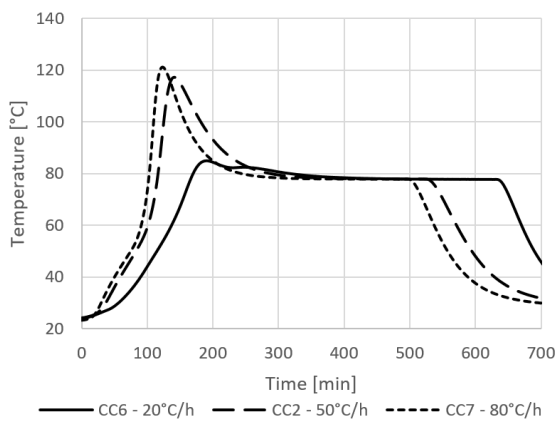
Figure 4.1: Temperature profile of laminate made with MRCC.



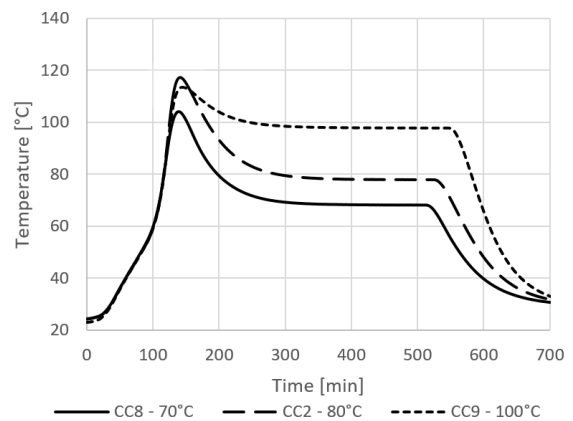
(a) Temperature profiles of sub-laminate E when increasing first dwell temperature.



(b) Temperature profiles of sub-laminate E when increasing first dwell time.

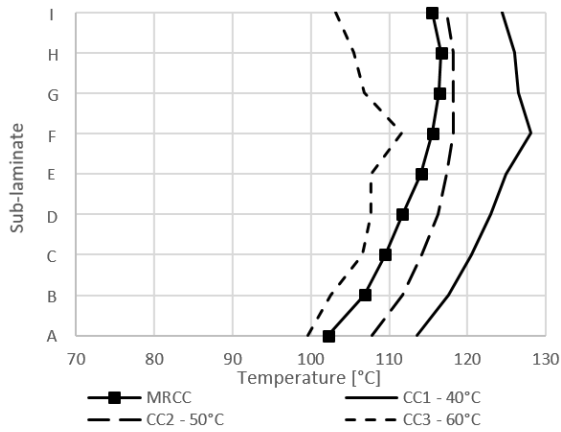


(c) Temperature profiles of sub-laminate E when increasing ramp rate.

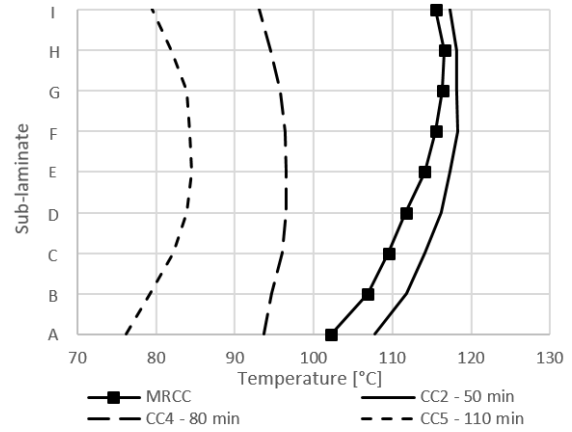


(d) Temperature profiles of sub-laminate E when increasing second dwell temperature.

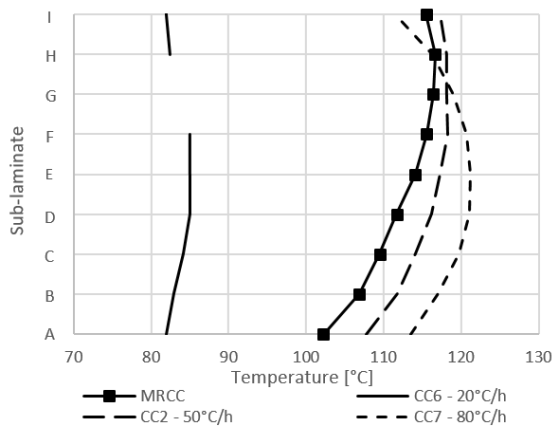
Figure 4.2: Temperature profiles of sub-laminate E.



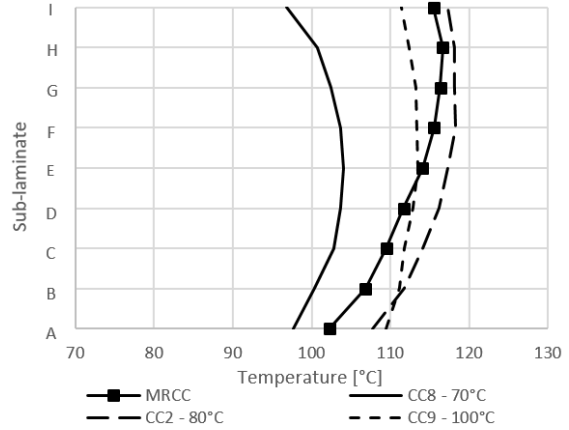
(a) Exothermic peak temperature when increasing first dwell temperature.



(b) Exothermic peak temperature when increasing first dwell time.



(c) Exothermic peak temperature when increasing ramp rate.



(d) Exothermic peak temperature when increasing second dwell temperature.

**Figure 4.3:** Exothermic peak temperature distribution through the thickness.

composite laminate with the same resin system as used in this project and found a symmetric temperature distribution through the thickness. The asymmetric temperature distribution will be further discussed in paragraph 4.3.

### 4.1.3 Thermal anisotropy in time

The evolution of the through-thickness temperature distribution in time for the MRCC and CC9 is visualised in Fig. 4.4 and Fig. 4.5. These cure cycles are chosen as they represent an asymmetric and symmetric through-thickness temperature distribution respectively.

For the laminate made with the MRCC (Fig. 4.4) it can be seen that the temperature distribution is uniform up to 140 minutes. From 150 minutes up to 200 minutes the maximum temperature is shifted towards the top side of the laminate. Finally, at 300 minutes the temperature distribution is again uniform.

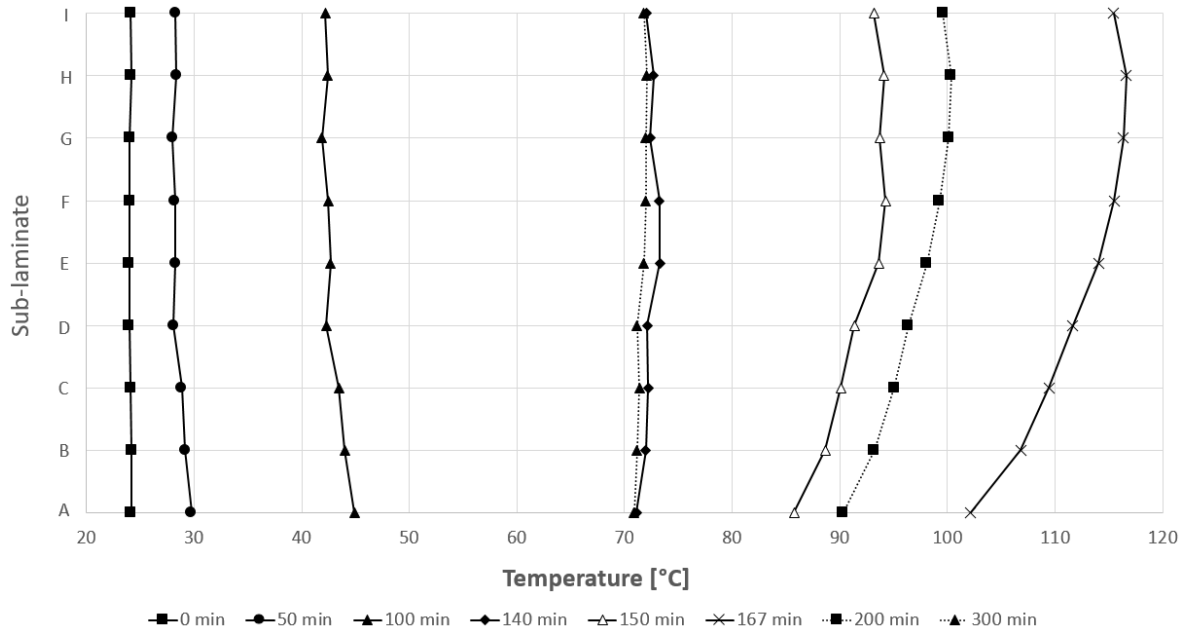


**Figure 4.4:** Through-thickness temperature distribution of the laminate made with MRCC at different points in time. The full lines represent the distributions from  $t = 0$  min up to the exothermic peak and the dashed lines represent the distributions from the exothermic peak up to  $t = 300$  min.

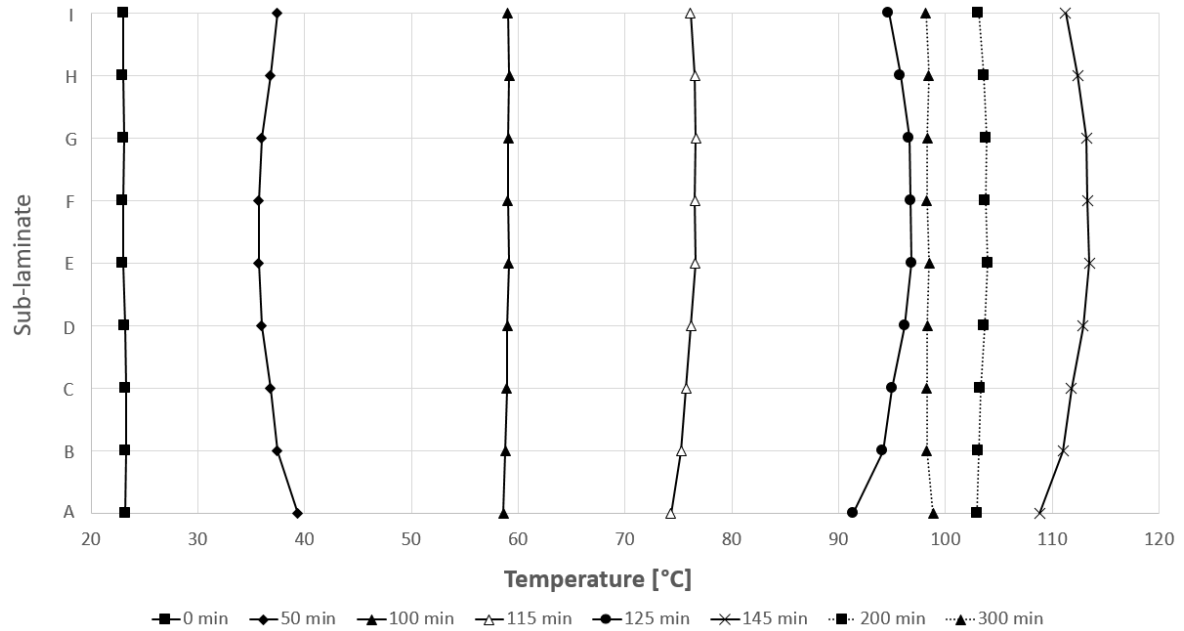


**Figure 4.5:** Through-thickness temperature distribution of the laminate made with CC9 at different points in time. The full lines represent the distributions from  $t = 0$  min up to the exothermic peak and the dashed lines represent the distributions from the exothermic peak up to  $t = 300$  min.

For the laminate made with CC9 (Fig. 4.5), at 50 minutes the outside of the laminate experiences higher temperatures than the inside of the laminate. From 100 to 115 minutes the temperature distribution is uniform after which the temperature of the inside gains upon the temperature on the outside of the laminate. After the exothermic peak the temperature distribution is again uniform.

The difference in temperature distribution over time between the laminates made with MRCC and CC9 can be explained by the different ramp rates. The laminate made with the MRCC has a ramp rate of 20°C/h which makes it easier for the inside of the laminate to follow the temperature increase. After 140 minutes the exotherm will start and the temperature on the inside will gain upon the temperature on the outside of the laminate because the low thermal conductivity of the resin and fibres. Cure cycle 9 has a ramp rate of 50°C/h which means that the outsides of the laminate will heat up first and the inside lags behind. After 115 minutes the exotherm starts and the temperature on the inside will gain upon the temperature on the outside of the laminate.

#### 4.1.4 Inside-out vs. outside-in curing

In paragraph 1.2.4 the distinction is made between inside-out and outside-in curing. In order to reduce the residual stresses,  $\alpha_{cross}$  should ideally be below  $\alpha_{AGP}$ . With the cure kinetics model described in paragraph 2.1, the degree of cure evolution for every sub-laminate can be calculated based on the thermocouple data. With the DiBenedetto equation described in paragraph 2.2.2 the corresponding  $T_g$  can be determined.  $\alpha_{cross}$  is the point at which the degree of cure on the inside is equal to the degree of cure on the outside of the laminate and is therefore calculated with the sub-laminates A and E.  $\alpha_{AGP}$  is the degree of cure at which  $T_g$  is equal to the temperature of the sub-laminate.  $\alpha_{AGP}$  is calculated for the sub-laminates A, C and E (Table 4.1). It can be seen that for all cure cycles and the sub-laminates A, C and E  $\alpha_{cross} < \alpha_{AGP}$ . This means that all laminates are cured inside-out. It is also observed that the exothermic peak always happens before  $\alpha_{AGP}$  which means that residual stresses caused by the exothermic peak can relax because the resin is still in its liquid phase.

**Table 4.1:**  $\alpha_{AGP}$  vs.  $\alpha_{cross}$ .

	$\alpha_{AGP}$			$\alpha_{cross}$
	A	C	E	
MRCC	0.95	0.97	0.97	0.59
CC1	0.97	0.98	0.99	0.73
CC2	0.97	0.97	0.98	0.56
CC3	0.96	0.97	0.97	0.57
CC4	0.95	0.96	0.96	0.47
CC5	0.95	0.95	0.95	0.46
CC6	0.95	0.95	0.95	0.66
CC7	0.97	0.98	0.98	0.61
CC8	0.94	0.95	0.95	0.56
CC9	0.99	0.99	0.99	0.90

**Table 4.2:** Density per sub-laminate for two glass fibre - epoxy laminates.

Sub-laminate	Cure cycle 7		Cure cycle 1	
	Density [g/cm <sup>3</sup> ]	SD [g/cm <sup>3</sup> ]	Density [g/cm <sup>3</sup> ]	SD [g/cm <sup>3</sup> ]
A	1.960	0.003	1.971	0.005
B	1.957	0.002	1.970	0.004
C	1.960	0.007	1.970	0.002
D	1.964	0.001	1.969	0.004
E	1.958	0.004	1.975	0.005
F	1.960	0.002	1.958	0.002
G	1.954	0.005	1.965	0.004
H	1.956	0.003	1.964	0.003
I	1.957	0.003	1.966	0.002

## 4.2 Density composite

The density of two composite laminates is measured in ethanol according to ASTM D792-13. Four samples (20 x 10 x 3.5 mm) per sub-laminate are tested for all nine sub-laminates of the laminates made with cure cycle 7 and cure cycle 1 (Table 4.2). These laminates are chosen as they represent respectively a symmetric and an asymmetric exothermic peak temperature distribution through the thickness with respect to the middle sub-laminate (paragraph 4.1.2). In this way it can be determined if a difference in density between the sub-laminates result in different through-thickness temperatures and/or mechanical properties.

### Cure cycle 7

There is no significant difference in density between the samples of the laminate made with cure cycle 7 except between sub-laminates B and D and between sub-laminates D and H. Also no trend is found between the results.

### Cure cycle 1

There is no significant difference in density of the laminate made with cure cycle 1 between sub-laminates A, C and E. However, a significant decrease in density occurs in the upper four sub-laminates (F, G, H and I). This could indicate that the matrix volume fraction is lower in the upper four sub-laminates.

## 4.3 Volume fractions

The FVF, MFV and VVF are measured according to D3171 procedure G with the same samples used in the density test described in paragraph 4.2. For the composite density, the specific values per sub-laminate are used as calculated in paragraph 4.2. The glass fibre density is assumed to be 2.61 g/cm<sup>3</sup> and the matrix density is 1.1566 g/cm<sup>3</sup> as described in paragraph 2.3.3.

**Table 4.3:** Volume fractions per sub-laminate for the laminate made with CC7.

Sub-laminate	FVF [%]	SD [%]	MVF [%]	SD [%]	VVF [%]	SD [%]
A	55.09	0.16	45.15	0.14	-0.24	0.03
B	54.77	0.16	45.59	0.20	-0.35	0.04
C	55.05	0.53	45.29	0.57	-0.34	0.07
D	55.30	0.05	45.03	0.10	-0.33	0.05
E	55.01	0.25	45.13	0.27	-0.13	0.04
F	55.15	0.14	45.03	0.12	-0.19	0.03
G	54.76	0.29	45.41	0.29	-0.17	0.12
H	54.84	0.14	45.37	0.13	-0.21	0.07
I	54.91	0.18	45.24	0.18	-0.16	0.02

### Cure cycle 7

There is no significant difference in FVF between the sub-laminates of the laminate made with CC7 except between sub-laminate D and H (Table 4.3). There is also no significant difference in MVF between the sub-laminates. The VVF is negative for all sub-laminates, which is physically impossible. This can be caused by an incorrect value for the fibre density. Although the VVF values are negative, the VVF for the sub-laminates E, F, G, H and I are slightly higher than for the sub-laminates A, B, C and D.

### Cure cycle 1

There is no significant difference in FVF between the sub-laminates of the laminate made with CC1 except between sub-laminate F and I (Table 4.4). There is no significant difference in MVF between sub-laminates A, C and E. However, the MVF tends to decrease between the sub-laminates F, G, H and I. No significant difference in VVF is found between the sub-laminates A, B, C, D and E and between the sub-laminates F, G, H and I. However, the VVF increases significantly between these two groups. The higher VVF and lower MVF on the upper side of the laminate causes the lower density on the upper side as described in paragraph 4.2.

For both laminates there is no significant difference in density, FVF, MVF and VVF between the sub-laminates A, C and E. Although this does not prove that this is true for all laminates, the mechanical performance of these three sub-laminates will be compared for all laminates in paragraph 4.4 and 4.5.

The lower MVF on the upper side of the laminate cured according to CC1 could be an explanation for the asymmetric through-thickness temperature distribution discussed in paragraph 4.1.2. The specific heat of epoxy resin above  $T_g$  is higher than the specific heat of glass fibres meaning that more energy is required to raise the temperature of epoxy resin than to raise the temperature of glass fibres [45]. The thermal conductivity of epoxy resin is lower than the thermal conductivity of glass fibres meaning that the heat will conduct faster through glass fibres than through epoxy resin [45]. When the MVF decreases towards the top, these two effects could lead to a higher temperature on the top side of the laminate, resulting in an asymmetric temperature profile. However, more research must be done to confirm this.

**Table 4.4:** Volume fractions per sub-laminate for the laminate made with CC1.

Sub-laminate	FVF [%]	SD [%]	MVF [%]	SD [%]	VVF [%]	SD [%]
A	55.74	0.34	44.65	0.38	-0.40	0.08
B	55.74	0.33	44.59	0.37	-0.33	0.05
C	55.70	0.13	44.64	0.12	-0.34	0.04
D	55.72	0.25	44.53	0.24	-0.25	0.02
E	56.11	0.31	44.17	0.31	-0.28	0.06
F	55.43	0.12	44.18	0.12	0.40	0.03
G	55.88	0.24	43.76	0.22	0.36	0.06
H	55.88	0.20	43.69	0.21	0.43	0.01
I	56.06	0.15	43.51	0.12	0.43	0.03

## 4.4 In-plane shear test

The in-plane shear test is performed according to ASTM D3518/D3518M. This standard recommends to calculate the maximum shear stress (4.4.1), shear modulus of elasticity (4.4.2), maximum shear strain (4.4.3) and offset shear strength (4.4.4). To indicate if different cure cycles affect the amount of defects due to the manufacturing process, acoustic emission sensors are used (4.4.5).

### 4.4.1 Shear stress

The maximum in-plane shear stress for every specimen is calculated according to:

$$\tau_{12}^m = \frac{P^m}{2A} \quad (4.1)$$

in which  $\tau_{12}^m$  is the maximum in-plane shear stress,  $P^m$  is the maximum force at or below 5% engineering shear strain and  $A$  is the cross-sectional area. The average  $\tau_{12}^m$  of 5 samples per sub-laminate with standard deviation is calculated for every cure cycle (Fig. 4.6). The results are analysed in 2 different ways. First it is determined if there is a significant difference in  $\tau_{12}^m$  between sub-laminates A and E and if a trend is found in the results. Then the  $\tau_{12}^m$  of sub-laminate E is compared for all cure cycles to determine the influence of different cure cycles on the in-plane shear stress. Sub-laminate E is chosen as it suffers most from the effects of residual stress.

There is a significant difference between  $\tau_{12}^m$  of sub-laminate A and E for 6/10 cure cycles (MRCC, CC2, CC5, CC6, CC7 and CC9). For these same 6 cure cycles, a downwards trend is found from sub-laminate A to sub-laminate E meaning that the  $\tau_{12}^m$  decreases towards the middle of the laminate.

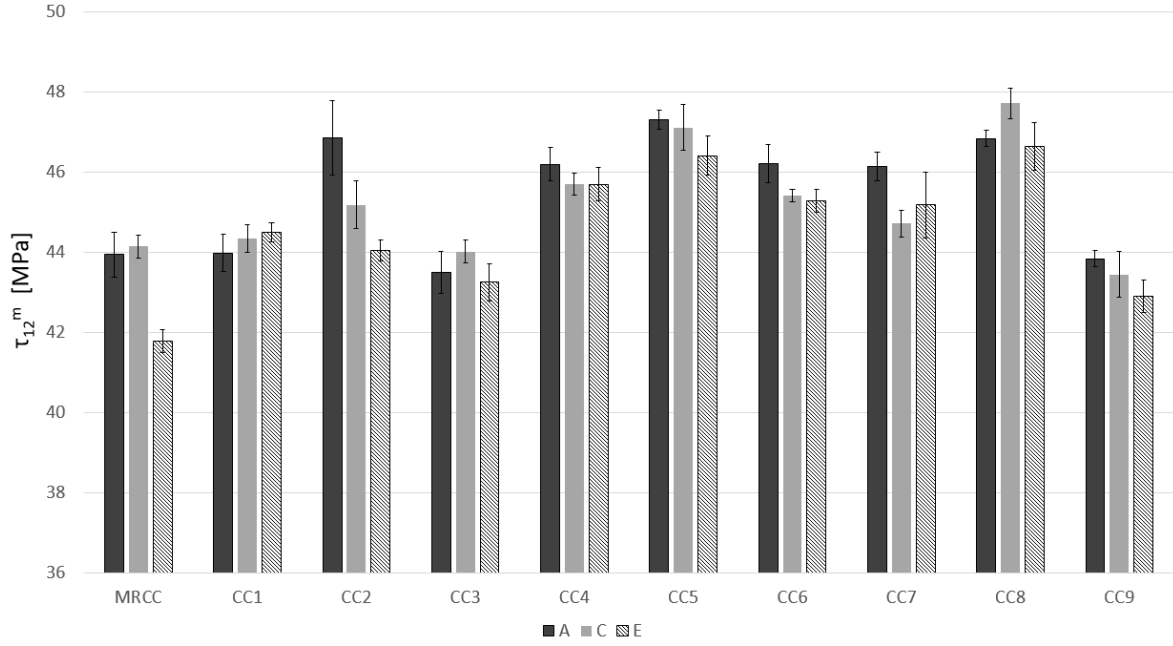


**Figure 4.6:**  $\tau_{12}^m$  per cure cycle for sub-laminates A, C and E.

Comparing  $\tau_{12}^m$  of sub-laminate E between different cure cycles, the following observations are noticed:

- $\tau_{12}^m$  of the laminate made with MRCC is significantly lower than  $\tau_{12}^m$  of all other cure cycles.
- Increasing the first dwell temperature will decrease  $\tau_{12}^m$  (CC1, CC2 and CC3). However, results are only significant between  $\tau_{12}^m$  of CC1 and CC3.
- Increasing the first dwell time will increase  $\tau_{12}^m$  (CC2, CC4, CC5). Results are significant between CC2 and CC4 and between CC2 and CC5. Results are not significant between CC4 and CC5.
- $\tau_{12}^m$  of the laminate made with CC2 (ramp rate of 50°C/h) is significantly lower than  $\tau_{12}^m$  of the laminates made with CC6 (ramp rate of 20°C/h) and CC7 (ramp rate of 80°C/h).
- Increasing the second dwell temperature will decrease  $\tau_{12}^m$  (CC8, CC2 and CC9). Results are significant between all three cure cycles.

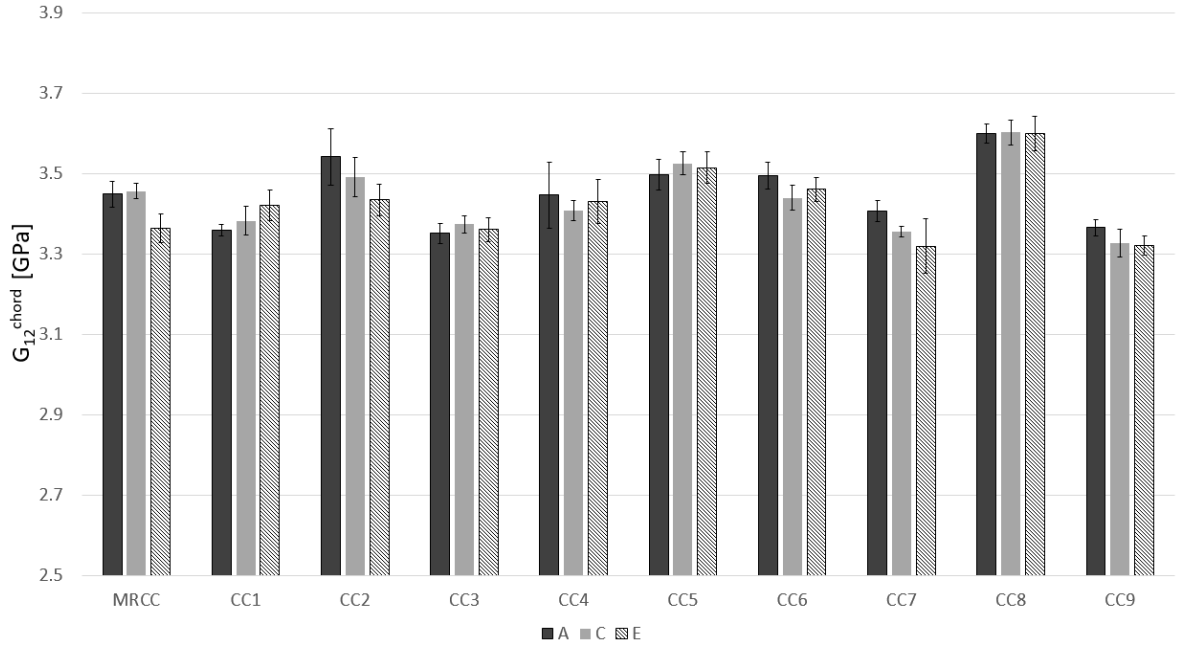


Figure 4.7:  $G_{12}^{chord}$  per cure cycle for sub-laminates A, C and E.

#### 4.4.2 Shear modulus

According to ASTM D3518/D3518M, the chord shear modulus of elasticity ( $G_{12}^{chord}$ ) is calculated using:

$$G_{12}^{chord} = \frac{\Delta\tau_{12}}{\Delta\gamma_{12}} \quad (4.2)$$

whereby  $\Delta\tau_{12}$  indicates the difference in applied engineering shear stress between the two shear strain points and  $\Delta\gamma_{12}$  is the difference between the two engineering shear strain points (Fig. 4.7). The engineering shear strain range is  $4000\mu\varepsilon$  starting with the lower strain point at  $1500\mu\varepsilon$ .

A significant decrease in  $G_{12}^{chord}$  between sub-laminates A and E is found for only 2/10 cure cycles (MRCC and CC2). Comparing  $G_{12}^{chord}$  of sub-laminate E between the laminates with different cure cycles, the following is observed:

- There is no significant difference in  $G_{12}^{chord}$  by increasing the first dwell temperature (CC1, CC2 and CC3).
- There is no significant difference in  $G_{12}^{chord}$  by increasing the first dwell time (CC2, CC4 and CC5).
- Increasing the ramp rate to  $80^\circ\text{C/h}$  (CC7) will significantly decrease  $G_{12}^{chord}$  compared to ramp rates of  $50^\circ\text{C/h}$  (CC2) and  $20^\circ\text{C/h}$  (CC6).
- Increasing the second dwell temperature will significantly decrease  $G_{12}^{chord}$  (CC8, CC2 and CC9).

### 4.4.3 Maximum shear strain

The engineering shear strain for every data point ( $\gamma_{12_i}$ ) is calculated using the DIC data according to:

$$\gamma_{12_i} = \varepsilon_{x_i} - \varepsilon_{y_i} \quad (4.3)$$

in which  $\varepsilon_{x_i}$  indicates the longitudinal normal strain and  $\varepsilon_{y_i}$  the lateral normal strain. The maximum engineering shear strain ( $\gamma_{12}^m$ ) is calculated using:

$$\gamma_{12}^m = \min \left\{ \begin{array}{l} 5\% \\ \gamma_{12} \text{ at maximum shear stress} \end{array} \right. \quad (4.4)$$

However, all samples failed beyond  $\gamma_{12} = 5\%$  which means  $\gamma_{12}^m = 5\%$  for all samples.

### 4.4.4 Offset shear strength

The offset shear strength ( $F_{12}^\circ$ ) is the shear stress value at which the stress-strain curve changes from linear to non-linear.  $F_{12}^\circ$  is calculated with an offset strain value of 0.2% (Fig. 4.8).

Comparing  $F_{12}^\circ$  between sub-laminates A and E for all cure cycles, a significant difference is found for only 3/10 cure cycles (CC6, CC7 and CC9). Comparing  $F_{12}^\circ$  of sub-laminate E per cure cycle it can be concluded that:

- There is a significant decrease in  $F_{12}^\circ$  by increasing the first dwell temperature from 50°C (CC2) to 60°C (CC3).
- There is no significant difference in  $F_{12}^\circ$  by increasing the first dwell time.
- There is no significant difference in  $F_{12}^\circ$  by increasing the ramp rate.
- There is a significant decrease in  $F_{12}^\circ$  between the laminates made with CC8 and CC9 (second dwell temperature of respectively 70 and 100°C).

### 4.4.5 Acoustic emission

During the in-plane shear test the AE activity is measured to determine the influence of different cure cycles on the amount of defects in the composite laminates. The AE sensors detect acoustic events (hits) and a typical graph of the  $\tau_{12}$  vs. average cumulative hits is shown in Fig. 4.9. The grey band indicates the standard deviation between the samples. A threshold of 50 dB is used to filter-out noise that is not related to the formation of defects in the laminate. At the start of the in-plane shear test, the grips of the test bench clamp into the specimen, causing high AE activity. Therefore, to reduce the variability between the tests, the hits during the first 100N are not taken into account.

Due to two measurement errors during the AE tests, no AE data is available after  $F = 10\text{kN}$  (approx. 56 MPa) for 6/30 sub-laminates and no data is available for CC5 sub-laminate A, CC7 sub-laminate E and CC8 sub-laminate C.

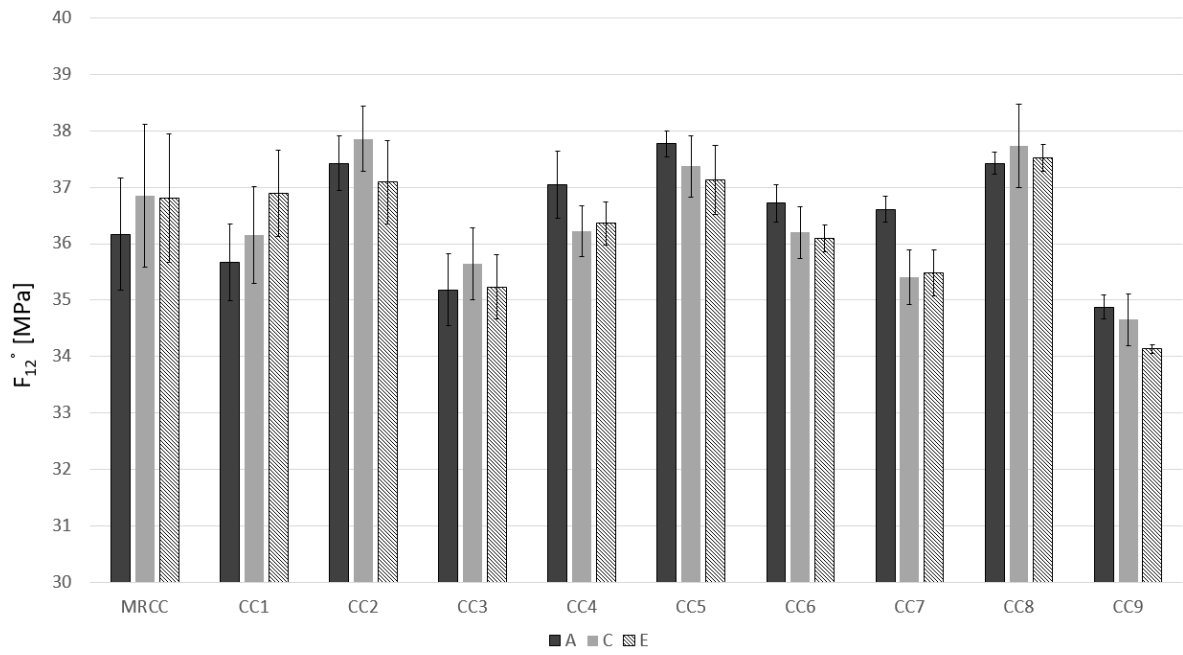


Figure 4.8:  $F_{12}^\circ$  per cure cycle for sub-laminates A, C and E.

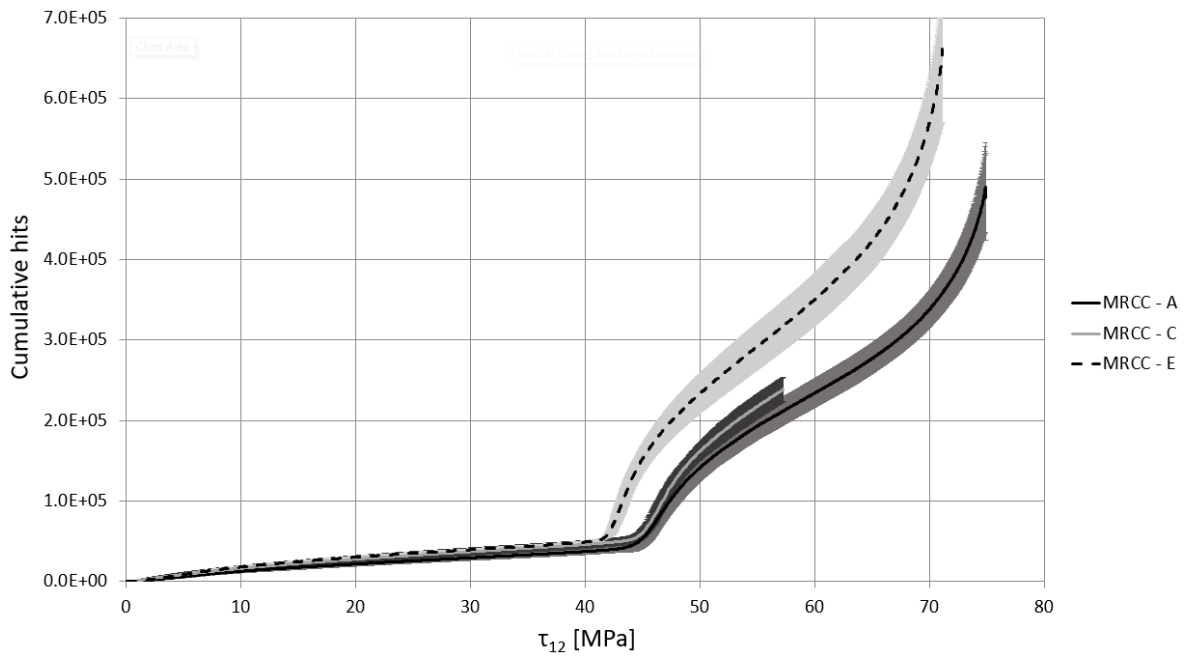
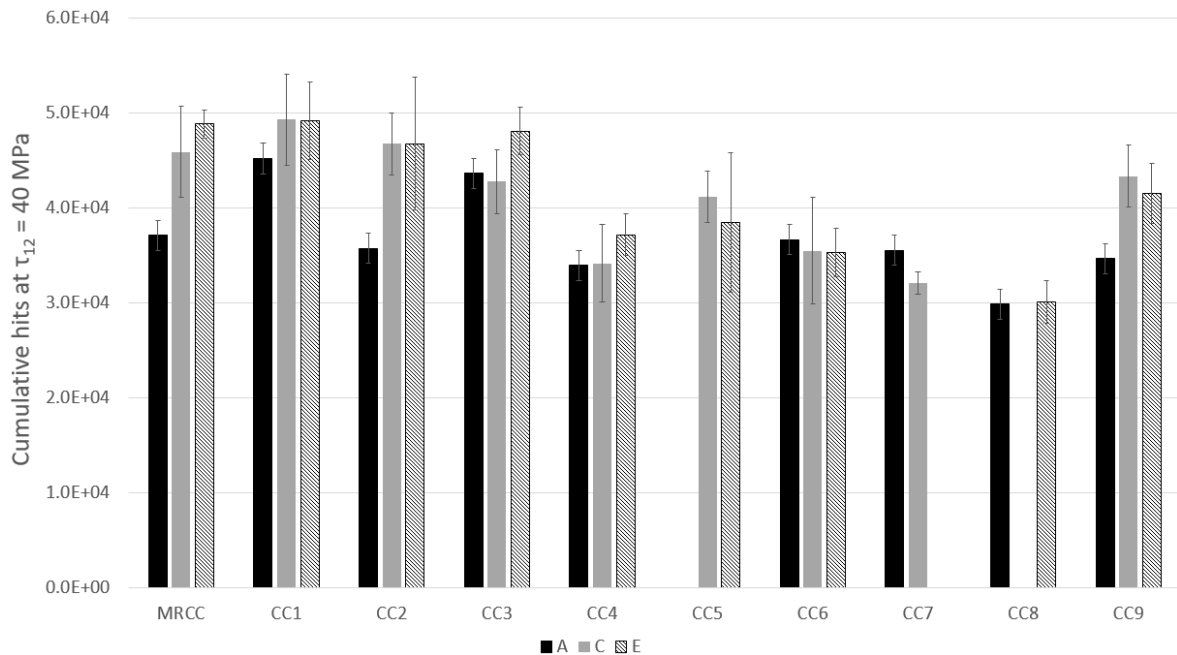


Figure 4.9:  $\tau_{12}$  vs. average cumulative hits of the laminate made with MRCC.



**Figure 4.10:** AE cumulative hits at  $\tau_{12} = 40$  MPa.

In Fig. 4.9 it can be seen that the  $\tau_{12}$  vs. cumulative hits graph experiences an increase in slope between  $\tau_{12} = 40$  MPa and  $\tau_{12} = 50$  MPa. This is related to the offset shear strength of the material. To compare data between laminates with different cure cycles, the average number of hits and its standard deviation at  $\tau_{12} = 40$  MPa (Fig. 4.10) and  $\tau_{12} = 50$  MPa (Fig. 4.11) are calculated.

Comparing the cumulative hits at  $\tau_{12} = 40$  MPa between sub-laminates A and E, a significant increase in AE activity is found for 3/8 cure cycles (MRCC, CC2 and CC9). For two cure cycles (CC5 and CC7) no data was available for either sub-laminate A or E. Comparing the number of hits of sub-laminate E between the laminates made with different cure cycles, the following can be observed:

- The AE activity of the laminate made with MRCC is significantly higher than 4/8 other cure cycles (CC4, CC5, CC6 and CC8).
- There is no significant difference in AE activity by increasing the first dwell temperature (CC1, CC2 and CC3).
- There is a significant decrease in AE activity by increasing the first dwell time from 50 minutes (CC2) to 80 minutes (CC4). However, no significant difference is found between CC2 and CC5 (first dwell time of 110 minutes) and between CC4 and CC5.
- Decreasing the ramp rate from 50°C/h (CC2) to 20°C/h (CC6) significantly reduces the AE activity.
- A second dwell temperature of 70°C (CC8) significantly decreases the AE activity compared to a second dwell temperature of 80°C (CC2) and 100°C (CC9). No significant difference is found between CC2 and CC9.

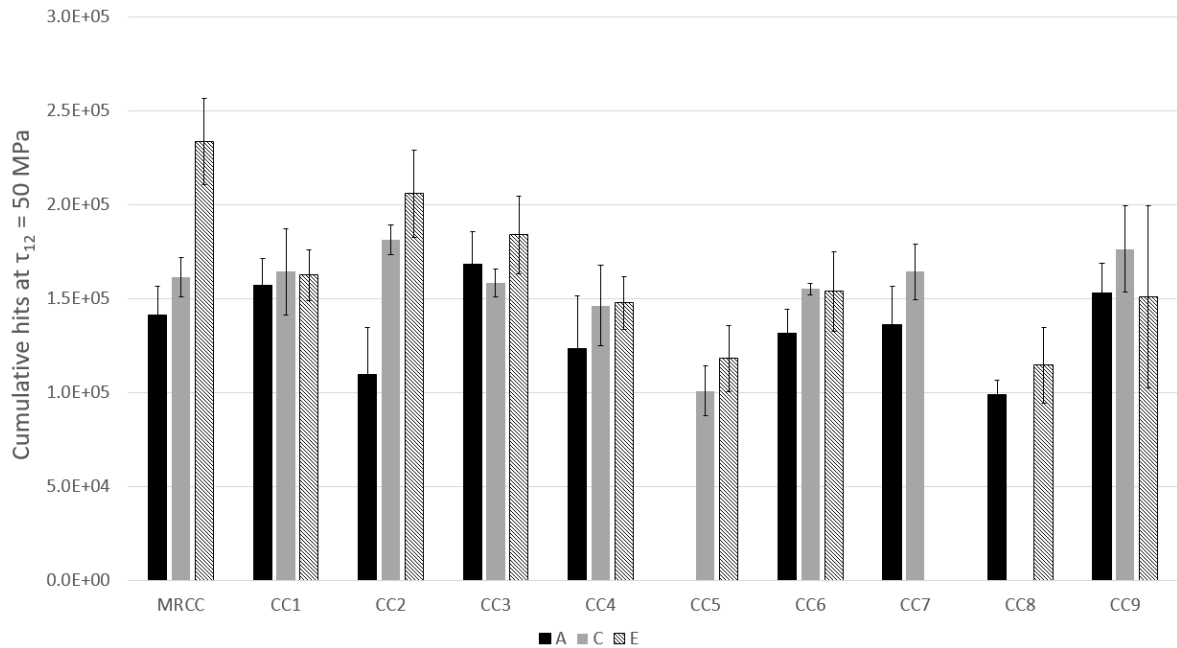


**Figure 4.11:** AE cumulative hits at  $\tau_{12} = 50$  MPa.

Comparing the cumulative hits at  $\tau_{12} = 50$  MPa between sub-laminates A and E, a significant increase in AE activity is found for 2/8 cure cycles (MRCC and CC2). Comparing the number of hits of sub-laminate E between the laminates made with different cure cycles, the following can be observed:

- The AE activity of the laminate made with MRCC is significant higher than 6/8 other cure cycles (CC1, CC4, CC5, CC6, CC8 and CC9).
- There is no significant difference in AE activity by increasing the first dwell temperature (CC1, CC2 and CC3).
- A decreasing trend in AE activity is found by increasing the first dwell time (CC2, CC4, CC5). There is a significant difference between CC2 and CC4 and between CC2 and CC5. However, no significant difference is found between CC4 and CC5.
- Decreasing the ramp rate from 50°C/h (CC2) to 20°C/h (CC6) significantly reduces the AE activity.
- A second dwell temperature of 70°C (CC8) significantly decreases the AE activity compared to a second dwell temperature of 80°C (CC2). Also increasing the second dwell temperature to 100°C (CC9) significantly decreases the AE activity compared to 80°C. No significant difference is found between CC8 and CC9.

The conclusions made with the cumulative hits at  $\tau_{12} = 40$  MPa and at  $\tau_{12} = 50$  MPa are comparable, except that the conclusions made with  $\tau_{12} = 50$  MPa are more significant. Therefore, from now on only the conclusions made with the cumulative hits at  $\tau_{12} = 50$  MPa are used.

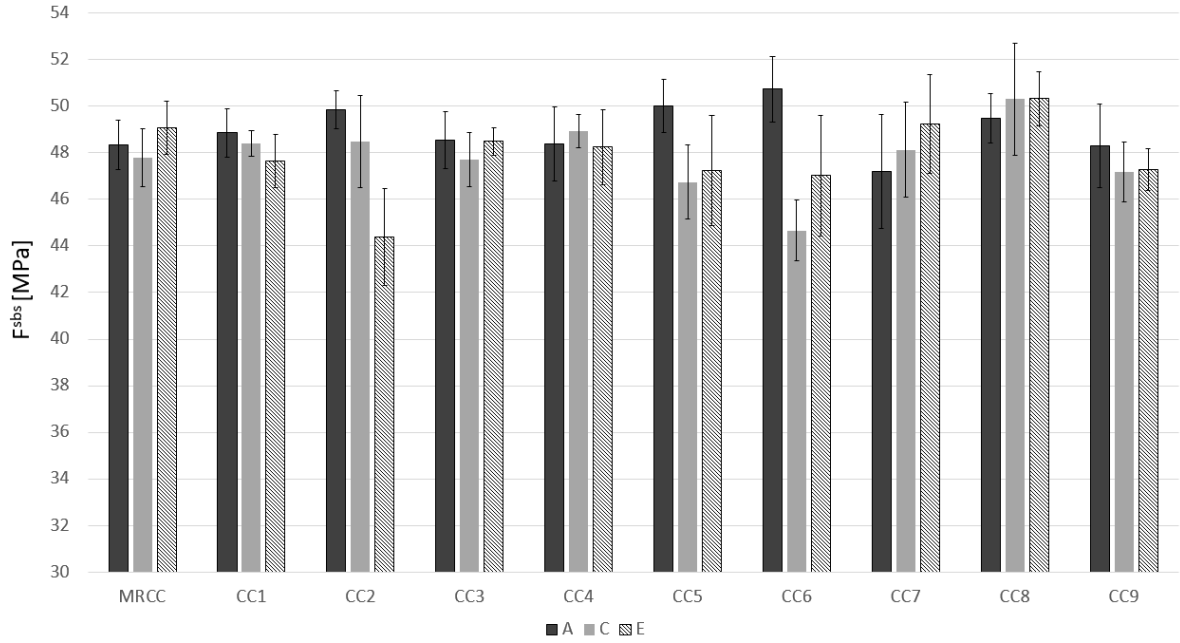


Figure 4.12:  $F^{sbs}$  per cure cycle for sub-laminates A, C and E.

## 4.5 Short-beam test

The short-beam strength is calculated according to ASTM D2344/D2344M using:

$$F^{sbs} = 0.75 \frac{P_m}{b \cdot h} \quad (4.5)$$

in which  $F^{sbs}$  is the short beam strength,  $P_m$  is the maximum load during the test and  $b$  and  $h$  are respectively the width and thickness of the specimen.  $F^{sbs}$  is calculated for the sub-laminates A, C and E for every cure cycle (Fig. 4.12). Comparing  $F^{sbs}$  between sub-laminates A and E, a downward trend is found for only 3/10 cure cycles (CC2, CC5 and CC6). Comparing  $F^{sbs}$  of sub-laminate E between the laminates made with different cure cycles, the following is observed:

- Increasing the first dwell temperature from 50°C (CC2) to 60°C (CC3) will significantly increase  $F^{sbs}$ .
- Increasing the first dwell time from 50 min (CC2) to 80 min (CC4) will significantly increase  $F^{sbs}$ .
- Increasing the ramp rate from 50°C/h (CC2) to 80°C/h (CC7) will significantly increase  $F^{sbs}$ .
- Decreasing the second dwell temperature from 80°C (CC2) to 70°C (CC8) will significantly increase  $F^{sbs}$ .

**Table 4.5:** Time to  $\alpha_{max}$ .

Cure cycle	Parameter	Setting	Time [min]	% time to MRCC
MRCC			385	
CC1	First dwell T	40°C	323	84%
CC2		50°C	360	93%
CC3		60°C	345	90%
CC2	First dwell t	50 min	360	93%
CC4		80 min	436	113%
CC5		110 min	587	153%
CC6	Ramp rate	20°C/h	599	156%
CC2		50°C/h	360	93%
CC7		80°C/h	295	77%
CC8	Second dwell T	70°C	372	97%
CC2		80°C	360	93%
CC9		100°C	376	98%

## 4.6 Time optimisation

In all two-dwell cure cycles, the time of the second dwell is set to 400 minutes to ensure that the degree of cure reaches a plateau. Now, the time needed to reach that plateau ( $\alpha_{max}$ ) is calculated with the cure kinetics model. Sub-laminate A is chosen to perform the time optimisation as this sub-laminate will experience the lowest temperature and thus will reach  $\alpha_{max}$  the latest. When the reaction rate ( $d\alpha/dt$ ) of the sub-laminate is below  $10^{-6}s^{-1}$  it is assumed that the degree of cure has reached a plateau (Table 4.5).

In Table 4.5 it can be seen that all two-dwell cure cycles will reduce the time to reach  $\alpha_{max}$  compared to MRCC except for CC4, CC5 and CC6. These cure cycles have either an extended first dwell time (CC4 and CC5) or a very slow ramp rate (CC6) which will considerably increase the time to  $\alpha_{max}$ .



---

## Chapter 5

---

# Discussion

In paragraph 1.2.2 is described that residual stresses are mainly caused by three mechanisms: thermal anisotropy that causes outside-in curing, cure shrinkage and differences in CTE between fibres and matrix. It was thought that the laminate made with MRCC would result in outside-in curing and a two-dwell cure cycle would result in inside-out curing because the exotherm would happen during the first dwell and therefore lowers  $\alpha_{cross}$  (Fig. 1.4). However, it turned out that all laminates, including MRCC, cured inside-out. Also, as described in paragraph 4.1.4, the exothermic peak always happens before vitrification which means that residual stresses caused by resin shrinkage and differences in CTE during the exothermic peak can relax because the resin is still in its liquid phase. These results were not expected during the cure cycle design phase and make comparison between the cure cycles more difficult as the differences are less outspoken.

It was thought that a first dwell time of 50 minutes was enough to ensure that the exothermic peak happens during the first dwell. However, for all cure cycles except CC5 (first dwell time of 110 min), the exothermic peak happened at the end of the second ramp or during the second dwell. This resulted in high exothermic peaks or very long cycle times.

The results of  $G_{12}^{chord}$ ,  $F_{12}^{\circ}$  and  $F^{sbs}$  confirmed some of the observations of  $\tau_{12}^m$  and AE activity by changing the cure cycle parameters. However, the differences between sub-laminates A and E and between the cure cycles are less pronounced for  $G_{12}^{chord}$ ,  $F_{12}^{\circ}$  and  $F^{sbs}$  and the variability is high. Therefore it is decided that  $G_{12}^{chord}$ ,  $F_{12}^{\circ}$  and  $F^{sbs}$  are no longer used for comparison.

### Through-thickness distribution

It was expected that a higher exothermic peak temperature would result in lower mechanical properties as it causes more residual stress. On the other hand, a higher exothermic peak temperature results in a higher  $\alpha$  and a higher  $\alpha$  results in higher mechanical properties. These two events contradict each other and could lead to inconclusive results. However,  $\alpha_{max}$ , which is almost similar as  $\alpha_{AGP}$  (Table 4.1), reached per sub-laminate differs maximum 2% between sub-laminate A and E. This will not lead to major differences in mechanical properties between sub-laminate A and E based on degree of cure.

Comparing the exothermic peak temperatures through the thickness (Fig. 4.3) with  $\tau_{12}^m$  of the laminates (Fig. 4.6), no relation is found between  $\tau_{12}^m$  and the exothermic peak temperature between sub-laminates A and E. A large difference in exothermic peak temperature between sub-laminate A and E will not result in significant differences in  $\tau_{12}^m$  between sub-laminate A and E. Also no relation is found between the AE activity of sub-laminate A and E and the exothermic peak temperatures of sub-laminate A and E.

### Cure cycle comparison

Comparing the exothermic peak temperature,  $\tau_{12}^m$ , AE activity and time to reach  $\alpha_{max}$  of sub-laminate E between the laminates made with MRCC and the two-dwell cure cycles, it can be concluded that curing with MRCC results in a high  $\Delta T$  at the exothermic peak temperature compared with the two-dwell cure cycles.  $\tau_{12}^m$  of the laminate made with MRCC is significantly lower than  $\tau_{12}^m$  of all two-dwell cure cycles. The AE activity for the laminate made with MRCC is higher than all two-dwell cure cycles and significantly higher for 6/8 two-dwell cure cycles. The time to reach  $\alpha_{max}$  for the laminate made with MRCC is higher than 6/9 two-dwell cure cycles. These results confirm the expectations that curing a thick-walled composite laminate with MRCC results in higher levels of residual stress and leads to longer cycle times than a thick-walled composite laminate cured with a two-dwell cure cycle.

Comparing the exothermic peak temperature,  $\tau_{12}^m$ , AE activity and time to reach  $\alpha_{max}$  of sub-laminate E between the laminates cured with different first dwell temperatures, it can be concluded that increasing the first dwell temperature will decrease the exothermic peak temperature, will decrease  $\tau_{12}^m$  and will not affect the AE activity and time. The fact that a decrease in exothermic peak temperature goes hand in hand with a decrease in  $\tau_{12}^m$  is not as expected as a lower exothermic peak temperature would result in less residual stress and thus higher mechanical properties.

Comparing the exothermic peak temperature,  $\tau_{12}^m$ , AE activity and time to reach  $\alpha_{max}$  of sub-laminate E between the laminates cured with different first dwell times, it can be concluded that increasing the first dwell time will decrease the exothermic peak temperature, increase  $\tau_{12}^m$  and decrease AE activity. Although results are as expected and one should say that a longer first dwell time will be beneficial for residual stress reduction, it will considerably increase the time to reach  $\alpha_{max}$ .

Comparing the exothermic peak temperature,  $\tau_{12}^m$ , AE activity and time to reach  $\alpha_{max}$  of sub-laminate E between the laminates cured with different ramp rates, it can be concluded that increasing the ramp rate will increase the exothermic peak temperature and increase the AE activity, but the time to reach  $\alpha_{max}$  is considerably reduced.  $\tau_{12}^m$  will be low at 20°C/h and at 80°C/h and will be high at 50°C/h. As described in paragraph 1.2.4, Kim and Daniel [21] found that lower ramp rates resulted in a higher curvature as a measure of residual stress and Bogetti and Gillespie [7] found that higher ramp rates results in outside-in curing. This can indicate that  $\tau_{12}^m$  goes through a peak by increasing the ramp rate of the cure cycle, which is also found in this research.

Comparing the exothermic peak temperature,  $\tau_{12}^m$ , AE activity and time to reach  $\alpha_{max}$  of sub-laminate E between the laminates cured with different second dwell temperatures, it can be concluded that increasing the second dwell temperature will increase the exothermic peak temperature, decrease  $\tau_{12}^m$ , increase AE activity, while not affecting the time to reach  $\alpha_{max}$ . It was expected that increasing the second dwell temperature would reduce the processing time, increase the maximum degree of cure and enhance the amount of residual stress. Although the last two statements are correct based on the exothermic peak temperature,  $\tau_{12}^m$  and AE activity, the processing time is not affected by increasing the second dwell temperature. It was also thought that a second dwell temperature above  $T_{g\infty}$  of the resin would relax the residual stresses and therefore increase  $\tau_{12}^m$ . However, increasing the second dwell temperature to 100°C will decrease  $\tau_{12}^m$  and increase AE activity which means that a second dwell temperature above  $T_{g\infty}$  is not beneficial for residual stress reduction.



---

## Chapter 6

---

# Conclusions

Thick-walled components of a wind turbine blade that are cured according to the MRCC result in low quality parts as the exothermic reaction of the epoxy resin causes thermal anisotropy through the thickness which will result in the formation of residual stresses. Thermal anisotropy can be reduced by increasing the cycle time of the cure cycle but this increases production costs. Therefore, it is important to optimise the cure cycle of thick-walled components in order to reduce the formation of residual stresses and minimise the cycle time. This master thesis project focused on the influence of different cure cycle parameters on the mechanical performance in order to make recommendations for improvement of the cure cycle for thick-walled components. In paragraph 1.3, three research questions were defined to be answered during this project.

### **1. What is the influence of temperature and degree of cure on the thermophysical properties of epoxy resin and composite laminates?**

A cure kinetics model is made in order to describe the influence of temperature and time on the degree of cure of the epoxy resin. The DiBenedetto model expresses the relation between degree of cure and the  $T_g$  of the resin. Thermo-mechanical characterisation is performed with samples with different degrees of cure. It is found that the storage modulus in glass and in rubbery state does not depend on degree of cure and frequency. CTE is constant in glass and rubbery state whereby  $CTE_{glass} < CTE_{rubber}$ . There is no relation between CTE and degree of cure. The density of the resin increases with increasing degree of cure until  $T_{gel}$ .

### **2. What is the influence of different ramp rates, dwell temperatures and dwell times on the through-thickness temperature distribution and the mechanical properties of thick-walled composites?**

Ten laminates with different cure cycles are manufactured and mechanically tested in order to determine the influence of different cure cycle parameters on its mechanical properties. The ten different cure cycles consist of the MRCC and nine two-dwell cure cycles with different cure cycle parameters. Curing according to the MRCC results in a laminate with a high exothermic peak temperature, low  $\tau_{12}^m$ , high AE activity and a long processing time compared to the two-dwell cure cycles.

Comparing the laminates with different two-dwell cure cycle parameters, the following can be concluded:

Increasing the first dwell temperature will:

- decrease the exothermic peak temperature
- decrease  $\tau_{12}^m$
- not affect AE activity
- not affect time.

Increasing the first dwell time will:

- decrease the exothermic peak temperature
- increase  $\tau_{12}^m$
- decrease AE activity
- increase time.

Increasing the ramp rate will:

- increase the exothermic peak temperature
- result in a peak in  $\tau_{12}^m$  at 50°C/h
- increase AE activity
- decrease time.

Increasing the second dwell temperature will:

- increase exothermic peak temperature
- decrease  $\Delta T$  between the exothermic peak temperature and the second dwell temperature
- decrease  $\tau_{12}^m$
- increase AE activity
- not affect time.

### **3. Which recommendations can be made for improvement of the cure cycle of thick-walled composites made by vacuum infusion in order to minimise the residual stresses and cycle time?**

The MRCC results in laminates with a lower  $\tau_{12}^m$  and higher AE activity than laminates made with a two-dwell cure cycle. Besides, the time to reach  $\alpha_{max}$  with the MRCC is higher than a two-dwell cure cycle for 6/9 two-dwell cure cycles. It is therefore recommended to use a two-dwell cure cycle compared to MRCC for thick-walled components with this resin system in order to reduce residual stresses and cycle time.

The effects of increasing the first dwell temperature of the cure cycle are inconclusive and more research needs to be done. Increasing the first dwell time will be beneficial for the mechanical performance. However, the time to reach  $\alpha_{max}$  is increased considerable and a trade-off should be made by the manufacturer. Based on this research, there is an optimum ramp rate to maximise mechanical performance. However, more research needs to be done to confirm this result. Decreasing the second dwell temperature to 70°C is beneficial for the mechanical performance while the time to reach  $\alpha_{max}$  is not affected. Therefore it is recommended to use a low second dwell temperature.

---

## Chapter 7

---

# Recommendations

Based on the discussion and conclusions described above, some recommendations can be made for future research.

- In this research only one thick laminate is made for every cure cycle. In order to determine the variability of the results, more laminates must be made with the same cure cycle.
- It is recommended for future research to perform density and volume fraction tests on all laminates and sub-laminates in order to relate this to the mechanical performance of the composite.
- With a thick laminate the temperature increases towards the middle which results in a higher  $\alpha$  and higher residual stresses towards the middle. A higher  $\alpha$  causes a higher  $\tau_{12}^m$  but higher residual stresses lead to lower  $\tau_{12}^m$ . In order to separate these events, thin laminates can be made with different cure cycles to investigate the influence of  $\alpha$  on  $\tau_{12}^m$  while the residual stresses are minimised. In this way it can be determined which event effects  $\tau_{12}^m$  the most.
- The fact that  $\tau_{12}^m$  goes through a peak by increasing the ramp rate must be investigated further either experimentally or by using a model to be able to prove this statement.
- All laminates in this research cured inside-out and the exothermic peak happened before vitrification of the resin which made the effects of different cure cycles on the mechanical performance less pronounced. A cure cycle can be designed that results in outside-in curing and/or an exothermic peak after vitrification such that the effects on the mechanical performance can be determined.
- The fact that some laminates experienced an asymmetric through-thickness temperature distribution at the exothermic peak with respect to the middle ply must be further investigated.



---

## References

- [1] L. Ma, S. R. Athreya, R. Mehta, D. Barpanda, and A. Shafi. Numerical modeling and experimental validation of nonisothermal resin infusion and cure processes in large composites. *Journal of Reinforced Plastics and Composites*, 36(10):780–794, 2017.
- [2] V. Antonucci, M. Giordano, K. T. Hsiao, and S. G. Advani. A methodology to reduce thermal gradients due to the exothermic reactions in composites processing. *International journal of heat and mass transfer*, 45(8):1675–1684, 2002.
- [3] D. J. Michaud, A. N. Beris, and P. S. Dhurjati. Thick-sectioned RTM composite manufacturing, part ii: Robust cure cycle optimization and control. *Journal of composite materials*, 36(10):1201–1231, 2002.
- [4] G. Struzziero and A. A. Skordos. Multi-objective optimisation of the cure of thick components. *Composites Part A: Applied Science and Manufacturing*, 93:126–136, 2017.
- [5] Z. Guo, S. Du, and B. Zhang. Temperature field of thick thermoset composite laminates during cure process. *Composites Science and Technology*, 65(3-4):517–523, 2005.
- [6] Y. A. Msallem, F. Jacquemin, N. Boyard, A. Poitou, D. Delaunay, and S. Chatel. Material characterization and residual stresses simulation during the manufacturing process of epoxy matrix composites. *Composites Part A: Applied Science and Manufacturing*, 41(1):108–115, 2010.
- [7] T. A. Bogetti and J. W. Gillespie. Process-induced stress and deformation in thick-section thermoset composite laminates. *Journal of composite materials*, 1992.
- [8] L. Shi. *Heat Transfer in the Thick Thermoset Composites*. Phd thesis, Delft University of Technology, 2016.
- [9] E. Ruiz and F. Trochu. Multi-criteria thermal optimization in liquid composite molding to reduce processing stresses and cycle time. *Composites Part A: Applied Science and Manufacturing*, 37(6):913–924, 2006.

- [10] L. Khoun, T. Centea, and P. Hubert. Characterization methodology of thermoset resins for the processing of composite materials - case study: CYCOM 890RTM epoxy resin. *Journal of Composite Materials*, 44(11):1397–1415, 2010.
- [11] M. K. Saraswat, K. M. B. Jansen, and L. J. Ernst. Cure shrinkage and bulk modulus determination for moulding compounds. In *Electronics Systemintegration Technology Conference, 2006. 1st*, volume 2, pages 782–787. IEEE, 2006.
- [12] P. P. Parlevliet. *Residual strains in thick thermoplastic composites: an experimental approach*. Phd thesis, Delft University of Technology, 2010.
- [13] M. R. Wisnom, M. Gigliotti, N. Ersoy, M. Campbell, and K. D. Potter. Mechanisms generating residual stresses and distortion during manufacture of polymer - matrix composite structures. *Composites Part A: Applied Science and Manufacturing*, 37(4):522–529, 2006.
- [14] M. M. Shokrieh. *Residual stresses in composite materials*. Woodhead Publishing, 2014.
- [15] W. J. Unger, J. S. Hansen, and H. Y. Ko. Method of reducing residual stresses in thermoplastic laminates, 1993.
- [16] M. M. Shokrieh and M. Safarabadi. Effects of imperfect adhesion on thermal micro-residual stresses in polymer matrix composites. *International Journal of Adhesion and Adhesives*, 31(6):490–497, 2011.
- [17] S. Laik and A. A. Skordos. Influence of residual stress on the delamination and shear response of carbon epoxy composites. In *European conference on composite materials, 15th*, 2012.
- [18] K. E. T. Kurdi and P. A. Olivier. Process-induced stresses and their influence upon some mechanical properties of carbon/epoxy laminates. part 2: study by acoustic emission. *Strain*, 3:2, 2004.
- [19] L. G. Zhao, N. A. Warrior, and A. C. Long. A micromechanical study of residual stress and its effect on transverse failure in polymer - matrix composites. *International Journal of Solids and Structures*, 43(18):5449–5467, 2006.
- [20] L. Sorrentino, W. Polini, and C. Bellini. To design the cure process of thick composite parts: experimental and numerical results. *Advanced Composite Materials*, 23(3):225–238, 2014.
- [21] Y. K. Kim and I. M. Daniel. Cure cycle effect on composite structures manufactured by resin transfer molding. *Journal of composite materials*, 36(14):1725–1743, 2002.
- [22] J. M. Balvers. *In situ strain & cure monitoring in liquid composite moulding by fibre Bragg grating sensors*. Phd thesis, Delft University of Technology, 2014.
- [23] J. S. Kim and D. G. Lee. Development of an autoclave cure cycle with cooling and reheating steps for thick thermoset composite laminates. *Journal of composite materials*, 31(22):2264–2282, 1997.
- [24] M. Li and C. L. Tucker. Optimal curing for thermoset matrix composites: Thermochemical considerations. *Polymer Composites*, 22.1:118–131, 2001.

- 
- [25] O. Sicot, X. L. Gong, A. Cherouat, and J. Lu. Influence of residual stresses on the mechanical behavior of composite laminate materials. *Advanced Composite Materials*, 14(4):319–342, 2005.
- [26] S. S. Kim, H. Murayama, K. Kageyama, K. Uzawa, and M. Kanai. Study on the curing process for carbon/epoxy composites to reduce thermal residual stress. *Composites Part A: Applied Science and Manufacturing*, 43(8):1197–1202, 2012.
- [27] D. Dykeman. *Minimizing uncertainty in cure modeling for composites manufacturing*. Phd thesis, The university of British Columbia, 2008.
- [28] P. I. Karkanis and I. K. Partridge. Cure modeling and monitoring of epoxy/amine resin systems. i. cure kinetics modeling. *Journal of applied polymer science*, 77(7):1419–1431, 2000.
- [29] J. Kratz, T. Mesogitis, A. Skordos, I. Hamerton, and I. K. Partridge. Developing cure kinetics models for interleaf particle toughened epoxies. *Proceeding of the 2016 International SAMPE Technical Conference*, 2016.
- [30] M. Reading and D. J. Hourston. *Modulated temperature differential scanning calorimetry: theoretical and practical applications in polymer characterisation*, volume 6. Springer Science & Business Media, 2006.
- [31] J. M. Barton. The application of differential scanning calorimetry (DSC) to the study of epoxy resin curing reactions. In *Epoxy resins and composites I*, pages 111–154. Springer, 1985.
- [32] J. P. Pascault and R. J. J. Williams. Glass transition temperature versus conversion relationships for thermosetting polymers. *Journal of Polymer Science Part B: Polymer Physics*, 28(1):85–95, 1990.
- [33] A. A. Skordos and I. K. Partridge. Cure kinetics modeling of epoxy resins using a non-parametric numerical procedure. *Polymer Engineering & Science*, 41(5):793–805, 2001.
- [34] A. P. Gray. A simple generalized theory for the analysis of dynamic thermal measurement. *Analytical calorimetry*, 1:209–219, 1968.
- [35] G. Li, P. Lee-Sullivan, and R. W. Thring. Determination of activation energy for glass transition of an epoxy adhesive using dynamic mechanical analysis. *Journal of thermal analysis and calorimetry*, 60(2):377–390, 2000.
- [36] M. Sadeghinia, K. M. B. Jansen, and L. J. Ernst. Characterization and modeling the thermo-mechanical cure-dependent properties of epoxy molding compound. *International Journal of Adhesion and Adhesives*, 32:82–88, 2012.
- [37] L. Khoun and P. Hubert. Cure shrinkage characterization of an epoxy resin system by two in situ measurement methods. *Polymer Composites*, 31(9):1603–1610, 2010.
- [38] K. M. B. Jansen, L. Wang, D. G. Yang, C. Van’t Hof, L. J. Ernst, H. J. L Bressers, and G. Q. Zhang. Constitutive modeling of moulding compounds [electronic packaging applications]. In *Electronic Components and Technology Conference, 2004. Proceedings. 54th*, volume 1, pages 890–894. IEEE, 2004.

- [39] W. Fisch, W. Hofmann, and R. Schmid. Chemistry of epoxide resins. xvii. influence of structure and curing conditions on the density, degree of cure, and glass transition temperature during the curing of epoxide resins. *Journal of Applied Polymer Science*, 13(2):295–308, 1969.
- [40] K.P. Pang and J.K. Gillham. Anomalous behavior of cured epoxy resins: density at room temperature versus time and temperature of cure. *Journal of Applied Polymer Science*, 37(7):1969–1991, 1989.
- [41] S. Huguet, N. Godin, R. Gaertner, L. Salmon, and D. Villard. Use of acoustic emission to identify damage modes in glass fibre reinforced polyester. *Composites Science and Technology*, 62(10-11):1433–1444, 2002.
- [42] W. Roundi, A. El Mahi, A. El Gharad, and J. L. Rebiere. Acoustic emission monitoring of damage progression in glass/epoxy composites during static and fatigue tensile tests. *Applied Acoustics*, 132:124–134, 2018.
- [43] F. Lahuerta Calahorra. *Thickness effect in composite laminates in static and fatigue loading*. Phd thesis, Delft University of Technology, 2017.
- [44] J. H. Oh and D. G. Lee. Cure cycle for thick glass/epoxy composite laminates. *Journal of composite materials*, 36(1):19–45, 2002.
- [45] A. A. Skordos. *Modelling and monitoring of resin transfer moulding*. Phd thesis, Cranfield University, 2000.
- [46] H. Cai, P. Li, G. Sui, Y. Yu, G. Li, X. Yang, and S. Ryu. Curing kinetics study of epoxy resin/flexible amine toughness systems by dynamic and isothermal DSC. *Thermochimica Acta*, 473(1-2):101–105, 2008.
- [47] S. Montserrat, C. Flaque, and J. Málek. Effect of the crosslinking degree on curing kinetics of an epoxy-anhydride system. *Journal of applied polymer science*, 56(11):1413–1421, 1995.

---

# Appendix A

---

## Dynamic DSC integration

Fig. A.1 and Fig. A.2 shows the integration of the two dynamic DSC tests to calculate total heat of reaction.

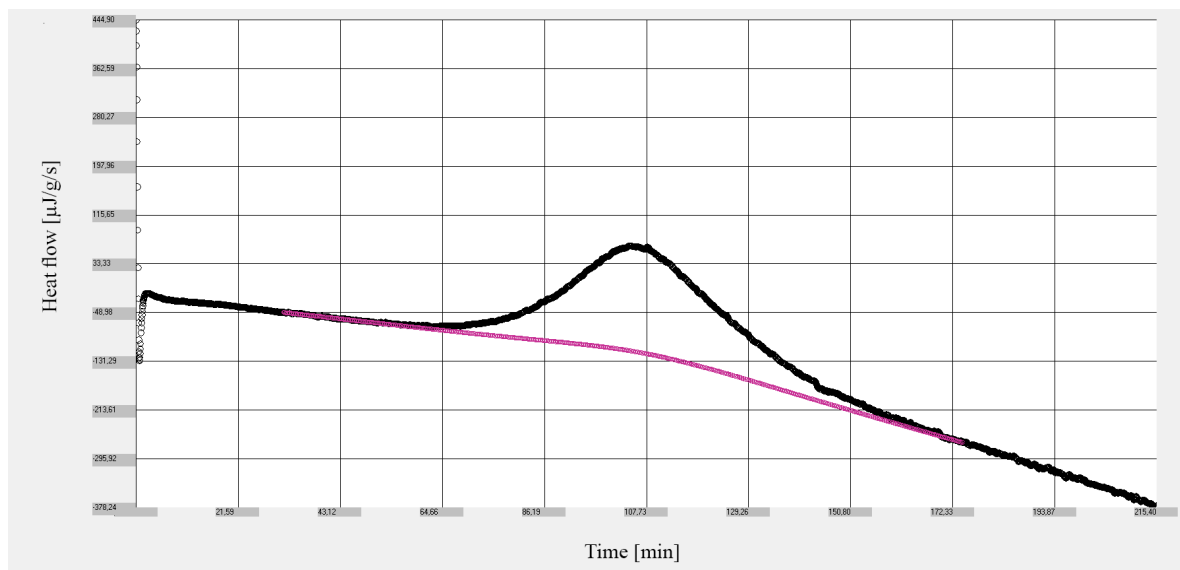


**Figure A.1:** Integration of first dynamic DSC test.

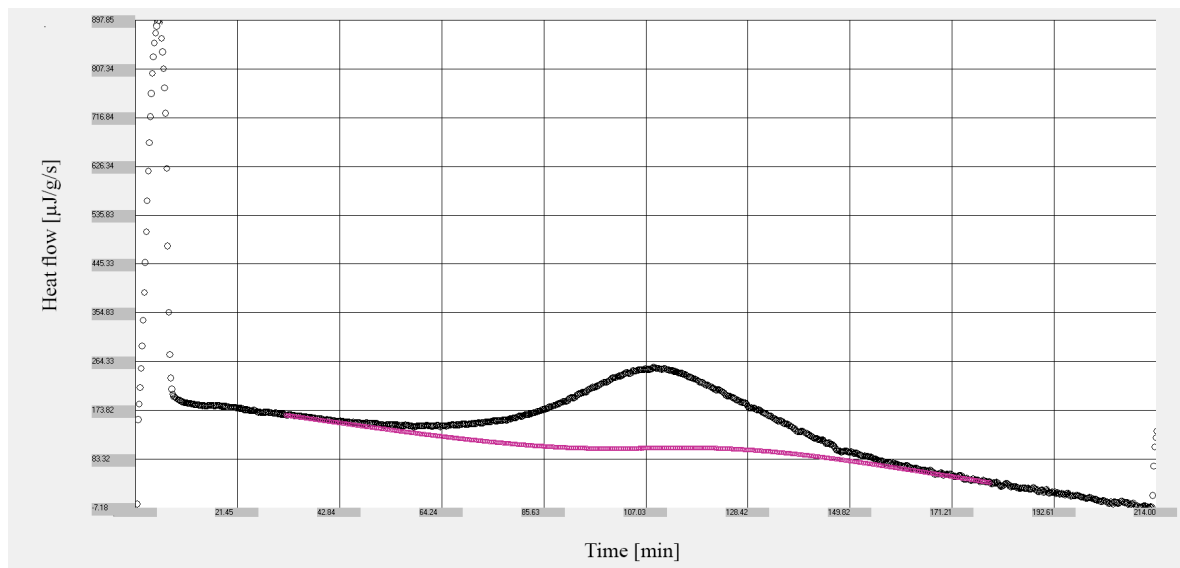


**Figure A.2:** Integration of second dynamic DSC test.

---

## Appendix B

---

# Determination of the glass transition temperature

Fig. B.1 shows the determination of  $T_g$  using the Pyris DSC software. The cure cycle used to determine the  $T_g$  is shown in Fig. B.2. The temperatures will differ for every  $T_g$  calculation. At  $T_g$ , there is a stepwise decrease in heatflow. The midpoint of this stepwise decrease is considered as  $T_g$ .

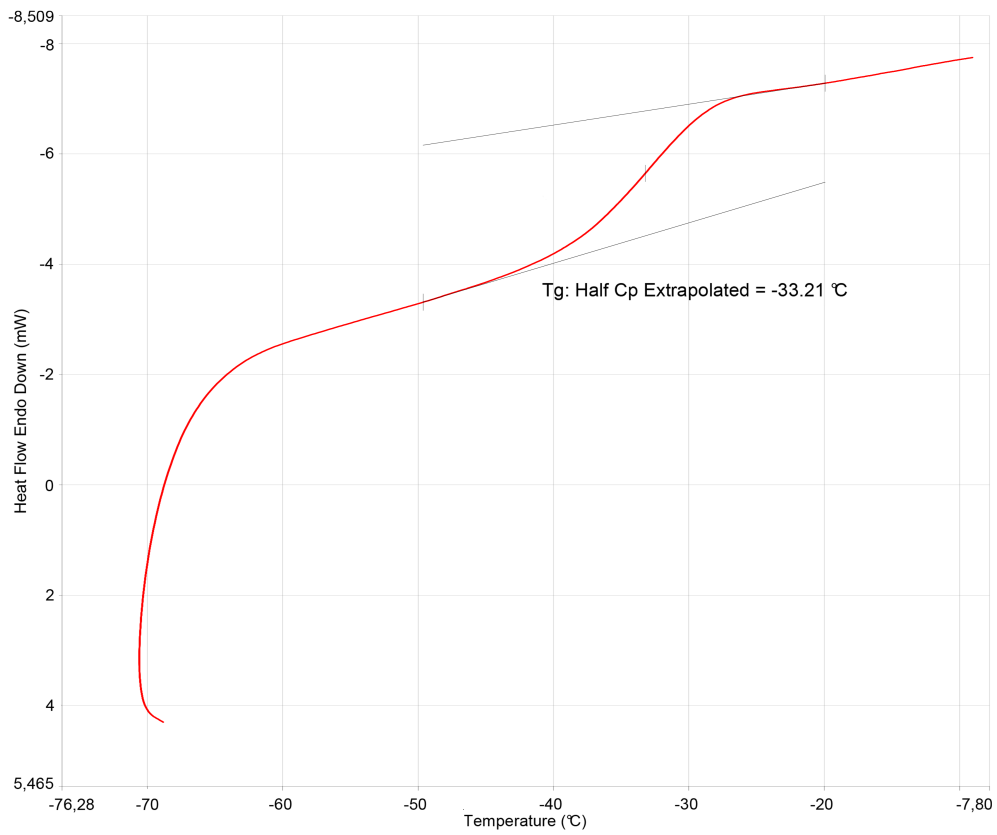


Figure B.1: Determination of  $T_g$  using the Pyris DSC software.

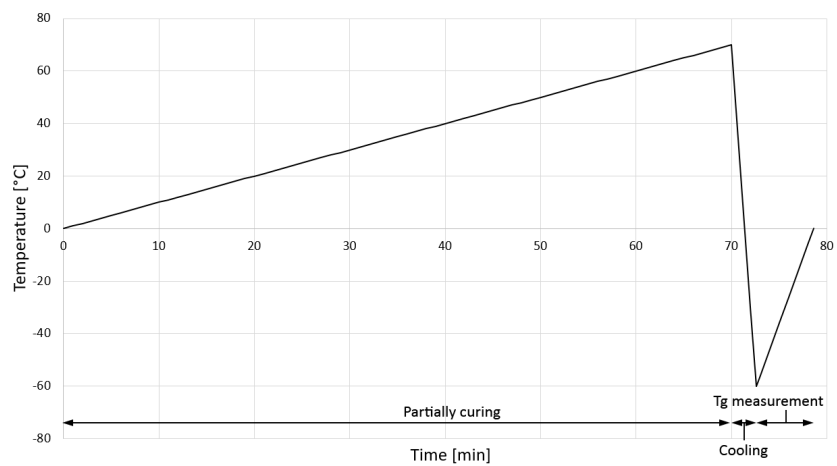
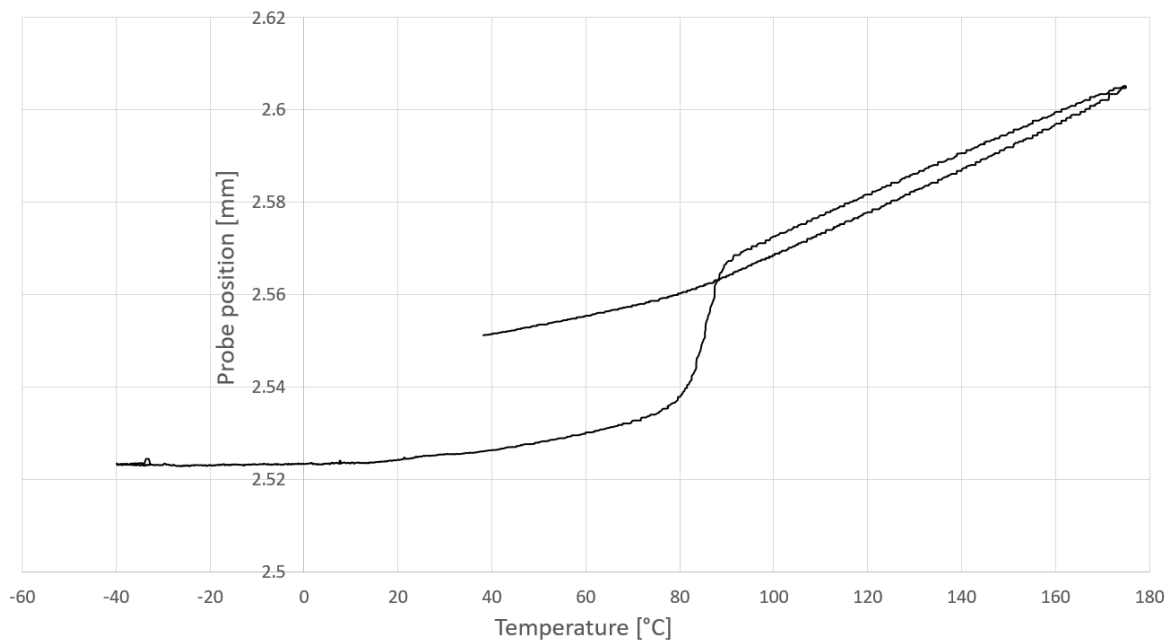


Figure B.2: Cure cycle to determine  $T_g$ .

## Malfunction of TMA

Fig. C.1 shows a constant probe position with increasing temperature which results in  $CTE = 0$ . This is physically not possible and is therefore seen as malfunctioning of the probe in the TMA.



**Figure C.1:** Malfunction of probe with TMA.



---

## Appendix D

---

# Resin crystallisation

When an epoxy resin is stored for a long time, crystallisation can occur due to cold temperatures or high temperature fluctuations. Crystallisation is a phase change of the resin whereby solid crystals are formed from the uniform liquid. The crystals will sink to the bottom as they have a higher density than the liquid. Crystallisation is completely reversible by heating the resin to about 50°C for 1 – 2 hours. The hardener will not undergo crystallisation.

The resin for this project (Airstone 780E) was stored in a barrel of 100L before it arrived at the TU Delft. The resin was poured into buckets of 20L for easier handling. However, as it was not known that the resin was crystallised in the big barrel and the crystals sank to the bottom, the small buckets contained resin with different compositions. Three laminates were infused and cured with a resin that contained a high level of crystals. While normally the laminate would be infused in about 90 minutes, these three laminates were barely infused in about 190 minutes. Barely infused because the resin started curing before the outlet was filled with resin. This is caused by the fact that the crystals lead to a higher viscosity of the resin which makes the infusion process slower. It was decided to disregard these laminates, order new resin and start over. Therefore, all laminates described in the report are infused with resin without crystals.

Since three laminates are infused and cured according to a certain cure cycle with both a good and bad resin system, the temperature profiles of these laminates can be compared. The cure cycles that are used with the bad resin system are MRCC, CC1 and CC3. By comparing the through-thickness exothermic peak temperature between the laminates made with a good and bad resin system it can be seen that the exotherm temperature of the good resin system is always between 4°C and 18°C higher than the exotherm temperature of the bad resin system (Fig. D.1). However, the shape of the through-thickness exothermic peak temperature is similar between the two resin types.

The difference in exothermic peak temperature can be explained by the longer infusion times of the bad resin system. Longer infusion times result in a higher initial degree of cure before the cure cycle starts. The initial degree of cure is calculated with the cure kinetics model and is between 0.12 – 0.14 for the laminates made with the good resin system while the initial degree of cure for the laminates made with the bad resin system is 0.19 – 0.24. Cai et al. [46]

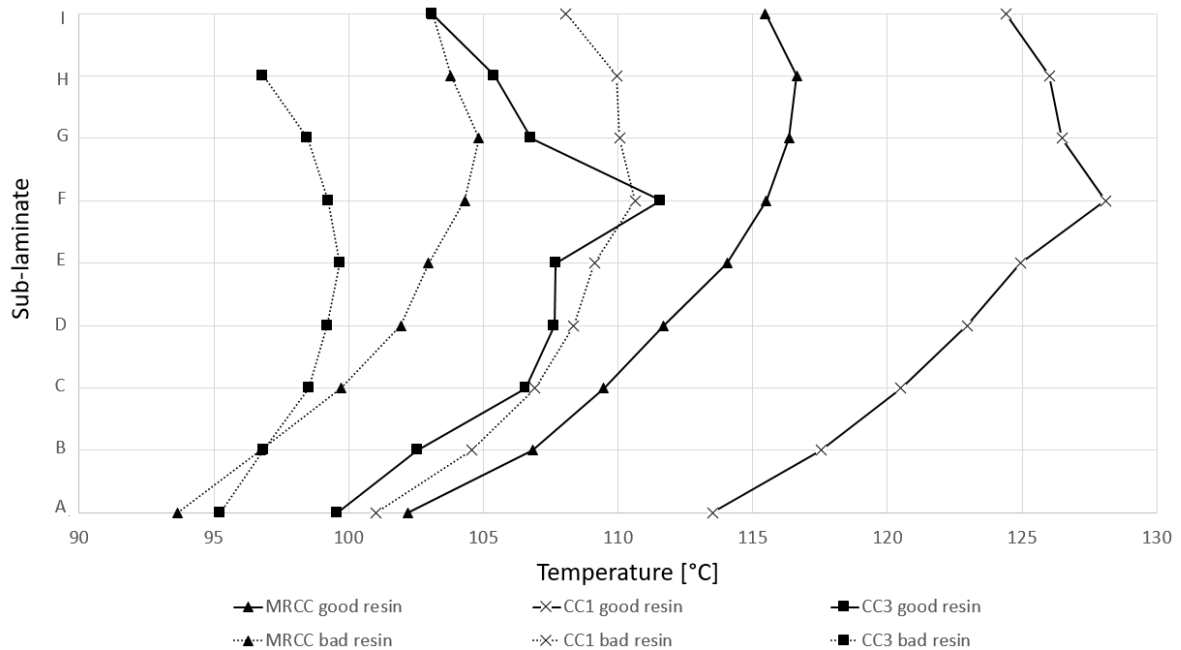


**Figure D.1:** Exothermic peak temperature of laminates made with a good and bad resin system.

and Montserrat et al. [47] researched the effects of degree of cure on the cure kinetics of an epoxy resin system. Both discovered that in the range of  $0.1 < \alpha \leq 0.4$  the activation energy increases with increasing degree of cure. The activation energy is the minimum energy required for a resin in order to react. A higher activation energy means a lower reaction rate ( $\frac{d\alpha}{dt}$ ) according to Eq. 2.3 and Eq. 2.4. Plotting  $\frac{d\alpha}{dt}$  vs.  $t$  for all six laminates it can be seen that the reaction rate of the laminates made with good resin is between  $5.0 \cdot 10^{-5}$  and  $1.5 \cdot 10^{-4} s^{-1}$  higher than laminates made with bad resin (Fig. D.2). This could clarify the difference in exothermic peak temperature between the laminates made with different resin qualities.

The shape of the through-thickness exothermic peak temperature is similar between the two resin types. Where the laminates made with MRCC follow a symmetric through-thickness temperature distribution, the laminates made with CC1 and CC3 are asymmetric for both resin qualities. This could be an indication that the variability of the thermocouple data is low, although more research must be done to prove this.

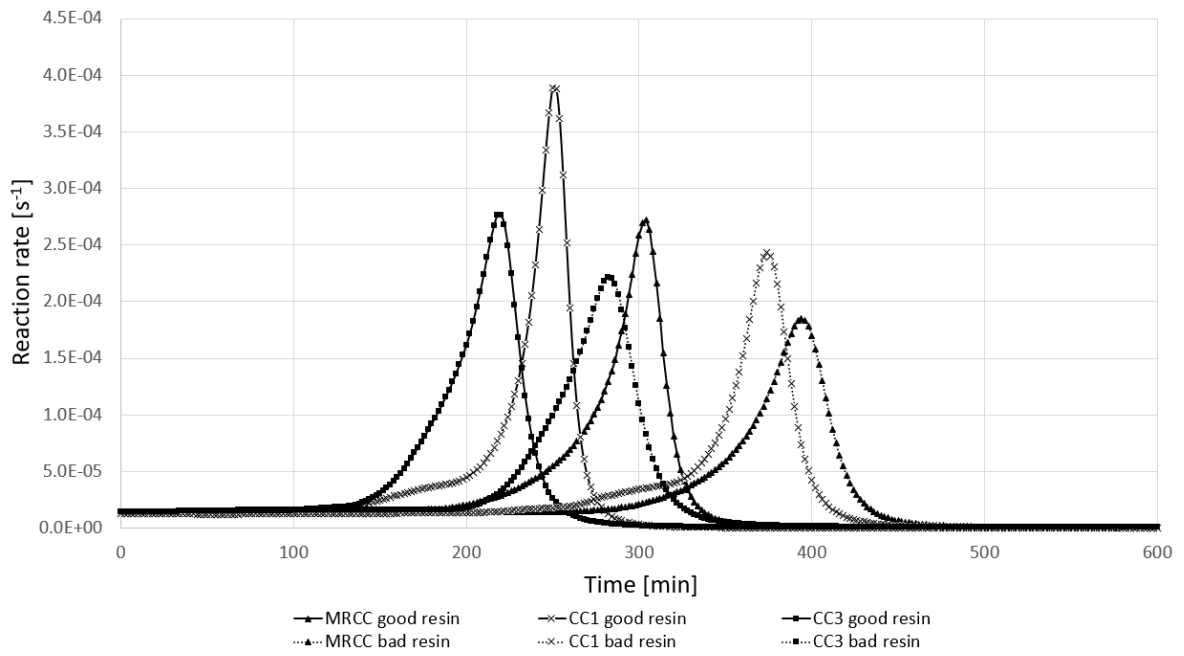


Figure D.2:  $\frac{d\alpha}{dt}$  of laminates made with a good and bad resin system.